MASARYKOVA UNIVERZITA
Přírodovědecká fakulta
Ústav Teoretické fyziky a Astrofyziky

Bakalářská práce

Brno 2020 Dominika Batková

MASARYKOVA UNIVERZITA
Přírodovědecká fakulta
Ústav Teoretické fyziky a Astrofyziky

Studium hvězd s velkou vlastní rychlostí

Bakalářská práce

Dominika Batková

Vedoucí práce: Mgr. Filip Hroch Ph.D. Brno 2020

Bibliografický záznam

Autor:	Dominika Batková Přírodovědecká fakulta, Masarykova univerzita Ústav Teoretické fyziky a Astrofyziky
Název práce:	Studium hvězd s velkou vlastní rychlostí
Studijní program:	Fyzika
Studijní obor:	Astrofyzika
Vedoucí práce:	Mgr. Filip Hroch Ph.D.
Akademický rok:	2019/2020
Počet stran:	$xvi + 74$
Klíčová slova:	hyper-rychlá hvězda; HVS; unikající hvězda; Gaia DR2; masivní černá díra; galpy; gala; dynamika Galaxie

Bibliographic Entry

Author:	Dominika Batková Faculty of Science, Masaryk University Department of theoretical physics and astrophysics
Title of Thesis:	On galactic high-velocity stars
Degree Programme:	Physics
Field of Study:	Astrophysics
Supervisor:	Mgr. Filip Hroch Ph.D.
Academic Year:	2019/2020
Number of Pages:	$xvi + 74$
Keywords:	hypervelocity star; HVS; runaway star; Gaia DR2; massive black hole; galpy; gala; Galactic dynamics

Abstrakt

V této bakalářské práci studujeme hvězdy s vysokou galaktickou rychlostí, které jsou v poslední době diskutovány v souvislosti se satelitem Gaia. Gaia poskytuje v současnosti nejpřesnější astrometrická měření společně v kombinaci se spektroskopií a fotometrií. Můžeme proto analyzovat pozice a pohyby miliard hvězd v Galaxii.

Rychlé hvězdy historicky dělíme na skupiny "runaway" a "hypervelocity". Existuje několik mechanismů jejich urychlení. Jejich původ hledáme v objektech Galaxie. Známý scénář využíva blízká setkání s černými dírami, které mohou narušit dvojhvězdný systém.

Nejprve jsme vyhledali nevázané objekty z katalogu Gaia, zpětnou integrací v čase našli průsečníky s rovinou galaktického disku a porovnali jsme je s pozicemi známých černých děr. Výsledky ukazují jistou vzájemnou korelaci.

Abstract

In this thesis we study high velocity stars which are lately very discussed in connection with Gaia satellite. Gaia has the most precise astrometric measurements in combination with spectroscopy and photometry. Therefore we may analyse positions and movements of billions of stars in the Galaxy.

These stars are historically divided into runaway and hypervelocity stars. There is several proposals for their ejection and it is essential to look for their origin in the Galaxy and objects that caused their velocity kick. The most known scenario uses close encounters with black holes that can tidally disrupt binary systems.

Firstly we found unbound objects from catalogue Gaia, found their intersections with the disk plane and compared to positions of possible stellar mass black holes in the Galaxy. Results show certain mutual correlation.

MUNI
SCI

MASARYKOVA UNIVERZITA
PŘÍRODOVĚDECKÁ FAKULTA
KOTLÁŘSKÁ 2, 611 37 BRNO
IČ: 00216224
DIČ: CZ00216224

ZADÁNÍ BAKALÁŘSKÉ PRÁCE

Akademický rok: 2019/2020

Ústav:	Ústav teoretické fyziky a astrofyziky
Studentka:	Dominika Batková
Program:	Fyzika
Obor:	Astrofyzika

Ředitel *Ústavu teoretické fyziky a astrofyziky* PřF MU Vám ve smyslu Studijního a zkušebního řádu MU určuje bakalářskou práci s názvem:

Název práce:	Studium hvězd s velkou vlastní rychlostí
Název práce anglicky:	On galactic high-velocity stars
Jazyk závěrečné práce:	angličtina

Oficiální zadání:
Poslední velmi přesná měření poloh a radiálních rychlostí, společně s nepřímými metodami jejich určení, otevírají cestu k seriozními studiu hvězd s velkou rychlostí vůči svému okolí. Hvězd, jež zaměstnávají astronomickou mysl už od dob svého objevu, poněvadž jde o poměrně nečekaný objev.

Jde o hvězdy, které by se dle stávajících teorii hvězdného vzniku, neměly vůbec pozorovat, jakožto dynamický vázaný objekt v Mléčné dráze. Musíme konstatovat, že hypotézy jejich zrodu nejsou nikterak přesvědčivé.

Cílem této práce je proniknout do podstaty problému prostřednictvím studia nejnovějších dat ze satelitů. Pro realizaci je nutná všeobecná znalost astronomického, statistického a počítačového zpracování dat.

Vedoucí práce:	Mgr. Filip Hroch, Ph.D.
Konzultant:	Mgr. Michal Prišegen
Datum zadání práce:	23. 10. 2019
V Brně dne:	23. 1. 2020

Souhlasím se zadáním (podpis, datum):

....	....	....
Dominika Batková	Mgr. Filip Hroch, Ph.D.	prof. Rikard von Unge, Ph.D.
studentka	**vedoucí práce**	**ředitel Ústavu teoretické fyziky a astrofyziky**

Poděkování

Na tomto mieste by som chcela poďakovať vedúcemu práce Mgr. Filipovi Hrochovi Ph.D. a konzultantovi práce Mgr. Michalovi Prišegenovi za cenné rady pri písaní práce. Mojej rodine ďakujem za podporu počas celého štúdia a priateľovi Martinovi za motiváciu pokračovať aj v zlých časoch.

Prohlášení

Prohlašuji, že jsem svoji bakalářskou práci vypracovala samostatně pod vedením vedoucího práce s využitím informačních zdrojů, které jsou v práci citovány.

Brno 16. srpen 2020 ....

Dominika Batková

Acknowledgement: This work has made use of data from the European Space Agency (ESA) mission *G*aia (https://www.cosmos.esa.int/gaia), processed by the *G*aia Data Processing and Analysis Consortium (DPAC, https://www.cosmos.esa.int/web/gaia/dpac/consortium). Funding for the DPAC has been provided by national institutions, in particular the institutions participating in the *G*aia Multilateral Agreement.

Contents

Introduction

With more precise measurents of positions and motions of stars we have opportunity to search for more high velocity objects in our Galaxy. However not only precision is the most important. Due to increasing range of measurable magnitudes we reveal more distant parts of our Galaxy. Nowadays, the most precise measurents of this type are fairly attributed to Gaia satellite which created the greatest catalogue of positions and velocities of stars with magnitudes up to 20. Even we call it the greatest catalogue it only cover about 1 % of Milky Way stars. It is neccessary to constantly cross our current limits to obtain data of more objects for a better understanding of our Galaxy.

The most important aspect in the analysis of high velocity stars is the place of their origin. We witnessed huge confusion among names of different types of high velocity stars and their ejection scenarios. With the knowledge of objects which possibly caused the ejection of high velocity stars we may confirm ejection proposals and later define precisely process of ejection and set borders among different types of scenarios and stars created by them. This is why it is very important to analyse obtained data and look for high velocity stars and their place of origin.

Through this thesis we are trying to dive deeper into problematics of high velocity stars and to understand processes behind the star ejections. We use the latest data release of the satellite Gaia. Firstly we want to create a Python script with help of the Python packages for galactic dynamics to analyze data of measured objects. Our goal is to find candidates of some high velocity objects and analyse their orbits to obtain information about these objects for improvements of script for analysing the future data release planned next year.

Subsequently we want to choose only unbound stars and integrate their orbits to past and future to find out when and where they cross the galactic disk to create tables with these data for future use.

Finally we want to compare places of intersections from the past with some exotic objects which may cause the ejection.

Chapter 1

High Velocity Stars

1.1 History

Astrometry is possibly one of the oldest segments of Astronomy. Measuring of exact position and movement of star across the sky was very important, but was limited by accuracy of the instruments. Barnard's star is one of the well-known discoveries of star with large proper motion that was not expected. Until the end of the 19th century it was not clear whether we would be able to measure the stars with sufficient accuracy. With the development of technology, we could begin to obtain the positions and motions with higher and higher accuracy and thanks to that we can study the morphology and dynamics of our Galaxy.

With the development of spectroscopy we were able to measure radial velocities due to Doppler's effect and we began to have an overall picture of what is happening with the movement of the stars. From these times on, it was as if a bag of articles about high velocity stars had been torn apart. Adams & Joy (1919) in their article analyse stars with large velocities in line of sight that were measured at the Lick and Mount Wilson observatories. Oort (1922) claims in his work that number of found stars with larger radial velocity is higher than would correspond to Maxwellian distribution. In this time measured stars with higher velocities were all moving towards one hemisphere of the sky. Works as Trumpler (1924) and Allen (1925) report findings of this type of stars and they were not alone. Even Oort (1926) deals with the stars of high velocities in his dissertation. Oort parses also asymmetry in stellar motions of high velocity stars and he assert that asymmetry appears above sharply defined limit of about 63 km.s^{-1}. Work also contains catalog of known high velocity stars.

Oort (1930) in his later work writes that the stars with corrected velocities for the motion of the sun larger than or equal to 63 km.s^{-1} have been called high velocity stars. This was first definition of high velocity stars. He also admits that some selection rule according to velocity is very probable to appear because of preference for certain spectral types of stars that can be measured with usable accuracy and limits of measuring equipments. This could be main reason why the majority of known high velocity stars pointed only toward one hemisphere. With spectra of high velocity stars astronomers were trying to find out their origin and properties. As Bidelman (1948) writes in his paper there was general opinion that high velocity stars are members of Baade's type II stellar population mainly because of their spectra which are different from normal stars. However he anounces discovery of two high velocity O- and B- type stars that are very early-type stars in comparison with Baade's type II stellar population which is very old.

Schwarzschild (1952) deals with perigalactic and apogalactic distances of high velocity stars. He works with an assumption that orbits of high velocity stars should remain the same during lifetime of Galaxy and therefore assumes that place of origin of high velocity star lies in a small area around its present orbit. His conclusions are that there is a number of Population II stars whose spherical distance from center in some parts of orbit exceeds twice the distance from the centre of Galaxy to our Sun. He also points out that orbits of most high velocity stars do not pass through the central bulge of the Galaxy and therefore they must have originated farther away in the Galaxy.

Firstly it looked like high velocity stars are mainly Population II stars and astronomers were trying to find their origin. We now know that Population II is defined by highly eccentric orbits passing through disk plane (Mikulášek & Krtička, 2005) and that is reason why they were included in group of high velocity stars. However it later became apparent that there was a more interesting group of high velocity stars. Greenstein et al. (1956) call them 'runaway' Population I objects. These are very young O- and B- type stars representing Population I among high velocity stars. Greenstein (1957) again mentions that these stars have been found above the galactic plane and their radial velocities are so high that they must have been even higher at the moment of passing through disk, around $200 - 300$ km.s^{-1}. He writes that these stars have been probably produced from high velocity interstellar clouds or in unstable OB associations.

From these times it was clear that these stars have a huge potential for analysing dynamics of our Galaxy. For now we will call them Runaway Stars and in the next section we will show what astronomers have found out about them.

1.2 Runaway Stars

The primacy in finding runaway stars is attributed to Humason & Zwicky (1947). In their search for faint blue stars they came across outstanding exceptions in velocities of some stars. They inform us about 8 stars in Hyades region with velocities +200 km.s^{-1} and 17 in the north galactic pole region with velocities -220 km.s^{-1}. Unfortunately, they did not draw any conclusions from these findings due to uncertainties.

These stars were studied mainly by Blaauw after their discovery. Blaauw (1956) firstly examines whole range of properties from luminosities to space distribution of some northern O-B stars. Later Blaauw (1959) determined luminosities and the 'expansion age' of some high-velocity O- and B-type stars which were discussed in previous paper. Expansion age is time elapsed since the star left the origin. For almost all of them he determined associations from which they probably originated.

The first vast article dealing only with problematics of runaway stars has been published by Blaauw (1961) whose article was trying to come up with theories for the explanation of these objects. He defined runaway star as object for which the direction of the space motion is sufficiently known and distance from left association is still small enough for identification. He also discusses differences between low and high velocity objects of this spectral type which include lack of double or multiple stars between found high velocity stars and different spectral distribution. These differencies were taken into consideration while the conclusions were made about explanations of these high velocity stars. He proposes that these stars were the secondary components of proto-double stars where the more massive star shed most of its mass and therefore the secondary is released with velocity equal to a large fraction of its original orbital velocity. Sheding of mass of proto-primary must be quick and thus this process is associated with the type II supernova.

An alternative explanation of high velocity O- and B- type stars was suggested by Poveda et al. (1967), who show that their origin may be a result of dynamical interactions during the collapse of small clusters consisting of massive stars. Results of simulations showed that it is easy to produce runaway stars through the collapse of small cluster. With lower initial velocities more runaway stars will be created with even higher velocities. Most of the runaways created in simulations were single stars what is in agreement with observations. Little difference is in ratio of a numbers of O-type stars and B-type stars which is smaller compared to observations. Allen & Poveda (1972) continued in simulations of collapsing clusters to test the stability of the trajectories of runaway stars. In introduction they remind that according to observations about 20 % of O stars belongs to high velocity stars while for B stars it is only 2 % of this spectral type.

Cherepashchuk & Kukarkin (1976) propose to search for the periodic optical variability of runaway stars due to suspicion of their binary nature and connection with relativistic objects as neutron stars and black holes. Cherepashchuk & Aslanov (1984) and Aslanov et al. (1984) launched a search for these non-X-ray binaries of which was thought to be thousands of them in the Galaxy. Due to supernova explosion theory for origin of runaway star it was shown that within a close binary system it is possible for system to stay gravitationally bound even after explosion and become runaway binary system with high velocity. List of runaway OB stars, which can possibly be a component of non-X-ray binary system with relativistic object was made. On account of interesting assumption there were another trials to confirm some binary systems of this type. (Aslanov & Barannikov, 1989; Sterken, 1988) However not even one have shown trustful evidence.

Scientists were creating different theories of high velocity star creation. Some were more believable than others which were rather exotic. The concept of black holes was at those times well known, but it was very uncertain whether they can be found in our Galaxy, what is their possible layout and if there is one massive black hole in the center of Milky Way. But these highly exotic objects became one of the candidates for high velocity phenomenon.

1.3 Hypervelocity Stars

While runaway stars were firstly detected and only after that were they explained, Hypervelocity Stars were firstly defined and only after very long time were they firstly detected. The dynamics of gas around the galactic centre suggested occurance of black hole with mass million times higher than mass of the Sun. This was reason why Hills (1988) made simulations of close encounters between a tightly bound binary system and such a massive black hole. These encounters may cause unbinding of binary system while one component stays bound to black hole and the other is running away from the galactic centre through space with velocities up to 4000 km.s^{-1}. He explains that most encounters happened beyond the last stable circular orbit. According to results of simulations he estimates that if 1 % of the stars ocurring in these types of encounters are binary systems with $a_0 = 0.01$ au then collision rate is $\sim 10^{-4}$ yr^{-1} and if other 1 % are systems with $a_0 = 0.1$ au then its collision rate is $\sim 10^{-3}$ yr^{-1}. He discusses that almost definitive evidence for a supermassive black hole in the galactic centre would be a discovery of such star.

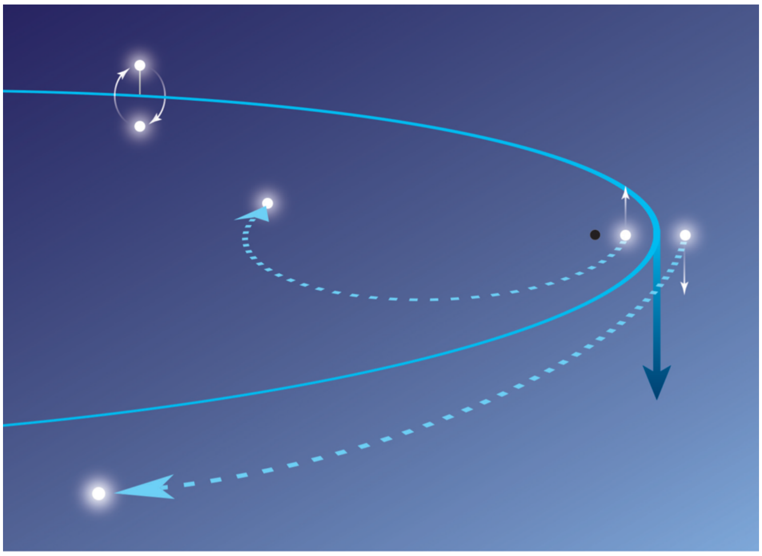

Figure 1.1: Illustrated Hills's mechanisms. (Brown, 2015)

While still searching for hypervelocity star, Yu & Tremaine (2003) made other simulations of ejections from the galactic centre. They propose 2 other possible encounters. First was an encounter of two single stars and second was interaction between a single star and binary black hole. For the first proposal rates are not so high $\sim 10^{-7}$ yr^{-1}. However second proposed mechanism has better results. If we admit an idea of having a binary black hole in the galactic centre then ejection rate would be $\sim 10^{-4}$ yr^{-1} and in the sphere with radius of our distance from the centre should be around 1000 of hypervelocity stars.

It took a long time to find the first hypervelocity star. Brown et al. (2005) inform us about their discovery. The star leaving the Galaxy with a galactic rest-frame velocity of 709 km.s^{-1}. However it is B-type star, it comes from the Galactic centre. According to them it is hard to imagine a formation of young and massive stars near the black hole but observations have shown these stars within 1 pc of the centre. That year 2 other hypervelocity stars were found. Second was found by Edelmann et al. (2005) and it had the galactic rest frame velocity at least 563 km/s. The problem with this star is that it needs more time to travel to its current position than is lenght of its lifetime. They propose two explanations. Either it is a blue straggler star or its origin is in the centre of the Large Magellanic Cloud. So in our Galaxy we do not have to find only local stars, but there is possibility of finding stars from neighboring galaxies. Hirsch et al. (2005) inform us about finding third hypervelocity star with a galactic rest frame velocity 751 km.s^{-1}. There is possibility that this star is formed by the merger of two helium white dwarfs in the close binary.

After these discoveries several targeted searches were launched. At this point it was all mixed together. There were so many different ejection possibilities. Found hypervelocity stars were mainly B-type stars located in the halo. And when we think about it, it is almost the same as for runaway stars. There are only two possible differences and they are ejection velocity and place of origin - whether it is from the galactic centre or disk. This is why Brown et al. (2006a) define a hypervelocity star as an unbound star with an extreme velocity that can be explained only by a massive black hole, but they forget to mention what should be its place of origin. Brown et al. (2006b) found in data of the velocity distribution a tail of objects with large positive velocities that may be a mix of low-velocity hypervelocity stars and high-velocity runaway stars.

However some definitions were made, not everyone use them and we have to warn that there are no exact borders between runaway and hypervelocity stars, because Przybilla et al. (2008) later found unbound star that was called hyper-runaway star and even speed of these two groups became comparable. They suggest that this star was created by supernova from the core collapse of very massive star and is an alternative to the Hills mechanism for moderate velocities. Even Brown et al. (2007a) change their mind and called a new found group with only large velocities as a new class of hypervelocity stars which should be ejected from the galactic centre with bound orbits. Brown et al. (2007b) infer from assymetry in the velocity distribution that hypervelocity stars must be short-lived stars. Bromley et al. (2006) finally simulated the spectrum of ejection velocities by a massive black hole from the galactic centre and they found out that full population of ejected stars include same number of unbound and bound hypervelocity stars of the same stellar type.

Name hypervelocity star was not very smart, because it should be used for stars with hyper velocity which means that ejection velocity should be above some defined limit. We admit that Hills (1988) used this nomenclature to highlight that only a massive black hole can create object with hyper velocity and he thought that there is only one of these in the galactic centre. Unfortunately there are no definitions and that is why reading scientific articles about high or hyper velocity stars is very confusing. There should be defined limit between high and hyper velocity - for example escape velocity. In that case, high velocity stars would be stars with bound excentric orbits and hyper velocity stars would be unbound to the Galaxy. Next division would be according to place of origin. While stars which are ejected from the disk have their name already - runaway stars, term for stars from the galactic centre is missing if we do not want to mistake them with other hyper velocity stars. We propose this division for easier orientation in the problematics. Of course this can not be the only selection. There are more proposals of creating hypervelocity star.

Abadi et al. (2009) found a large fraction of hypervelocity star cluster around the constellation of Leo that share a common travel time. They used numerical simulations to show that disrupting dwarf galaxies may contribute halo stars with velocities sometimes exceeding the nominal speed of the system. In their paper they proposed a new mechanism of creating the hypervelocity star with a tidally disrupting dwarf galaxy passing through the center of the Galaxy. Last known possible variant of creating the hypervelocity star was suggested by Silk et al. (2012) who argue that the hypervelocity stars may be generated by the interactions of an active galactic nucleus jet from the central black hole with a dense molecular cloud.

All ejection scenarios proposed are shown on the Figure 1.2 with their possible spatial distribution of ejected stars. With all these proposals and simulations of ejection scenarios, selection to specific group is even more important, because there could be a great number of extragalactic stars but also some of the proposals may not work in reality.

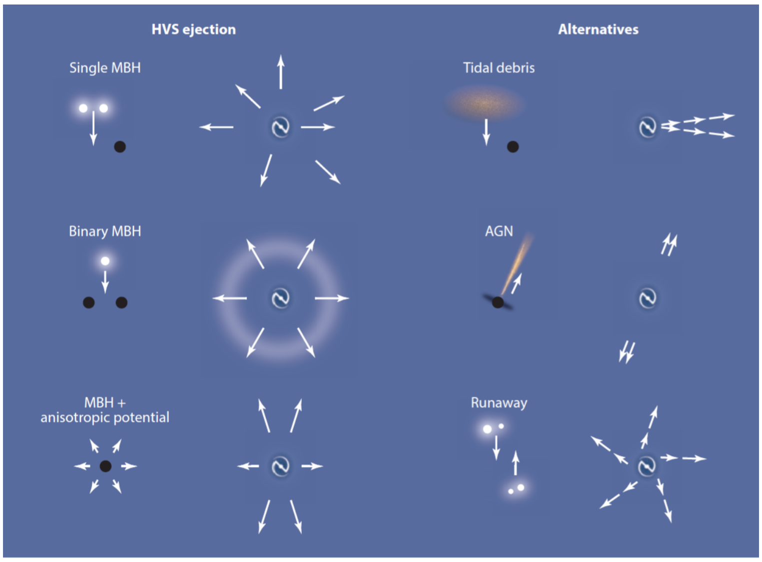

Figure 1.2: Spatial distribution of the ejected stars by different types of the origin mechanisms. (Brown, 2015)

1.3.1 Intermediate or stellar mass black holes

Fragione & Gualandris (2019) noticed that data from Gaia mission suggest that only those fastest hypervelocity stars can be traced to the galactic centre and others have their origin somewhere in the disk. They propose that they originated by Hills-type mechanism in star clusters with intermediate mass black hole. Binaries should be tidally disrupted by intermediate mass black hole and ejected with high velocity. These are stars that can be mistaken with hyper-runaway stars, but due to interaction with black hole they call them hypervelocity. These stars may have unbound trajectories and if traced back they may suggest positions of intermediate mass black holes.

With more data about possible intermediate or stellar mass black holes we may compare positions of black holes with intersections of the galactic disk. There is not many of these surveys with positions in the Galaxy to be used. Black hole could be connected with two different scenarios. First is cluster hosting black hole and the other is supernova explosion of very massive star whose core may collapsed into black hole. According to Fragione & Gualandris (2019) the first scenario has higher change of higher ejection velocity. However according to Przybilla et al. (2008) even supernova explosion may cause unbinding from the Galaxy.

1.4 Extreme findings

1.4.0.1 The fastest found hyper-runaway star

The most interesting hyper-runaway star was confirmed by Hattori et al. (2019). It is a massive subgiant star ejected from stellar disk of the Galaxy 33 Myr ago with ejection velocity around 568 $km.s^{-1}$. It is almost the velocity limit with which can be a runaway star ejected and that makes it hyper-runaway. These hyper-runway stars are ejected with rate $\sim 10^{-7}yr^{-1}$. It is aproximatelly 1 % of hypervelocity stars ejection rate. LAMOST-HVS1 is probably ejected by 3 or 4 body dynamical interaction and its natal star cluster may be currently located near the Norma spiral arm. The data used for identifying LAMOST-HVS1 were the proper motion measurements from Gaia DR2 and their special high-resolution spectrometry.

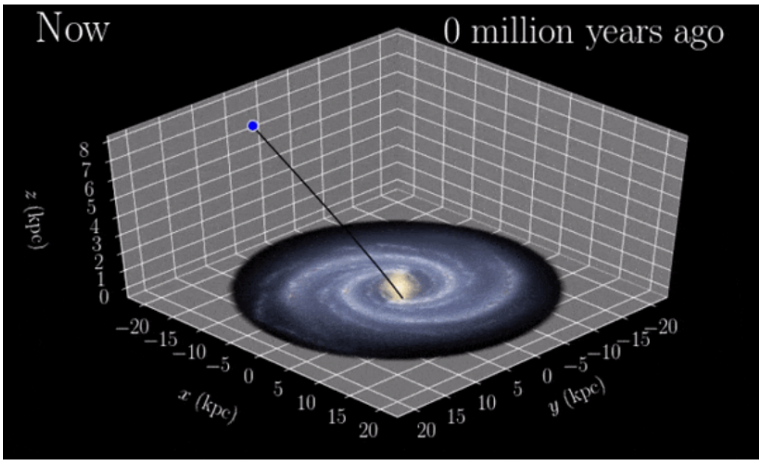

Figure 1.3: The simulated trajectory of a massive hyper-runaway subgiant star LAMOST-HVS1 from the Galactic disk. (University of Michigan, 2019)

1.4.0.2 The fastest found hypervelocity star

The latest article about finding of a new hypervelocity star was published in January. Koposov et al. (2020) used the Southern Stellar Stream Spectroscopic Survey (S^5) and unintentionally discover the fastest main-sequence hypervelocity star. They called it S5-HVS1 and its velocity in the Galactic frame is $1755 \pm 50 kms^{-1}$. Koposov et al. (2020) claim that S5-HVS1 is the only hypervelocity star assuredly correlated with the Galactic center. The fact that velocity of S5-HVS1 is almost two times higher than the velocities of other hypervelocity stars related to the Galactic center is very strange. Koposov et al. (2020) wonder whether they are ejected by the same mechanism.

Chapter 2

The satellite Gaia

2.0.1 Introduction

Astrometry is one of the oldest disciplines used by astronomers to obtain the accurate positions of the objects in the sky. However, measuring the precise parallaxes from Earth is very difficult considering the systematic errors and disturbing effects of our atmosphere.

The change came in 1997 with the Hipparcos satellite, which obtained the absolute parallax with milli-arcsecond precision. Even with its limitations, it made significant progress in understanding of the structure and dynamics of Milky way.

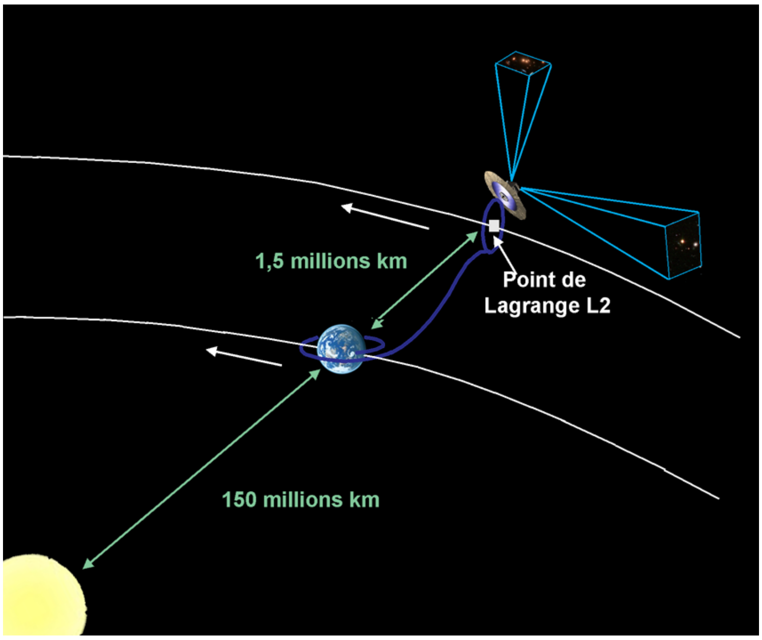

Figure 2.1: Orbit of Gaia. (Pline, 2013)

Gaia is one of the main missions of the European Space Agency(ESA), as was the Hipparcos. On December 19 2003 the satellite Gaia was launched from Earth. After one month it was transferred to the orbit around the second Lagrange point of the Sun - Earth - Moon system, which is around 1.5 million kilometres from Earth. It moves around this point in a Lissajous-type orbit, that has several advantages over an Earth-bound orbit. For example, stable thermal conditions, a benign radiation environment and high observing efficiency in which the Sun, Earth and Moon are outside of its view. (Kramer, 2002)

Amazing is that after processing, calibration, and validation of data, they will be made available to the world without limitations.

2.0.2 The aims and goals of the Gaia mission

The scientific goals of the design reference mission were relying on astrometry combined with its photometric and spectroscopic surveys. The location in space and design of satellite enable a great accuracy, sensitivity, dynamic range and sky coverage impossible to obtain with ground-based observatories. (Gaia Collaboration et al., 2016)

Main task of Gaia is detailed observation of the Galaxy in order to understand the formation, dynamics and current state of the Milky way. The goal is to make a catalogue of 1 billion stars with precise measurements of the three - dimensional spatial and the three - dimensional velocity distribution of stars and to determine their astrophysical properties, such as surface gravity, effective temperature and composition. Each star will be observed 70 times during 5 years of expected lifetime of the satellite. Astrometric data are obtained with an extraordinary precision. The satellite is able to get data from stars with magnitudes up to 20. Gaia sample will only cover about 1 % of the stars in the Galaxy. With this number we realise, how much there is to discover. (Gaia Collaboration et al., 2016; Kramer, 2002)

2.0.3 The spacecraft and payload

The spacecraft consists of a payload module, a mechanical service module and an electrical service module. The payload module has three scientific functions: astrometric, photometric and spectroscopic. So the instruments are divided to these three categories according to their functions.

An astrometric instrument (AI) sums the two telescopes, an area of $7+7$ CCDs in the focal plane commited to the sky mappers and an area of 62 CCDs in the focal plane where the two fields of view are connected to the astrometric field. A photometric instrument (PI) determines the spectral energy distribution of all observed bodies and a spectroscopic instrument (SI), known as the radial-velocity spectrometer (RVS), gains spectra of the bright end of the Gaia sample to provide radial velocities, coarse stellar parametrisation, interstellar reddening, atmospheric parameters, rotational velocities and individual element abundances. The PI and SI are higly integrated with the AI by operating the same telescopes, focal plane and sky-mapper function. (Gaia Collaboration et al., 2016; Kramer, 2002)

The wavelength coverage of the AI is 330 – 1050 nm. The PI has two prisms dispersing incoming light. First disperser is blue photometer and works in the wavelength range 330 – 680 nm and second is red and refer to the wavelength range 640 – 1050 nm. The SI consists of a blazed-transmission grating plate, four prismatic lenses and a multilayer-interference bandpass-filter plate to limit the wavelength range to 845 – 872 nm centred on the Calcium triplet region, which is suitable for radial-velocity

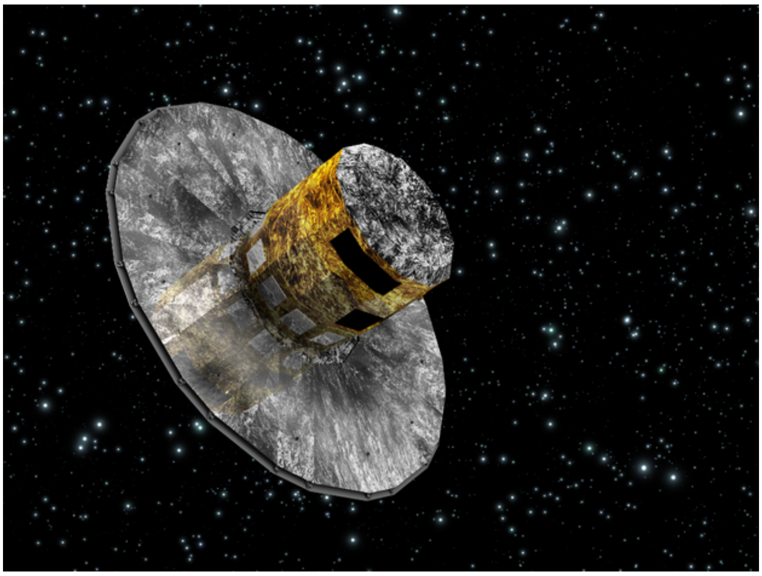

Figure 2.2: Artistic impression of the satellite Gaia. (ESA, 2017)

determination over a wide range of stars. (Cropper et al., 2018)

The AI can handle object densities up to 1050000 objects deg^{-1}, the PI is limited to 750000 objects deg^{-1} and the SI 35000 objects deg^{-1}. Only brightest objects are observed in denser areas. (Gaia Collaboration et al., 2016)

2.1 Data from Gaia

2.1.1 The data releases

Gaia data release was planned to be divided into three parts. The first data(DR1) was released on 14 September 2016 and second(DR2) on 25 April 2018. The final update of data(DR3) is expected in the second half of 2021. (ESA, 2014-2020)

The DR1 was the first whiff of results from Gaia with over 2 million parallaxes and proper motions. It was very quickly established as a reference for calibration of other surveys. However, it is based on a limited amount of input data and in some cases suffers from systematic errors due to shortcomings in the calibrations caused by simplifications in the data processing. The major advances are represented in Gaia DR2. (Gaia Collaboration et al., 2018)

The DR2 consists not only of new data types, but also much expanded and effectively improved astrometric and photometric data. The largest radial velocity survey was added together with astrophysical information for 161 million sources and variability information for 0.5 million sources. Nevertheless DR2 is still intermediate and represents only 22 months of the nominal mission lifetime and is still troubled by simplifications of input data. The problems are caused also by partly inadequate calibrations and an incomplete understanding of the behaviour of the satellite. On the bright side, astrometry in DR2 shows a great improvement over DR1. The parallax uncertainties are generally below 0.1 mas. The uncertainty of the radial velocities is above 20 km.s^{-1}. (Lindegren et al., 2018)

The expectation of the last data release are huge. With more measured data it should be more accurate to process them without any simplifications and to make better calibrations that will not cause any systematic errors as it was with DR1 and DR2. We hope that a real advantage will be gained from the higher precision due to the longer time span of the input data. (Gaia Collaboration et al., 2018)

2.1.2 Problems and Access of Data

2.1.2.0.1 Access of Data The way how to access data from Gaia is very straightforward. During our research we encountered two different ways how to obtain and download data from Gaia. First way is through Gaia Archive Website and second is through Jupyter Notebook.

Gaia Archive

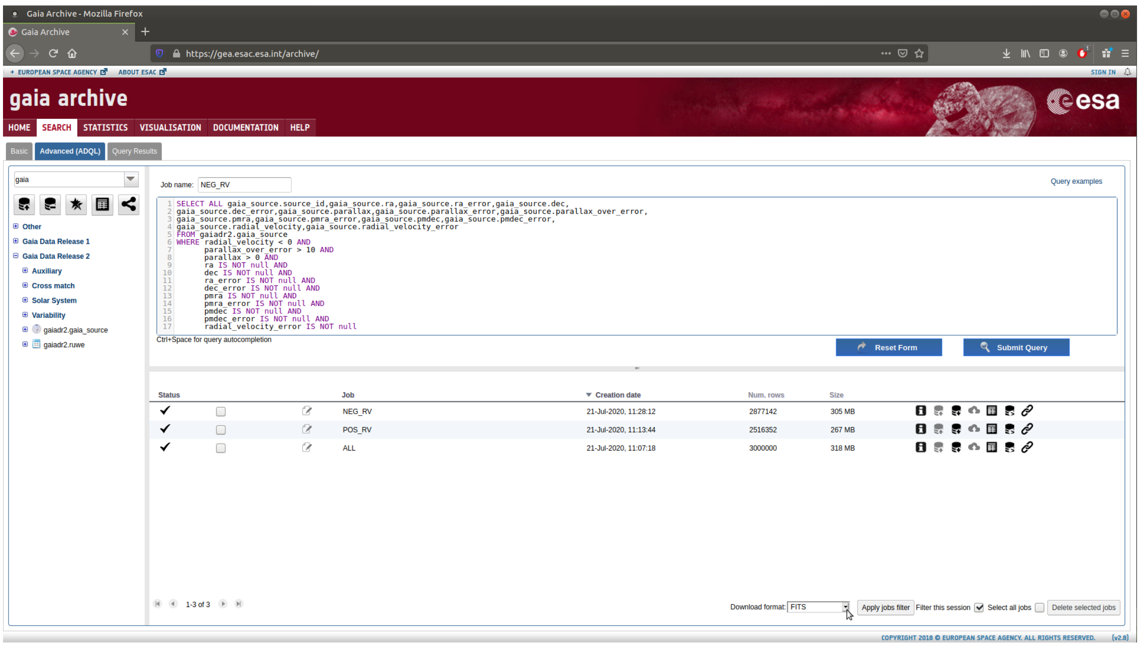

Figure 2.3: Gaia archive query.(ESA, 2018)

Benefits of using Gaia Archive from https://gea.esac.esa.int/archive/ are mainly in loading speed of huge amount of data. Its disadvantages are in limited amount of objects that can be loaded at once, but still it is more than through Jupyter Notebook and can be taken more as an advantage. Secondly it is not so comfortable, because it is not included in script and we have to firstly download data before using them. Eventually we used this method because of higher amount of data that can be loaded at once. We have to admonish that limit of rows=objects that can be loaded at once is apparently 3 millions. We can notice on the Figure 2.3 that when we take whole range of radial velocities (ALL) there is number of rows 3 millions. We would logically assume that sum of objects with positive and negative radial velocities is equal to number of objects with whole range of radial velocities. Though it would be logical, the truth is that there is more objects than 3 millions and we were only limited by number of rows that can be loaded at once.

Jupyter notebook

Using Jupyter Notebook to get data from Gaia is very easy and pleasant way because is implemented in script itself. However, there are some disadvantages with its usage. We personally ran into a problem with memory error that was main reason why we did not use this method, but also we noticed slower loading of data. This method is more convenient for downloading and using less data maybe for some tests of script or packages from Python.

```
ValueError: 1:0: no element found
```

Figure 2.4: Error in Jupyter Notebook while uploading too much data.

Here we can see example of code from Jupyter Notebook that can be used for obtaining data from Gaia through this method.

```
from astroquery.gaia import Gaia
from astropy.table import QTable

query_text = '''SELECT TOP 200 gaia_source.source_id,gaia_source.ra,
gaia_source.ra_error,gaia_source.dec,gaia_source.dec_error,
gaia_source.parallax,gaia_source.parallax_error,
gaia_source.parallax_over_error,gaia_source.pmra,
gaia_source.pmra_error,gaia_source.pmdec,gaia_source.pmdec_error,
gaia_source.radial_velocity,gaia_source.radial_velocity_error
FROM gaiadr2.gaia_source
WHERE radial_velocity >=500 AND
parallax_over_error > 10 AND
parallax > 0 AND
ra IS NOT null AND
dec IS NOT null AND
ra_error IS NOT null AND
dec_error IS NOT null AND
pmra IS NOT null AND
pmra_error IS NOT null AND
pmdec IS NOT null AND
pmdec_error IS NOT null AND
radial_velocity_error IS NOT null
'''
job = Gaia.launch_job(query_text)
gaia_data_posrv = job.get_results()
gaia_data_posrv.write('gaia_data_posrv.fits')
gaia_data_posrv = QTable.read('gaia_data_posrv.fits')
```

2.1.2.0.2 Problems Unfortunatelly, the range of possible radial velocities is limited to $|v_{\text{rad}}| < 1000$ km.s^{-1}. We have to highlight the fact that for the 613 sources with absolute value of radial velocity above 500 km.s^{-1} were looked after with special care. Because of data processing limitations this small subset can be contamined by outliers. So their spectra were visually checked and only 202 of 613 sources were included to DR2 as valid high velocity sources. We have to be carefull with using this data, because reliability of the remaining radial velocities is not guaranteed. (Gaia Collaboration et al., 2018; Katz et al., 2019; Soubiran et al., 2018)

One more problem for us comes with negative parallaxes. DR2 contains parallaxes of faint bodies measured only few times and for many of them the parallax value listed in the processed data may be negative. According to Luri et al. (2018) the presence of these negative values is natural due to a linearised astrometric source model with which the Gaia observations are described. For sources with parallax close to zero it is expected to measure negative parallax for half of them. Gaia Collaboration et al. (2018) say that negative parallaxes are perfectly valid measurements, although we have to take special care with them and take into consideration possibilities of effective treatment of them with help from Luri et al. (2018).

2.1.3 Chosen Dataset

According to problematics of this thesis we have chosen data that define place and velocity of object in space. These are right ascension and declination, parallax, proper motion in right ascension and declination and at the end radial velocity. Their errors were also added to data. We have taken whole ranges of right ascension, declination, proper motions and radial velocities. First condition was range of parallax. As was written in Problems of data, parallax may be for some objects negative and we wanted to eliminate this problem. Therefore we have chosen only positive values of parallax. On the other hand we have wanted to prevent data contamination by huge errors in parallax, so we have chosen only those objects whose parallax errors were maximally 10 % of parallax values. The last condition was that all selected parameters were measured and have numerical value, because sometimes it happens that they are missing.

Chapter 3

Galactic Dynamics

3.1 Morphology and dynamics of Galaxy

The Milky Way is a barred spiral galaxy which consists of nucleus, bulge, disk, stellar halo and dark matter halo. In the galactic nucleus there is a supermassive black hole with thousands of millions solar masses and it is the site of wide range of wild activities powered by its main inhabitant. Measurements are indicating that it si very rich area in star occurance what has not been considered in the past. Its diameter is around 300 pc. The central bulge is nearly spherical extension of the galactic nucleus and primarily consists of Population II stars with nearly radial orbits around the nucleus. In this area we can also find several globular clusters. Its mass is estimated at $4 \cdot 10^{10} M_{\odot}$ and its effective radius is around 2000 pc. The galactic disk is the main part of our Galaxy where stars are born. Its radius is around 25 kpc and thickness varies with respect to different parts of disk, but its approximatelly 0.6 kpc. The galactic disk is divided to more specific parts according to age and type of stars. Over and under disk we can find the stellar halo which is extension of central bulge. Its almost spherical shape is home for outer globular clusters but also many individual field stars of Population II. The stellar halo extends to approximatelly 100 kpc from the galactic center. The latest found part of Galaxy is dark matter halo. It was found by its effect on the outer rotation of Galaxy, which was not consistent with model made by mass estimation of our Galaxy from visible matter. Its mass is estimated to be several times greater than the mass of the rest of the Galaxy and it exceeds approximately $500 - 600$ kpc from the galactic center. (Hodge, 2020)

In our Galaxy we may found around $250 - 500$ billion of stars. Among these stars is one very special for us and this star is the Sun. Its parameters in the Galaxy are included in all models of Milky Way Potential and are used as capture points. Sun's distance from the galactic center is around $7.86 - 8.32$ kpc with circular velocity approximately 230 km.s^{-1}. Sun's galactic rotation orbits takes 240 Myr and its escape velocity is 550 km.s^{-1}. (Wikipedia, 2020b)

When we connect composition of our Galaxy with types of stars in it, we can conclude that in different parts are different types of stars according to age, kinematics and metal abundance. We mainly divide them into disk and spheroidal star populations, in other words Population I and II. Population II consists of very old stars, sometimes old as our Galaxy and these stars mainly occur in spherical parts of our Galaxy - stellar halo, galactic

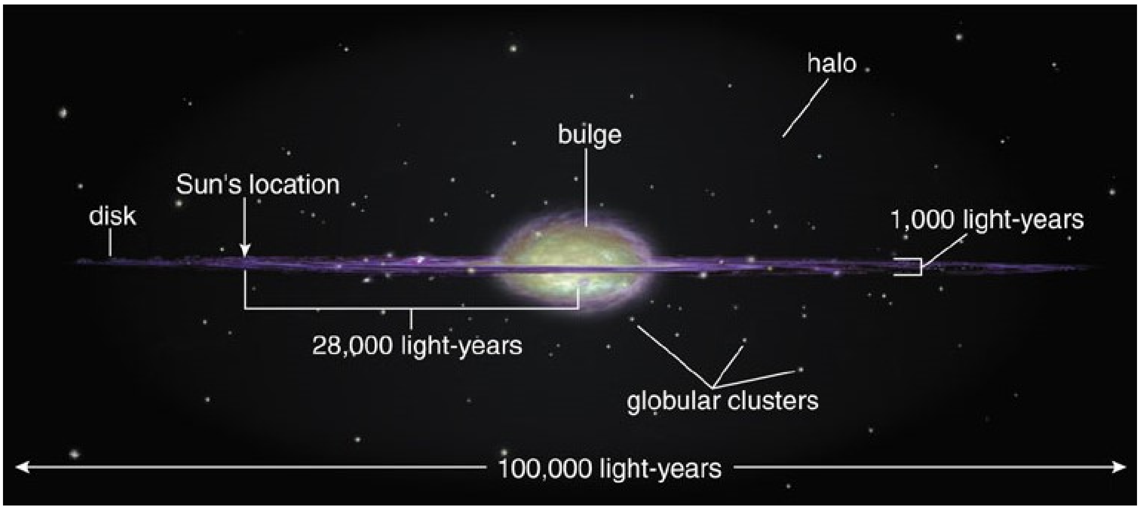

Figure 3.1: Anatomy of the Milky way. (Pearson Education, 2004a)

bulge and galactic nucleus. However we can find them almost everywhere in the Galaxy. Their trajectories are unclosed, very eccentric and they cross the galactic disk at random angles. Their orbits are main reason why they are for us among high-velocity stars, because according to orderly circulating stars of Population I, where Sun also belongs, their relative velocities are very high. Population I type stars are younger, but their age is different for different parts of the galactic disk. There are 4 distinct parts - the youngest, young, middle and old disk. According to their names we may conclude the age of stars found in them. These stars are orbiting center of Galaxy in one direction along almost circular trajectories and moreover in almost same plane, that is why we call them disk star population. This type of stars cannot be found in any other part of the Galaxy unless they encounter some massive object which cause velocity kick so high that they run away from their place of origin. These are stars we are interested in.(Mikulášek & Krtička, 2005)

3.2 Python Packages for Galactic Dynamics

3.2.1 Introduction

Gala is an Astropy-affiliated Python package for galactic dynamics. Python flexibility and user-friendly interface also enable implementation of low-level languages(C) for speed and thus its application is beneficial. Therefore Gala is easy to use and efficient helper for calculations focused on galactic dynamics.(Price-Whelan, 2017)

Benefits of the package Gala include commonly used Galactic gravitational potentials, extensible and easy to define new potentials, extremely fast orbit integration (parts implemented in C), precise integrators, easy visualization and Astropy units support. (Price-Whelan et al., 2020)

During our research we came across another Python package for galactic dynamics called Galpy. This package is older than Gala and it appears little more complicated to use at the first sight, but their functions are very similar. Galpy has its own definition of Milky Way Potential called MWPotential2014 and it is composed of a bulge modeled as

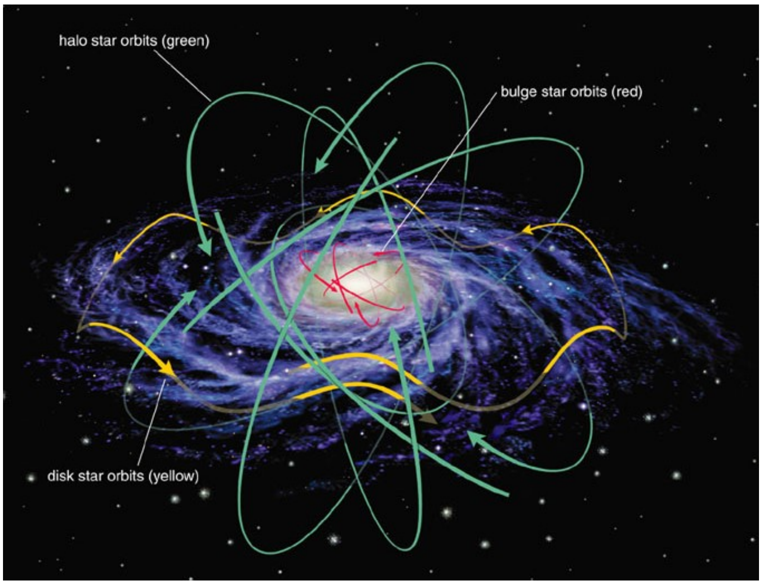

Figure 3.2: Orbits of stars in different regions of our Galaxy. (Pearson Education, 2004b)

a power-law density profile that is exponentially cut-off (PowerSphericalPotentialwCutoff) with a power-law exponent of -1.8 and a cut off radius of 1.9 kpc, a MiyamotoNagaiPotential disk, and a dark-matter halo described by an NFWPotential. The relative amplitudes for each part of the MWPotential2014 are fit to some measured data, for more info see Bovy (2015). Bovy (2015)'s potential is also available in Gala as BovyMWPotential2014.

Difference of Milky Way Potential defined in Gala and Galpy is mainly in measured data which where used for fitting the potential. But also in Gala there is forth component of Milky Way Potential, namely the nucleus potential. This is one of the reason why we have chosen Gala as an auxiliary package for galactic dynamics in our script. Whole definition of used Milky Way Potential is described in the following part.

3.2.2 Definition of used Milky Way Potential from Gala

Whole definition of MW Potential can be found at `https://gala-astro.readthedocs.io/en/latest/potential/define-milky-way-model.html` from where we drew information.

Milky Way Potential can be found in package Gala as an approximate mass model which parameters are obtained by least-squares method fitting the enclosed mass profile of a pre-defined potential form to recent measurements compiled from the literature. These data are shown in Table 3.1.

Pre-defined potential form is composed of four potentials each representing certain part of Galaxy namely nucleus, bulge, disk and halo. Parameters of the disk and bulge are chosen with respect to Bovy (2015). Parameters of the halo and nucleus where left free for least-squares fit of data from table.

Table 3.1: Measured data for the enclosed mass at some spherical distance from galactic center with errors and references. (Price-Whelan, 2020a)

r [kpc]	M_{enc} [10^{10} $M_{\odot}$]	M_{enc} error$_{neg}$ [10^{10} $M_{\odot}$]	M_{enc} error$_{pos}$ [10^{10} $M_{\odot}$]	References
0.01	0.003	0.001	0.001	Feldmeier et al. (2014)
0.12	0.080	0.020	0.020	Launhardt et al. (2002)
8.1	8.950	0.499	0.486	Bovy et al. (2012)
8.3	11.042	0.448	0.439	McMillan (2011)
8.4	10.242	1.673	1.547	Koposov et al. (2010)
19	20.802	4.432	3.483	Kuepper et al. (2015)
50	53.988	2.000	26.849	Wilkinson & Evans (1999)
50	52.989	1.000	3.854	Sakamoto et al. (2003)
50	39.991	10.998	7.270	Smith et al. (2007)
50	41.991	4.000	3.817	Deason et al. (2012)
60	39.991	6.999	6.434	Xue et al. (2008)
80	68.985	29.994	11.036	Gnedin et al. (2010)
100	139.970	89.981	83.134	Watkins et al. (2010)
120	53.988	19.996	12.385	Battaglia et al. (2005)
150	75.000	25.000	25.000	Deason et al. (2012)
200	67.985	40.991	31.365	Bhattacherjee et al. (2014)

```python
def get_potential(log_M_h, log_r_s, log_M_n, log_a):
    mw_potential = gp.CCompositePotential()
    mw_potential['bulge'] = gp.HernquistPotential(m=5E9, c=1., units=galactic)
    mw_potential['disk'] = gp.MiyamotoNagaiPotential(m=6.8E10*u.Msun, a=3*u.kpc, b=280*u.pc,
                                                      units=galactic)
    mw_potential['nucl'] = gp.HernquistPotential(m=np.exp(log_M_n), c=np.exp(log_a)*u.pc,
                                                  units=galactic)
    mw_potential['halo'] = gp.NFWPotential(m=np.exp(log_M_h), r_s=np.exp(log_r_s), units=galactic)

    return mw_potential
```

Figure 3.3: Definition of Milky Way Potential in Gala. (Price-Whelan, 2020a)

Bulge and nucleus are defined by Hernquist potential (Hernquist, 1990). Parameters of Hernquist potential which is used for spheroid are m = mass and c = core concetration.

$$\rho(r) = \frac{m}{2\pi c^3} \frac{c^4}{r(r+c)^3}, \tag{3.1}$$

where c and m are constants. (Ponman, 2013)

Disk is determined by Miyamoto-Nagai potential (Miyamoto & Nagai, 1975) which is potential for a flattened mass distribution. Its parameters are m = mass, a = scale lenght and b = scale height.

$$\rho(R,z) = \frac{b^2 m}{4\pi} \frac{aR^2 + [a + 3(z^2+b^2)^{1/2}][a + (z^2+b^2)^{1/2}]^2}{\{R^2 + [a + (z^2+b^2)^{1/2}]^2\}^{5/2}(z^2+b^2)^{3/2}}, \tag{3.2}$$

where $R = (x^2+y^2)^{1/2}$ and therefore $r = (R^2+z^2)^{1/2}$ is spherical distance from centre.

Last component of used Milky way potential is halo which is specified by Navarro-Frenk-White potential. Its defining parameters are m = mass and r_s = scale radius. (Wikipedia, 2020c)

$$\rho(r) = \frac{\rho_0}{\frac{r}{r_s}\left(1+\frac{r}{r_s}\right)^2} \tag{3.3}$$

```
# Initial guess for the parameters- units are:
#     [Msun, kpc, Msun, pc]
x0 = [np.log(6E11), np.log(20.), np.log(2E9), np.log(100.)]
init_potential = get_potential(*x0)
```

Figure 3.4: Initial guess of free parameters of MW potential. (Price-Whelan, 2020a)

For free parameters of nucleus and bulge potentials was firstly made initial guess which we can see on the Figure 3.4. On the Figure 3.5 we can see plot of potential with intial guess and measured data with their errors from table. We can notice that potential with initial guess of free parameters is fitting very nicely over the data already. Subsequently was used least - squares fitting to optimize free parameters. Thus defined Milky Way Potential is available in the package Gala after using command 'from gala.potential import MilkyWayPotential'.

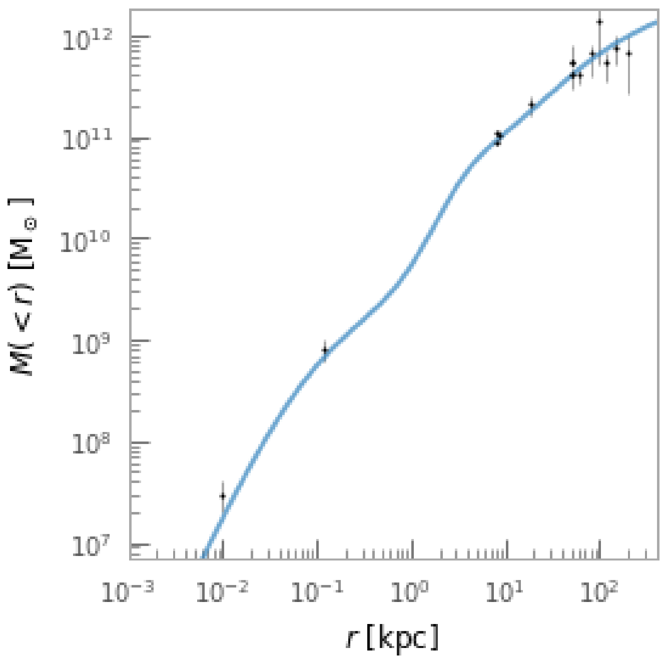

Figure 3.5: Plot of MW potential with intial guess and measured data with their errors from table. (Price-Whelan, 2020a)

Finally we have made plots of equipotentials contours of Milky Way Potential in 2D sections.

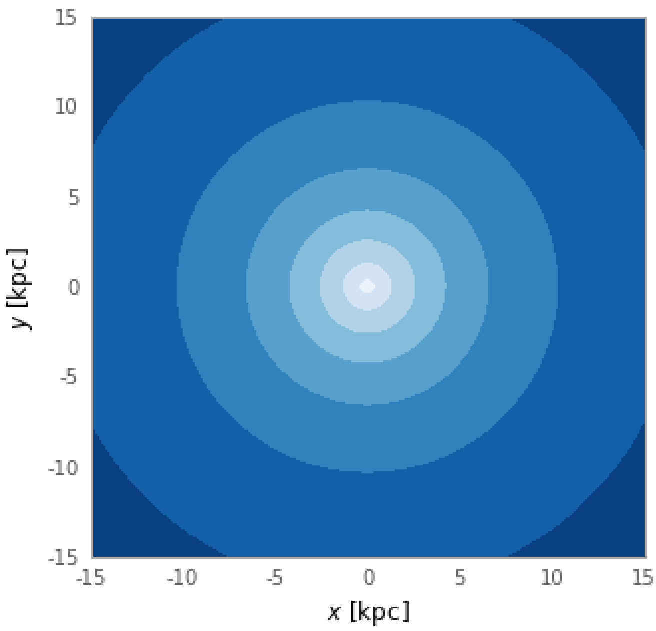

Figure 3.6: Equipotentials contours of MW Potential in xy-plane where z=0.

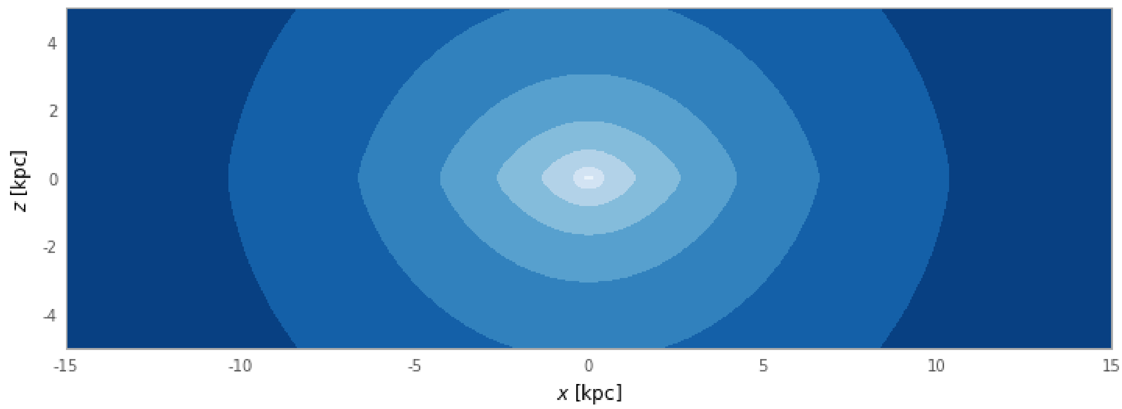

Figure 3.7: Equipotentials contours of MW Potential in xz-plane where y=0.

3.2.3 Functions used in script

In addition to used Milky Way Potential we used other 2 functions from Gala and these are Hamiltonian and PhaseSpacePosition. PhaseSpacePosition clearly represents phase-space positions of objects which are subsequently used as initial conditions for integration. In our script galactocentric cartesian coordinates were used for representation of phase-space positions. (Price-Whelan, 2020d)

Hamiltonian is firstly used to represent a composition of a gravitational potential, in our case Milky Way Potential. After defining Hamiltonian for our potential we used function Hamiltonian.integrate_orbit() where we gave it initial conditions and specifications of how long to integrate. For static frames is generally used LeapfrogIntegrator. If a function for computing time derivatives of the phase-space coordinates is given then integrator computes the orbit at specified times. (Price-Whelan, 2020b,c)

Leapfrog integration is a second-order method for numerically integrating differential equations of the form

$$\frac{\mathrm{d}^2x}{\mathrm{d}t^2} = A(x), \tag{3.4}$$

which can be rewrited as

$$\frac{\mathrm{d}v}{\mathrm{d}t} = A(x), \; \frac{\mathrm{d}x}{\mathrm{d}t} = v. \tag{3.5}$$

Leapfrog integration (Wikipedia, 2020a) is equivalent to updating positions and velocities at interleaved time points, staggered in such a way that they 'leapfrog' over each other. The equations for updating position and velocity are

$$a_i = A(x_i) \tag{3.6}$$
$$v_{i+1/2} = v_{i-1/2} + a_i \Delta t \tag{3.7}$$
$$X_{i+1} = x_i + v_{i+1/2} \Delta t \tag{3.8}$$

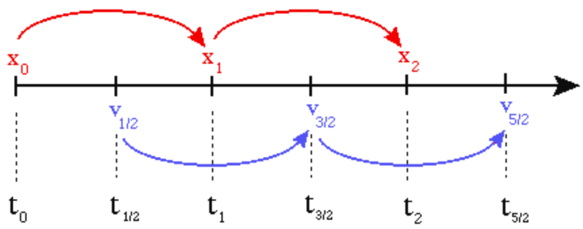

Figure 3.8: Picture showing the structure of the leapfrog method. (McMillan, 2019)

Two benefits of this method are time-reversibility nad symplectic behaviour which means it conserves energy of dynamical system.

Chapter 4

Orbits of hypervelocity stars

4.1 Results of the integration

Firstly, we have to point out that from conditions required for data written in Chosen dataset we got $5,393,494$ objects, from which $2,877,142$ is with negative radial velocity and $2,516,352$ objects have positive radial velocity. In the script we firstly integrate stars to future during 100 Myr with step 0.001 Myr and we set condition that we want just objects that in this timescale reach minimal spherical distance from radius 30 kpc. This condition was set to eliminate normal stars rotating in galactic disk and of course bulge and halo stars since almost 90 % of galactic halo objects is within 30 kpc from centre. After integration we end up with 904 candidates on high velocity object, from which 442 objects were with negative radial velocity and 462 with positive.

Even though there are tons of articles with different methods how to choose those unbound objects, we have chosen to analyze every orbit to understand what is really going on and to get deeper into the topic. We were interested in trajectory shapes and we wondered whether there is some special characteristic according to which we can classify these objects. After seeing 904 trajectories we came to a conclusion that we can somehow put them into classes.

We mainly noticed that there are several objects orbiting in the disk plane but unlike normal disk stars their orbits are eccentric. When we think about populations of stars, we may wonder what is chance of them being only members of Population I. We admit an idea that these stars may be runaway stars from disk which were created in such act that gave them energy kick only in x or y axis and therefore they stayed orbiting in the disk but not with the traditional almost round orbits. In some articles was written that origin of stars may be found in apocenter or in pericenter of object's orbit. Since this was not the goal of our thesis we are just proposing this to be possible future topic for some article. Even though it would not be easy work to collect all positions of apocenters and pericenters and look for possible origins but it is definitely worth the effort.

There is also group that goes farther away from center and are 'almost unbound' and 'unbound' objects. These names are just makeshift. We have noticed that there are trajectories that are coming back for the first time after long run from center and we called them almost unbound just to emphasize that they are coming back for the first time in 100 Myr. Second group is called unbound just to show that they are still running from center. Here we have to be very careful and we have to define our own definition of 'unbound' star. Therefore we have decided to make new integration and we have increased time of integration to 10 Gyr. More than half of them stayed unbound and therefore we report 50 unbound objects, 27 with negative radial velocity and 23 with positive.

The creation of last group was not pleasant and this group contains all objects that were left. Their trajectories are chaotic and therefore there is no special sign to be found to classify them. If we want to analyze them more we will need more data about their characteristics, mainly their metalic abundance to determine their Population type. For Population I there would be purpose to look for their apocenters and pericenters to find their origin, but as we have written when we were introducing disk objects, this process is very time consuming and very difficult.

In sections Sample Orbits and Tables we use first division according to pattern of orbit during integration to 100 Myr, while in section Unbound we work only with those unbound objects which stayed unbound even after integration to 10 Gyr.

4.1.1 Samples of Orbits

This part of thesis is present to show samples of orbits according to which we were classifying objects and to clear thoughts behind decisions.

4.1.1.1 Unboud Group

First group is called unbound according to trajectory which does not appear to close and come back to center from where it is coming. Often their spherical distance from galactic centre exceeds hundreds of kpc. Orbits of samples made from normal distribution of position and velocity errors are made only to inform us about their size of impact and to count with them when we need to analyse precision. This type of orbit is beautifully determined by relation of spherical distance from galactic center on time. We can see that it is growing function back to past and it would be similar to future.

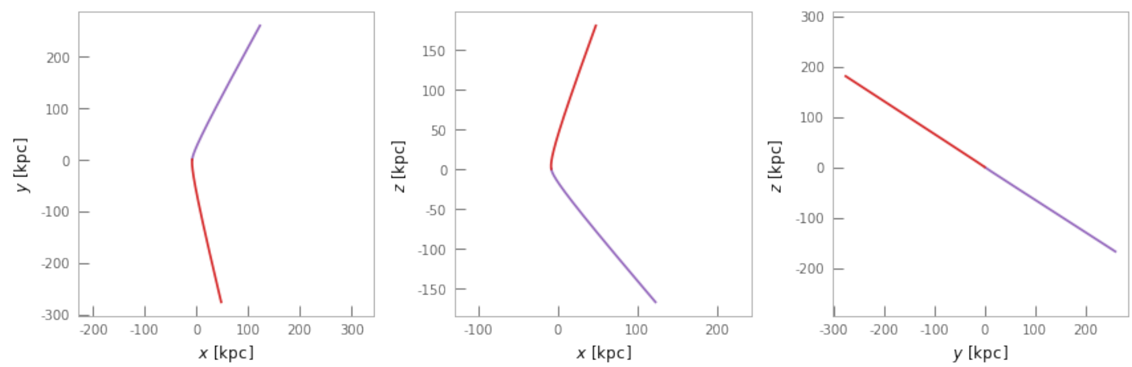

Figure 4.1: Orbit of one of objects falling to group called unbound during 100 Myr to future(purple) and 100 Myr to past(red).

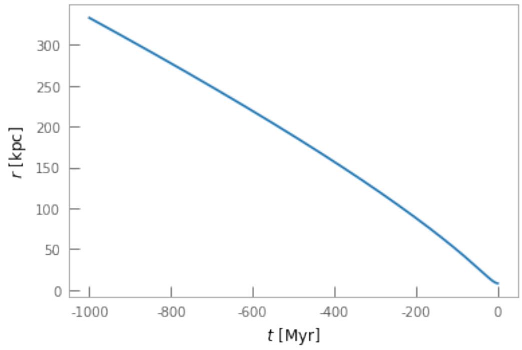

Figure 4.2: Relation between spherical distance from galactic center and time of integration.

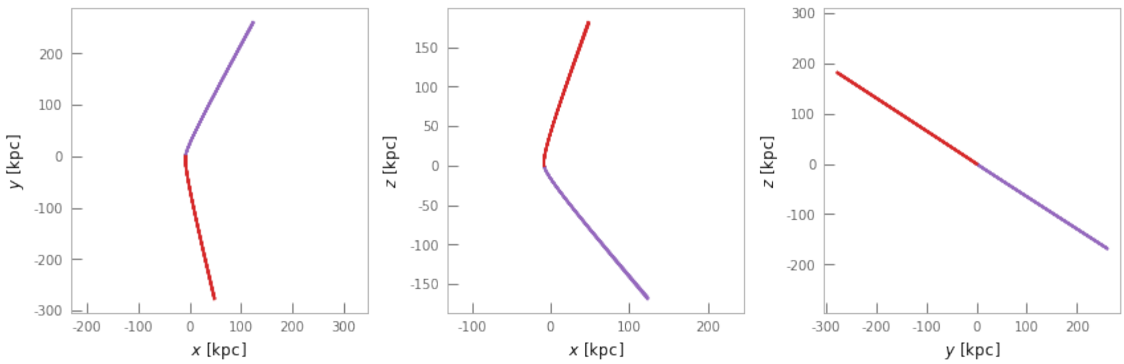

Figure 4.3: Orbit of one of objects falling to group called unbound with counted errors during 100 Myr to future(purple) and 100 Myr to past(red). As we can see in this particular case errors are not so long.

4.1.1.2 Almost Unbound Group

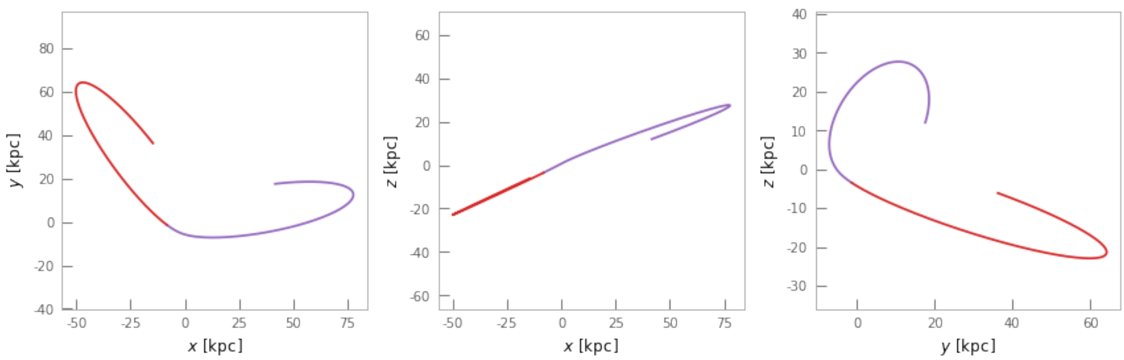

Figure 4.4: Orbit of one of objects falling to group called almost unbound during 100 Myr to future(purple) and 100 Myr to past(red).

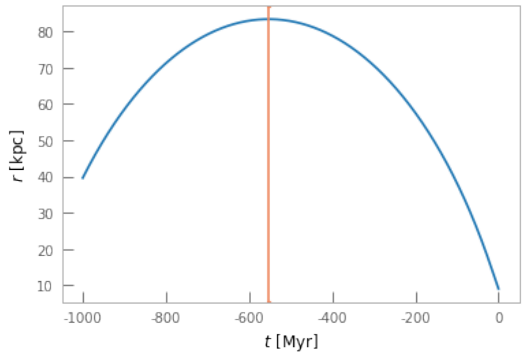

Figure 4.5: Relation between spherical distance from galactic center and time of integration.

Special sign of this group is that orbits are starting to close for the first time during 100 Myr. Objects usually reach more than 50 kpc and we can expect that they have high velocity according to distance to which they get. Therefore this group with Unbound group is worth studying, because they have high velocities assumed by huge reached spherical distance from centre. Particularly in this group errors are very important because as we can see on Figure 4.5, sometimes it reveals high inaccuracy of measurents and these objects should be treated with special care. Errors also cause larger range of pericenter, apocenter and eccentricity values. Histograms are clear indicators od accuracy of measurements.

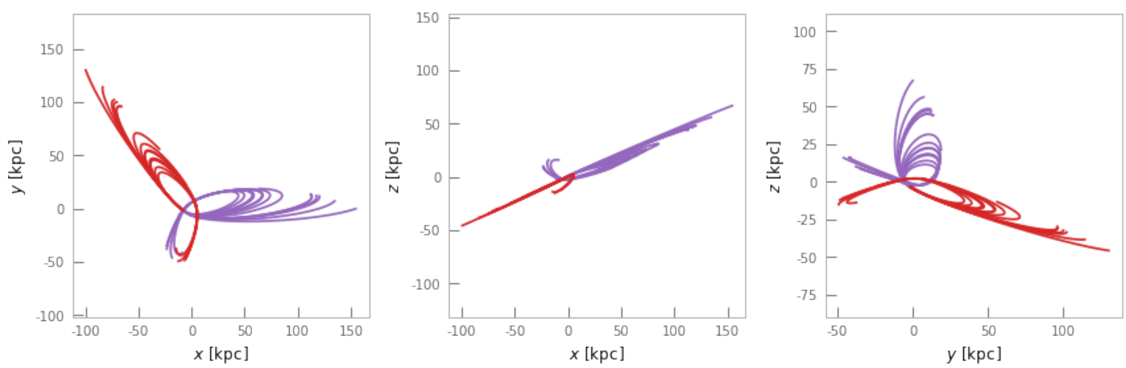

Figure 4.6: Orbit of one of objects falling to group called almost unbound with counted errors during 100 Myr to future(purple) and 100 Myr to past(red). As we can see in this particular case errors caused also already closed orbits.

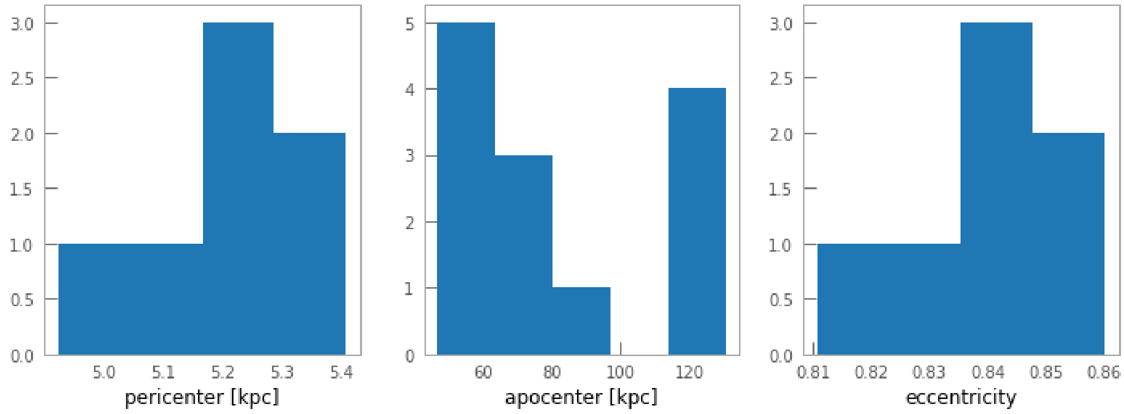

Figure 4.7: 3 histograms showing numbers of specific values of pericenter, apocenter and eccentricity appearing in orbits containing counted errors.

4.1.1.3 Disk Group

Disk group is special because of reasons why it was created. Reasons are mainly connected with Population type of stars. While studying high velocity stars it is convenient to focused on Population I type of stars because as they are naturally located in galactic disk, it is unnatural to found them somewhere over galactic plane. But what if they orbit near the disk but on highly eccentric trajectories which exceeds around 30 – 40 kpc. This is what hit our minds and we assume that these objects may be Population I type which were kicked by some event from place where they originated with high velocity distributed only in the direction of the disk plane. We discussed early that it would be worth it to find places of possible apocenters and pericenters to find place and cause of this high velocity object. Unfortunately problems are mainly in an insufficient knowledge about high mass objects in our Galaxy and in multiplicity of places of apocenters and pericenters due to rotation of orbit.

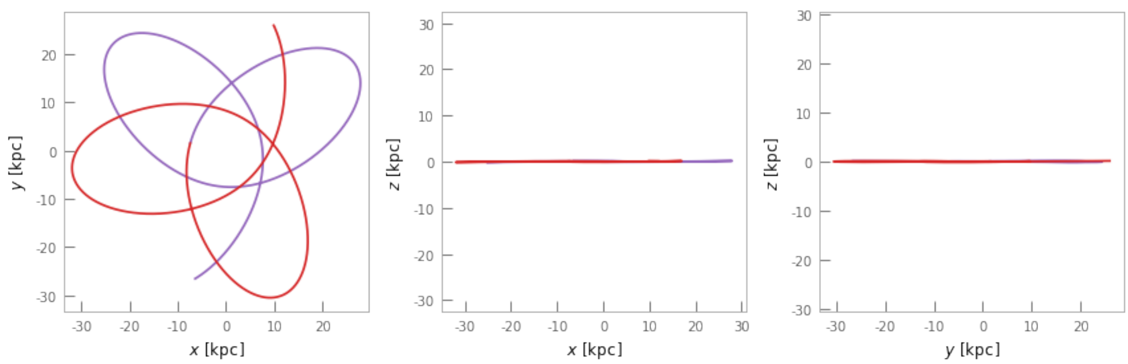

Figure 4.8: Orbit of one of objects falling to group called disk during 100 Myr to future(purple) and 100 Myr to past(red).

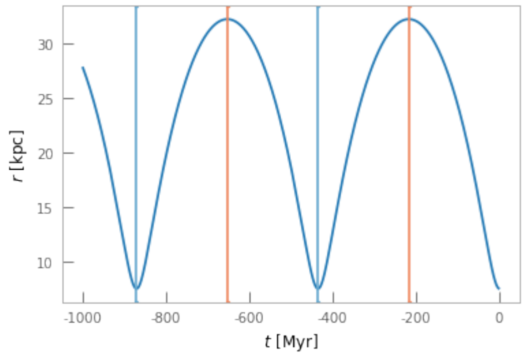

Figure 4.9: Relation between spherical distance from galactic center and time of integration.

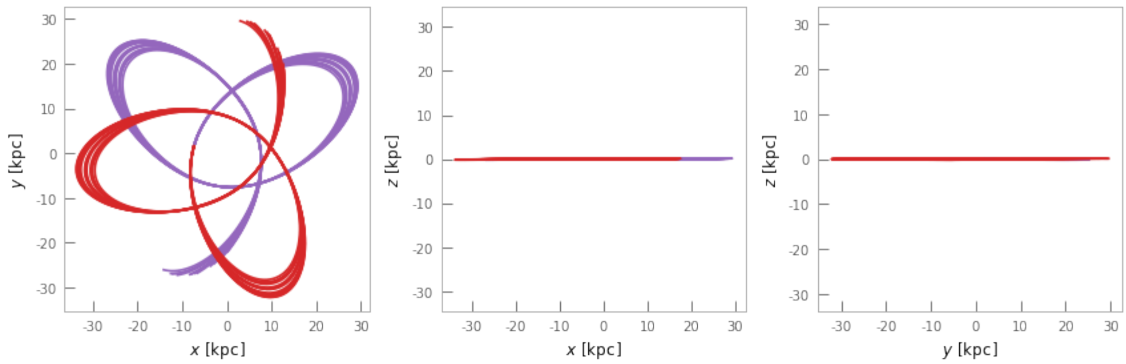

Figure 4.10: Orbit of one of objects falling to group called disk with counted errors during 100 Myr to future(purple) and 100 Myr to past(red).

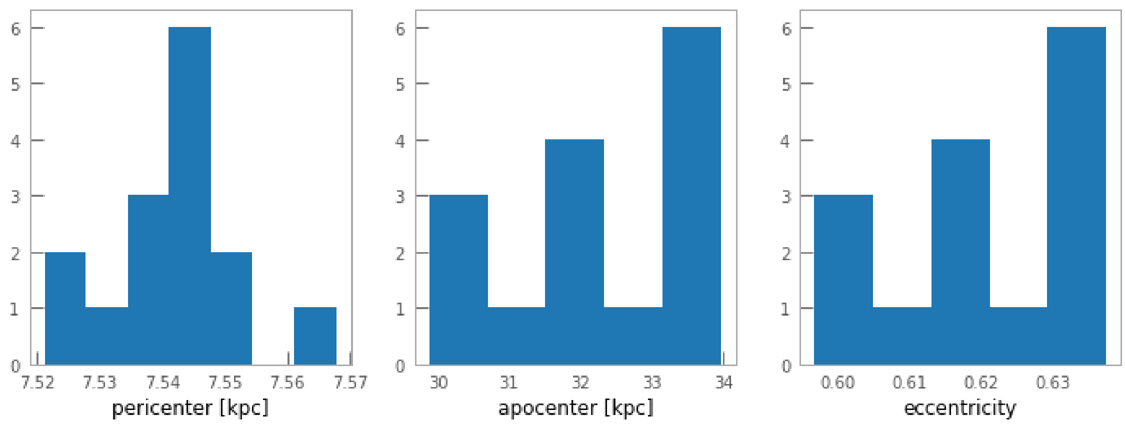

Figure 4.11: 3 histograms showing numbers of specific values of pericenter, apocenter and eccentricity appearing in orbits containing counted errors.

4.1.1.4 Chaotic Group

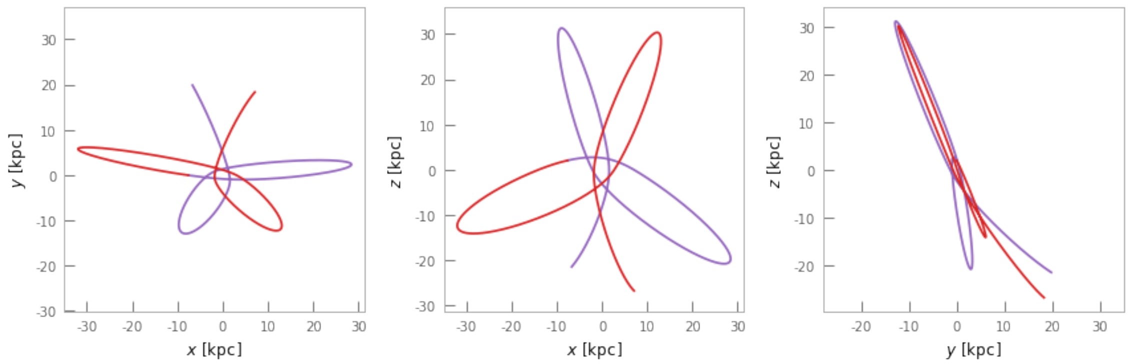

Figure 4.12: Orbit of one of objects falling to group called chaotic during 100 Myr to future(purple) and 100 Myr to past(red).

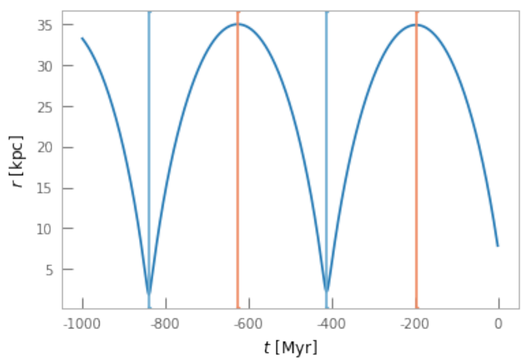

Figure 4.13: Relation between spherical distance from galactic center and time of integration.

Chaotic group contains leftovers from creation of first three groups. These orbits are highly eccentric and may cross disk plane at various angles so from their look we cannot specify nothing particular. These objects can belong to any type od Population type and looking for places of apocenters and pericenters appears very complicated. We are not sure wheter it is worth it to deal with this group for anyone. We just propose to analyze ratio of metals to specify their Population type and then it would be worth considering searching for their origin.

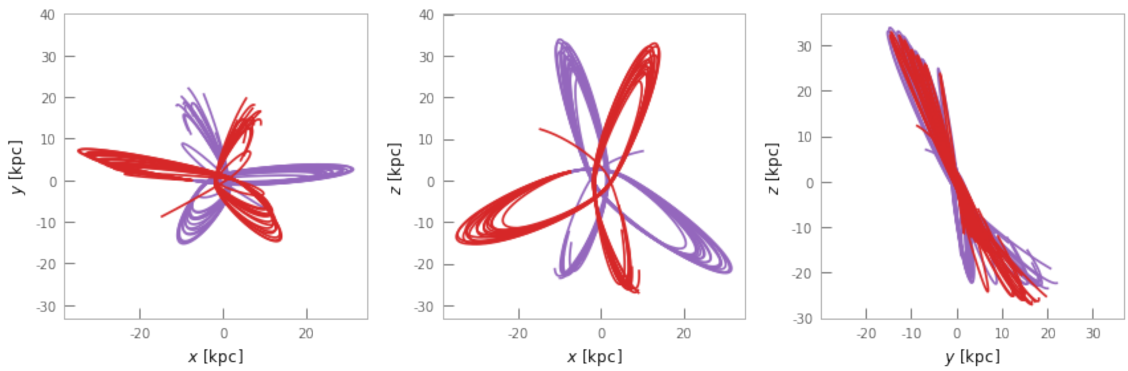

Figure 4.14: Orbit of one of objects falling to group called chaotic with counted errors during 100 Myr to future(purple) and 100 Myr to past(red).

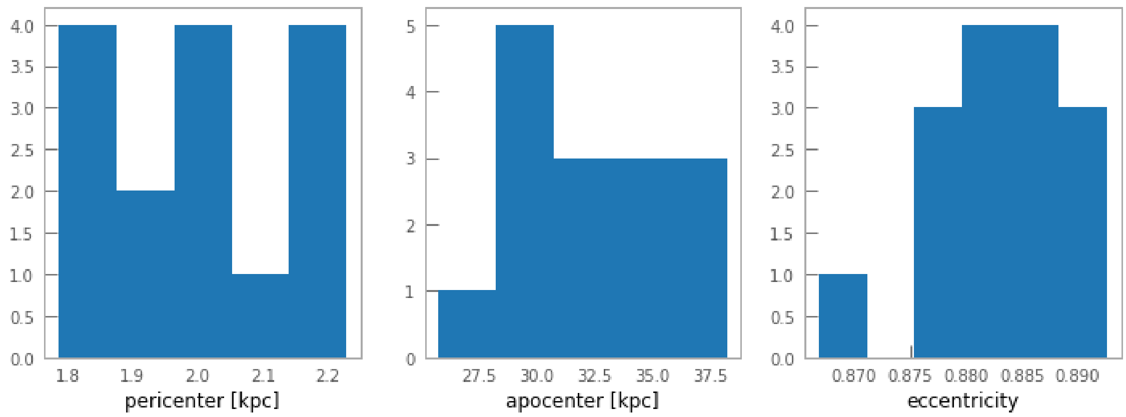

Figure 4.15: 3 histograms showing numbers of specific values of pericenter, apocenter and eccentricity appearing in orbits containing counted errors.

4.1.2 Trials of orbits - runaway stars

Mainly because of disk and chaotic orbit objects, we have made some trial orbits for runaway stars. As a capture point we have chosen position in galactic disk 8 kpc from galactic center, where we expect orbiting velocity 220 km.s^{-1} - inspired by Sun. Subsequently we were integrating orbits while we were changing some parameters of velocities. We were working with galactocentric cartesian coordinates. So we have chosen position at $x = -8$ kpc and y and z equal zero. Then we have set expected orbiting velocity $v_y = 220\,\mathrm{km.s}^{-1}$. Pictures of orbits are to be found in Appendix A with comments about changed parameters. We have been changing velocity components to get an idea of how orbits of kicked stars look like depending on the direction of the kick.

From trial orbits we may conclude that many of patterns of higher changes in velocity were found within orbits of chaotic and disk group. So we cannot exclude any pattern from possible candidates. For now we need to leave this problematics due to difficulty of issue. Currently it is smarter to study those objects whose spherical distance from center exceeds 50 kpc.

4.1.3 Tables

After analyzing orbits of all candidates for high velocity stars, we have decided to search for all these objects at Simbad catalogue and to find out what is known about these objects. We have created tables with found information to make a clear picture about these objects we have got from script. Objects are divided into tables according our first division to unbound, almost unbound, disk and chaotic orbit groups. Tables can be found in Appendix B.

Very shocking fact was that there are objects that were not identified by Simbad. We think that these are objects not yet found on the map to be identified as star, so therefore they are not included in catalogue for now. These objects do not have any specific information about them, only those measured by Gaia. Because of them we created special column which says wheter this object is found in Simbad catalogue.

Another group which was often found was that this object is only measured by Gaia but it is found on the map and therefore is identified as Star. These objects do not have any other data about them.

Lastly we found objects that were measured by other missions and therefore have different names, they may be identified as specific type of star and also some of them have specified group of stars to which they belonged or still belong. Because of these data we were doing this research to see how much are these data contamined by Population II and to find frequent types of stars. Firstly we thought that there would be a lot of hypervelocity stars, but we really have not found any. Limitations of Gaia's spectroscopy are the most possible reason.

Every group is divided according to sign of radial velocity. 'Unboud' group with negative radial velocity consists of 23 not found objects and 27 identified stars. These found objects consist of 7 High proper-motion Stars, 1 High-velocity Star, 1 Peculiar Star and finally 18 not specified Stars. For group with positive radial velocity applies that only 9 objects are not found. 30 stars are divided into 2 Higher proper-motion Stars, 26 not classified Stars and 2 objects which are not expected to be included here. One is possible Star of RR Lyr type and second is Variable Star of RR Lyr type which are classified as Population II. But since we have made another test to confirm unboudness of these objects we found out that these RR Lyr type stars have disappeared from this group and they are not really unbound. Main cause of occurence of these stars are high errors in measurents.

Second group called 'Almost Unbound' has not very different results. For negative radial velocity we have 30 not found and only 16 found objects. We can find among them 7 High proper-motion Stars, 1 Peculiar Star and 8 Stars. Between objects with positive radial velocity there is more found objects -25- and 21 not found. Among found stars are 15 High proper-motion Stars, 1 Peculiar Star and 9 Stars.

Following group is very interesting to analyze because if our assumption will be confirmed for these data, it would be possible for these objects to be mostly of Population I type. Of course nothing is for 100 percent always true. Even between groups with different radial velocity it is not different. For negative radial velocity we have 23 not found and same amount of found objects. New types of stars appeared among the found objects - 2 Spectroscopic binaries, 1 Variable Star of RR Lyr type and 1 Variable Star of RS CVn type. Another types are 12 High proper-motion Stars, 1 Peculiar Star and 6 Stars. Positive radial velocity group contains 34 not found and 27 objects. New type of stars appeared also here and it is 1 Be Star and 2 Emission-line Stars. Among rest we can find 1 Spectroscopis binary, 2 Variable Stars of RR Lyr type, 1 Peculiar Star, 14 High proper-motion Stars and 6 Stars. Reasons why Population II type stars appeared in Disk group may be mainly caused by selected insufficiently small height above plane of the disk during orbit or high errors in position and velocity parameters. So we propose to upgrade these criteria when choosing objects for Disk group to confirm or deny our proposal.

Last group called Chaotic have so much members that we just used those found to bring closer results of our survey. Among negative radial velocity objects there are 171 not found and 129 found. Found stars consists of one new type - 1 Horizontal Branch Star - and others contain 60 High proper-motion Stars, 56 Stars, 2 Spectroscopic binaries, 1 High-velocity Star, 4 Variable Stars of RR Lyr type and 5 Peculiar Stars. Within positive radial velocity group can be found 136 stars and 180 are not identified. New types of stars appeared again - 2 Red Giant Branch Stars and 1 Variable Star. Others types contain 3 Peculiar Stars, 56 High proper-motion Stars, 70 Stars, 3 Variable Stars of RR Lyr type and 1 Spectroscopic binary.

From these findings we can see that most of Stars are High proper-motion Stars and not specified Stars. Unfortunatelly we can not specify how many of all stars are Population II, but at least we can notice that among found type are Variable Stars of RR Lyr type which are taken as Population II and we can conclude that we cannot avoid this type of Population until we do not have their metal abundance. Therefore it is very important to measure and analyse types of stars to use their data for futher research.

4.2 Unbound stars intersecting the galactic disk

This part is dedicated to new definition of unbound star. We consider star to be unbound if its trajectory during integration to 10 Gyr still heads from Galaxy. From firstly selected 89 unbound stars we are left with 50 stars - 27 with negative radial velocity and 23 with positive.

We have made pictures of orbits for all of them and also with usage or errors. These pictures are to be found in zip file named ’unbound.zip’.

We have made tables with positions of galactic plane crossings and time it happened. We have find 4 types of crossings. First group have common only one crossing which happened in the past, these stars are most likely members of our Galaxy kicked from somewhere in the disk or nuclues. Another group have 2 crossings in the past. These also may be either from the Galaxy or can be extragalactic. Special extragalactic group is with only one crossing in the future. These are definitely extragalactic if their errors are not too big. Last group consist of 2 crossings, one in the past and one in the future. This group is similar to group with two crossings in the past and we cannot say with certainty whether they are extragalactic or from the Galaxy.

We can only try to analyse places of crossings and decide whether it is close enough to Sun to determine massive objects which could cause these high-velocity objects since most objects in our Galaxy are still not found because of bad observational conditions caused by extiction.

Data in tables and on the pictures are from orbits in static frame in galactocentric coordinates and they were not changed yet for comparing with other galactic objects.

For galactocentric coordinates we used is exactly defined position of the Sun which is always on the negative x-axes for any time. Rotating of coordinates is explained in next section where we will compare corrected positions of crossings from the past with some exotic objects measured in our Galaxy.

4.2.1 Negative radial velocity

Within group with negative radial velocity we have 4 stars with one crossing in the past, 2 stars with 2 crossings in the past, 14 stars with 1 crossing in the future and 7 stars with 1 crossing in the past and 1 crossing in the future. In the tables we may see galactocentric cartesian coordinates of crossings and time which has passed or will pass to cross the disk. We may assume that 14 stars with one crossing in the future are possibly extragalactic objects running through our Galaxy. When we compare this to objects with positive radial velocity there are only 3 from 23. We may see that different sign of radial velocity have different ratio between galactic objects and extragalactic ones.

Table 4.1: Places of crossing of the galactic disk for stars with only one crossing in the past.

Gaia DR2	X-cross [kpc]	Y-cross [kpc]	Time [Myr]
1598160152636141568	−2.926	6.437	−12.267
5878409248569969792	−7.525	−0.813	−0.735
6505889848642319872	1.433	1.218	−12.870
1552278116525348096	4.888	2.444	−22.502

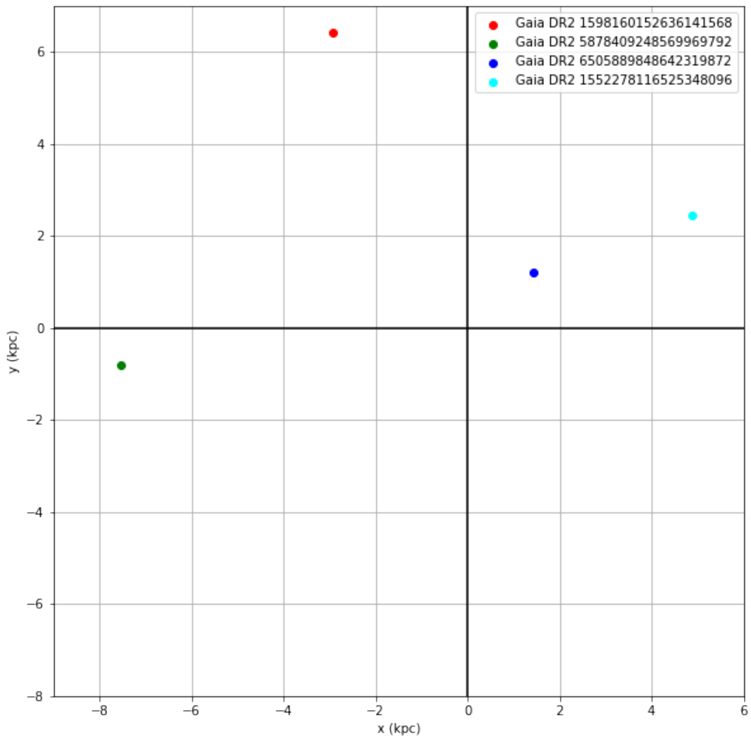

Figure 4.16: Places of crossing for stars with only one crossing in the past.

Table 4.2: Places of crossing of the galactic disk for stars with two crossing in the past.

Gaia DR2	X-cross [kpc]	Y-cross [kpc]	Time [Myr]	X-cross [kpc]	Y-cross [kpc]	Time [Myr]
2629296824480015744	−5.940	0.762	−3.281	42.301	−0.627	−95.586
5966712023814100736	−6.825	−0.362	−0.064	26.682	−13.801	−34.784

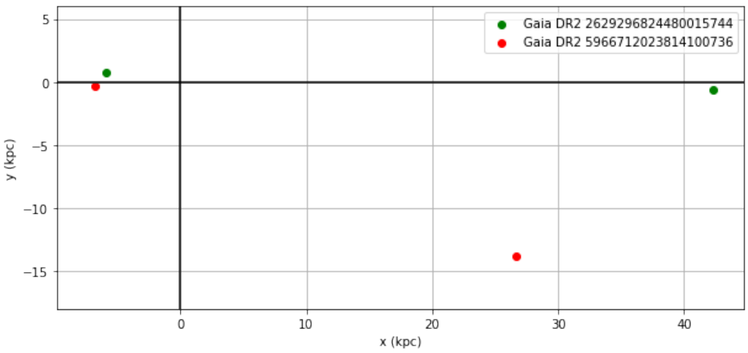

Figure 4.17: Places of crossing for stars with two crossing in the past.

Table 4.3: Places of crossing of the galactic disk for stars with one crossing in the past and one in the future.

Gaia DR2	X-cross [kpc]	Y-cross [kpc]	Time [Myr]	X-cross [kpc]	Y-cross [kpc]	Time [Myr]
4065480978657619968	2.683	−0.958	−13.938	−8.166	0.125	0.730
4103096400926398592	0.232	−0.016	−8.522	−21.434	1.459	21.565
5931224697615320064	12.577	−13.709	−32.862	−8.039	0.937	3.878
5953456066818230528	22.579	−11.241	−45.121	−7.427	0.086	1.228
5932173855446728064	9.861	−11.976	−26.376	−8.995	1.503	5.175
5956359499060605824	10.013	−6.318	−27.650	−8.328	0.295	1.261
5916830097537967744	107.613	−61.874	−326.925	−7.655	0.738	4.046

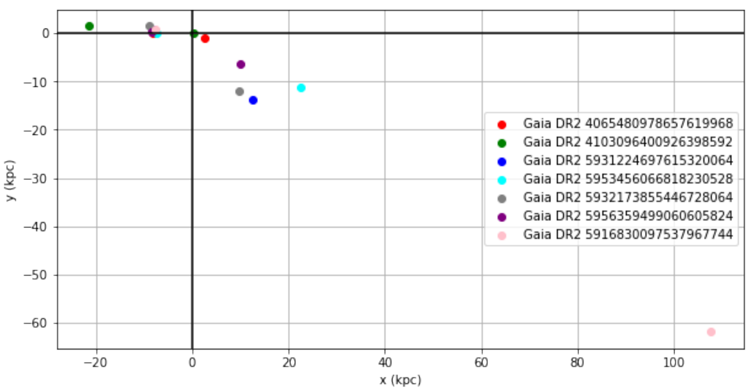

Figure 4.18: Places of crossing for stars with one crossing in the past and one in the future.

Table 4.4: Places of crossing of the galactic disk for stars with only one crossing in the future.

Gaia DR2	X-cross [kpc]	Y-cross [kpc]	Time [Myr]
5951114420631264640	−8.034	0.231	0.958
3793467471202249472	−8.095	0.027	0.108
5716044263405220096	−8.318	0.316	3.061
5253575237405660160	−8.610	1.707	4.750
6385725872108796800	−6.346	−3.662	5.639
5412495010218365568	−8.118	0.348	1.686
5672759960942885376	−8.116	0.739	2.766
5305975869928712320	−9.315	3.627	6.730
3006234119426679936	−8.114	0.289	1.255
2233912206910720000	−8.251	3.501	1.569
2041630300642968320	−8.111	0.043	0.215
6397497209236655872	−0.846	−0.912	9.033
1995066395528322560	−8.154	0.460	1.326
5231593594752514304	−8.099	0.019	0.087

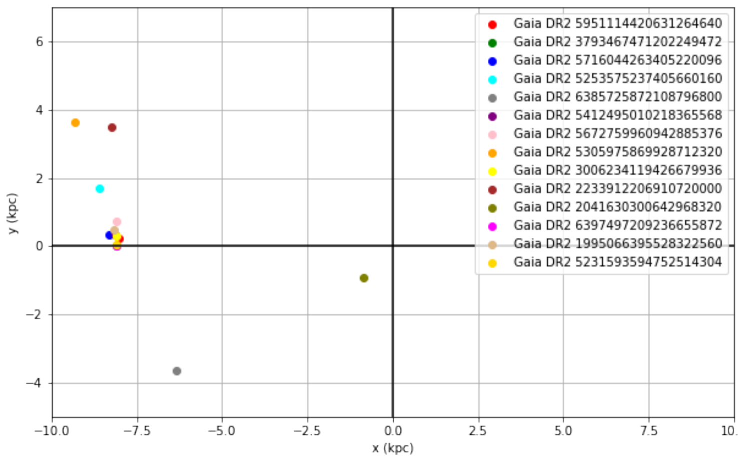

Figure 4.19: Places of crossing for stars with only one crossing in the future.

4.2.2 Positive radial velocity

Within group with positive radial velocity we have 15 stars with one crossing in the past, 1 star with 2 crossings in the past, 3 stars with 1 crossing in the future and 4 stars with 1 crossing in the past and 1 crossing in the future. In the tables we may see galactocentric cartesian coordinates of crossings and time which has passed or will pass to cross the disk. In this group is higher number of stars crossing one time disk in the past and lot of them are very close to each other. We may assume they may have the same place of origin. Even placement how they go on after another is almost identical with time when they were crossing the disk. Is this coincidence or do they have same place of origin? Is there object which kicks stars from galactic plane? We have to highlight that even from different groups there is some stars which cross plane near this place. 2 are from group with one crossing in the past and one in the future and that only star which cross the plane 2 times in the past has one of crossings near this place. This place is very strange and is worth studying.

Table 4.5: Places of crossing of the galactic disk for stars with only one crossing in the past.

Gaia DR2	X-cross [kpc]	Y-cross [kpc]	Time [Myr]
413902566644674432	−8.160	−0.140	−0.881
2251311188142608000	−8.105	−0.113	−0.461
5195254636665583232	3.708	0.398	−18.132
1752925794453337600	−8.095	−0.032	−0.158
4296894160078561280	−8.019	−0.143	−0.944
1825842828672942208	−7.980	−0.076	−1.560
1774513537034328704	−8.101	−0.051	−0.233
1732532430739244544	−8.077	−0.086	−0.479
4076739732812337536	−6.357	−0.076	−1.609
1949388868571283200	−8.109	−0.208	−0.780
3252546886080448384	−9.988	0.821	−2.618
6101408687905214208	−8.027	−0.292	1.042
5482348392671802624	4.342	0.626	−25.645
2099408640243333632	−8.090	−0.012	−0.096
1334468195956624768	−8.084	−0.121	−0.592

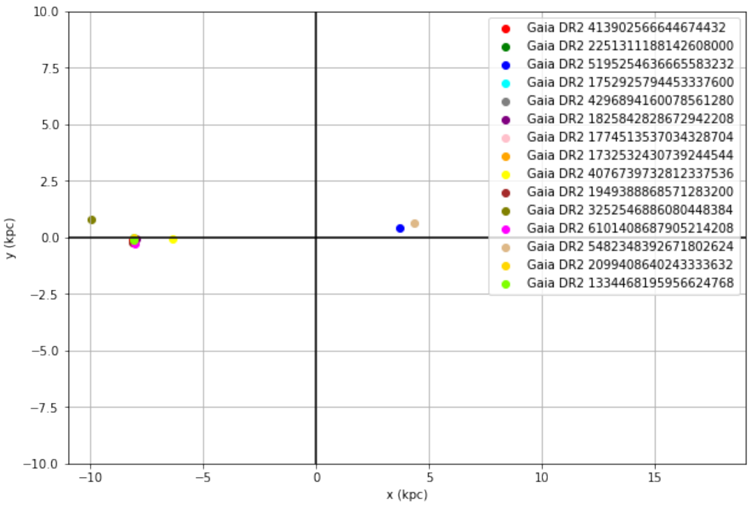

Figure 4.20: Places of crossing for stars with only one crossing in the past.

Table 4.6: Places of crossing of the galactic disk for stars with two crossing in the past.

Gaia DR2	X-cross [kpc]	Y-cross [kpc]	Time [Myr]	X-cross [kpc]	Y-cross [kpc]	Time [Myr]
939821616976287104	−8.100	−0.022	−0.092	150.330	−22.948	−363.782

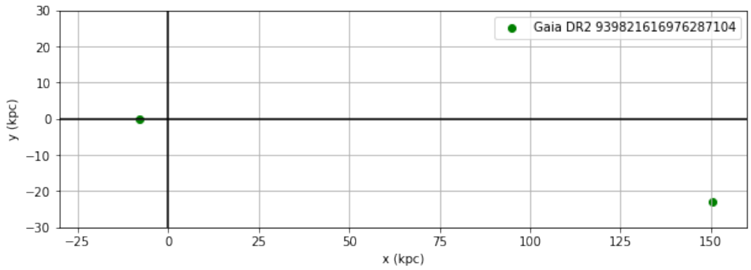

Figure 4.21: Places of crossing for stars with two crossing in the past.

Table 4.7: Places of crossing of the galactic disk for stars with one crossing in the past and one in the future.

Gaia DR2	X-cross [kpc]	Y-cross [kpc]	Time [Myr]	X-cross [kpc]	Y-cross [kpc]	Time [Myr]
4038969206316480512	−8.363	−0.357	−1.753	3.065	2.225	16.958
5212110596595560192	−52.179	−7.184	−97.583	3.581	−0.310	17.097
4150939038071816320	−8.147	−0.101	−0.366	13.174	10.295	33.926
5300505902646873088	−13.488	−6.594	−11.226	6.988	0.914	24.289

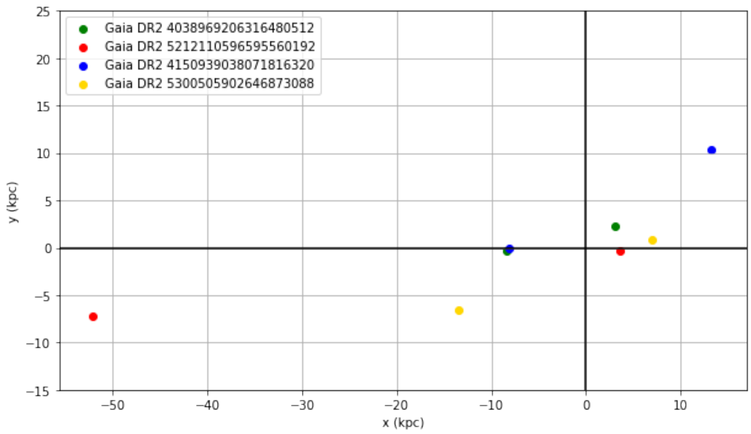

Figure 4.22: Places of crossing for stars with one crossing in the past and one in the future.

Table 4.8: Places of crossing of the galactic disk for stars with only one crossing in the future.

Gaia DR2	X-cross [kpc]	Y-cross [kpc]	Time [Myr]
3705761936916676864	3.247	−2.317	17.686
5212817273334550016	−9.958	−4.687	6.303
1042515801147259008	−13.307	−0.363	7.460

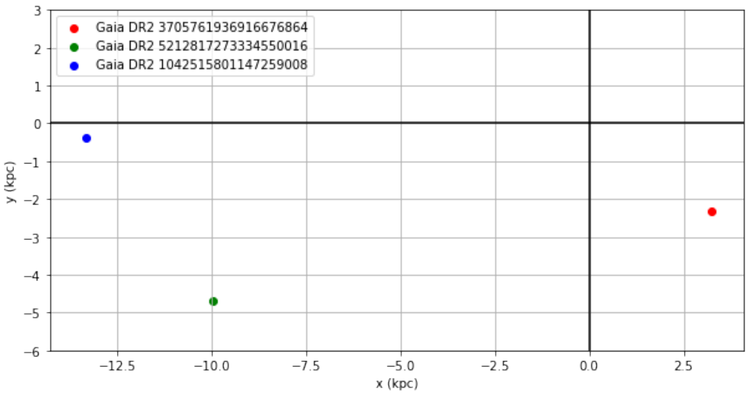

Figure 4.23: Places of crossing for stars with only one crossing in the future.

4.2.3 Looking for possible cause of ejection

Table 4.9: Places of (first) crossing of the galactic disk for stars in the past rotated according to their crossing time. In the last column there is absolute velocity which corresponds to velocity right after ejection.

Negative radial velocity			
Gaia DR2	$X_{\rm rot}$ [kpc]	$Y_{\rm rot}$ [kpc]	$V_{\rm int}$ [km.s^{-1}]
2629296824480015744	−6.005	1.657	607.033
1598160152636141568	−8.036	8.458	571.459
4065480978657619968	3.285	−4.946	739.768
4103096400926398592	0.140	0.209	866.484
5878409248569969792	−7.506	−0.655	898.631
5931224697615320064	100.006	−93.888	616.642
5953456066818230528	30.944	−29.715	610.544
5932173855446728064	42.901	−39.081	670.497
5956359499060605824	20.002	−22.808	607.973
5916830097537967744	175.275	−186.147	307.674
6505889848642319872	−1.231	−0.270	690.326
1552278116525348096	−0.183	−1.631	578.082
5966712023814100736	−6.825	−0.347	1041.440

Due to the integration of orbits within galactocentric coordinates in static frame we have got positions of crossings not corrected to the galactic rotation. So the easiest way how to correct positions of intersections is to rotate them with circular velocity corresponding to their position in the Galaxy during time which had passed from possible ejection from the galactic disk. So according to exact position of crossing we calculated circular velocity and divided into velocity components in x and y axis. The script with particular procedure can be seen in Appendix C. So we have exact position and velocity which is perpendicular to line connecting the galactic centre and position of intersection oriented in direction of rotation of Galaxy. While using the galactocentric coordinates we have to realize that position of the Sun lies always at negative side of x-axis. Intersections happened in the past, so when we take galactocentric coordinates of intersections from the orbits that mean that position of the Sun had to be rotated backwards. So the easiest way how to get right coordinates of crossings is to rotate them in the direction of the galactic rotation during time that had passed from ejection.

Table 4.10: Places of (first) crossing of the galactic disk for stars in the past rotated according to their crossing time. In the last column there is absolute velocity which corresponds to velocity right after ejection.(* before Gaia DR2 ID marks object with similar place of intersection of the galctic plane)

Positive radial velocity			
Gaia DR2	$X_{\rm rot}$ [kpc]	$Y_{\rm rot}$ [kpc]	$V_{\rm int}$ [km.s^{-1}]
*413902566644674432	−8.154	0.065	580.582
*2251311188142608000	−8.102	−0.005	957.606
*4038969206316480512	−8.335	0.040	545.995
5195254636665583232	0.973	−2.734	611.106
*1752925794453337600	−8.095	0.005	692.451
*939821616976287104	−8.100	−0.000	604.093
*4296894160078561280	−8.012	0.077	940.659
5212110596595560192	−46.208	9.802	394.576
*1825842828672942208	−7.968	0.290	843.012
*1774513537034328704	−8.100	0.004	603.283
*1732532430739244544	−8.075	0.026	905.611
*4150939038071816320	−8.145	−0.015	676.474
4076739732812337536	−6.341	0.306	661.311
*1949388868571283200	−8.102	−0.027	574.626
3252546886080448384	−10.025	1.483	590.122
*6101408687905214208	−8.014	−0.054	615.105
5482348392671802624	−0.467	−3.115	597.193
*2099408640243333632	−8.090	0.011	732.366
*1334468195956624768	−8.081	0.017	574.301
5300505902646873088	−12.459	−4.809	530.468

In the tables 4.9 and 4.10 we may see rotated positions of intersections of the star with crossing in the past. For objects with two crossings in the past we have taken only the first one. In the table we may also see velocity of object during intersecting the disk so this velocity corresponds to velocity right after ejection. There is a wide range of velocities.

As possible candidates of ejection cause we have chosen catalogue of stellar mass black holes from Corral-Santana et al. (2016). We used those objects with right ascesion, declination and distance. We changed their coordinates to galactocentric to compared their positions with positions of intersections where possible ejection happened. On the Figures 4.24, 4.25 and 4.26 we see plotted positions of stellar mass black holes in dark blue color and positions of corrected intersections in cyan color. All three pictures shows the same picture, but we tried to zoom densier parts of plot. We may see that their distribution is anisotropic and we may assume that these stellar black holes may be potential cause of ejection. There are two possible scenarios of this. One is ejection by supernova explosion and subsequent collapsed of core of massive star to black hole or this ejection is caused by Hills-type mechanism which means encounter of binary system with black hole and their tidal disruption.

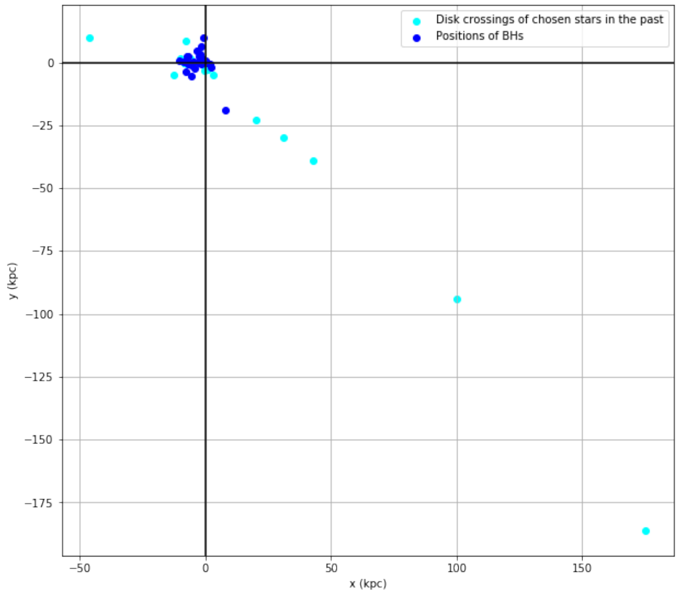

Figure 4.24: Graph with plotted positions of stellar massive black holes and positions of intersections of stars with crossing of the galactic plane in the pass.

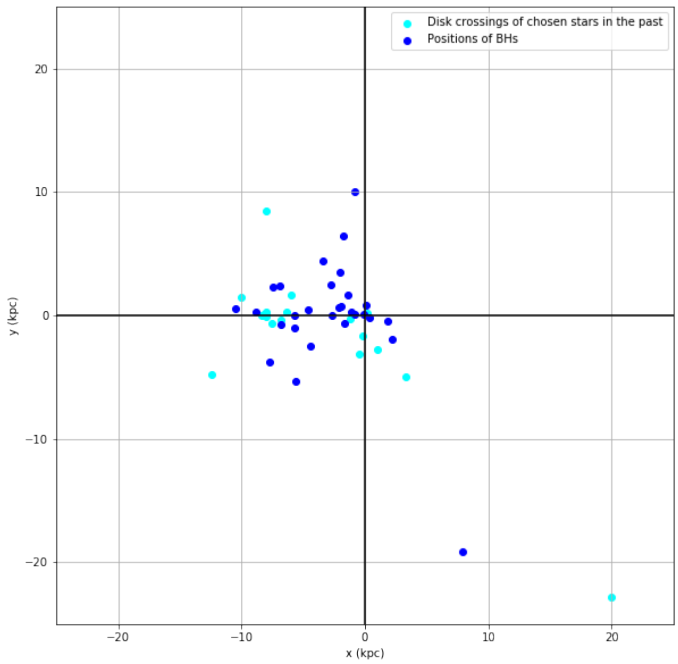

Figure 4.25: Zoomed graph of densier part with plotted positions of stellar massive black holes and positions of intersections of stars with crossing of the galactic plane in the pass.

On the last picture we may notice group of stars with similar place of intersection with the galactic plane around $x \approx -8$ kpc and $y \approx 0$ kpc. In the Table 4.10 we marked these stars with * before their Gaia DR2 ID. We transform rotated coordinates of these objects to Sky coordinates and almost all these stars overlay area in the direction around galactic center. We have tried to find any possible objects for their ejection, for example some cluster with intermediate black hole, but unfortunatelly we have not found anything satisfactory. There is identified a lot of star clusters, but for most of them there is not given their distance. Distance of these intersections from the Sun is around 160-300 pc what is relatively close.

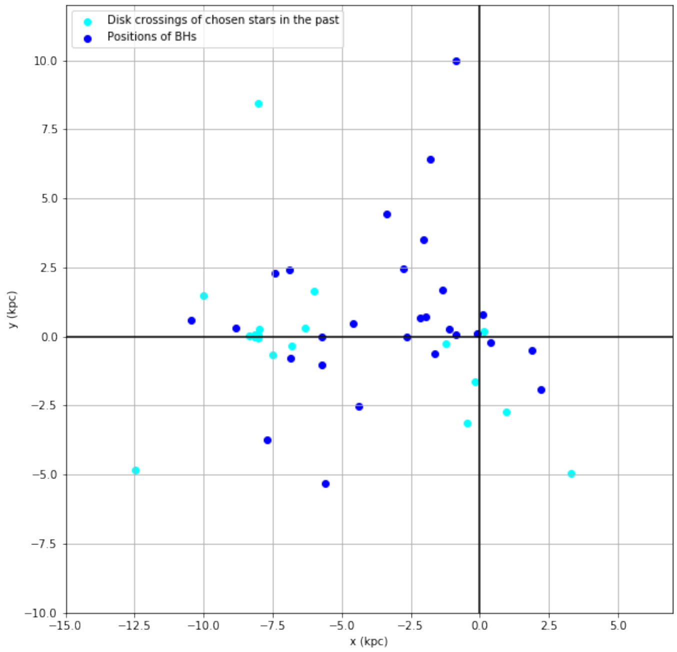

Figure 4.26: Twice zoomed graph of densier part with plotted positions of stellar massive black holes and positions of intersections of stars with crossing of the galactic plane in the pass.

4.3 Script for a future release

At the end we represent improved script for finding unbound stars in the data that can be found in Appendix D. We noticed that for unbound stars there is special property that can distinguish them from bound stars. That property is eccentricity of orbit. For those unbound it was always 'nan' which means there is not enough data to calculate it and that is sign that if during 10 Gyr it is not curved enough for calculating eccentricity it may be with high possibility unbound. So we made script with condition that saves number only of those objects which eccentricity is 'nan'. Of course, someone can dispute that it is not only possibility. For covering whole range it would be essential to add another condition and that would be eccentricity value over some special limit like 1 for parabola. When some object correspond to the condition script creates folder with its number.

When search for unbound stars is done then script looks for intersections of the galactic disk. For every object it looks for positions in the orbit where $z < 0.000005$ kpc. Those places are saved in text files which are located in created folders of every object. The intersections are in galactocentric coordinates and their are not correct to rotation of the Galaxy. Of course due to our condition there would be couple of following points around one place, but this condition is important for objects with more intersections in the past. According to small number of unbound objects it is not so big problem to select from them those with the smallest z and then use script from Appendix C to rotate them a compare them with positions of interesting objects. For now we are left waiting for the upcoming data release from Gaia. This script is made to be used for analysing them in the future.

Discussion and Future Insights

In our work we used only data from Gaia satellite. We have to highlight that for more effective search for high velocity stars with hyper velocities it is essential to use higher number of surveys, especially spectroscopic. Gaia is specialized for astrometry and in this respect it is unrivaled. Unfortunatelly, its spectroscopy is not so good and is limited. For example it can only measure radial velocities under 1000 km.s^{-1} and errors for those above 500 km.s^{-1} are large. We propose to use combinations of surveys to become more effective in research in the future.

In results we have shown a figure with compared positions of stellar mass black holes and rotated intersections of objects with at least one crossing of the galactic centre in the past. This result fits very well even when we may expect uncertainties of crossings and possible uncertainties in positions of measured stellar mass black holes. Uncertainties of used objects may be seen in zip file named 'unbound.zip' on figures named errors. There are in fact uncertainties in integration and we have to admit that also positions of black holes might be different now. After all, it may be only coincidence that plotted positions are distributed anisotropically and that they fit very nicely. In the future it would be better to calculated uncertainties of intersections to have better image about accuracy of the result.

We created a script for future use, because we are expecting the last data release by Gaia next year. We used our gained experience and we used eccentricity as identification mark for unbound stars. We hope that more data will be corrected and improved in the last release, mainly negative parallaxes.

Summary and Conclusion

In our thesis, we were analysing data from the latest data release of Gaia catalogue. We had used the specialised Python package called Gala intended for the galactic dynamic. Selection of stars has been made on base of the condition: it takes those objects which exceeds 30 kpc during 10 Myr. We analysed their orbits and classified into groups according to the shape of orbits (see Section 4.1.1). We made also trials of orbits for runaway stars for better imaginations. We has been looking for these objects also in known catalogues to find their basic characteristics.

Subsequently we selected only the unbound stars, and we defined our new unbound group to have to head away from the Galaxy during 10 Gyr of integration. We have used these objects and found their intersections with the disk plane. As we used a static frame we did necessary back- time Milky Way rotation on per star basis. Following the correction, we compared them with positions of known stellar mass black holes. Their an-isotropic distribution of positions shows certain degree of mutual correlation (see Figure 4.24).

The correlation may be due Hills mechanism (see Section 1.3); the stars are in close encounters accelerated during passing near some stellar mass black holes. However, another acceleration mechanism may be a supernova explosion and subsequent anisotropic collapse of a core into a stellar mass black hole.

Finally we included our knowledge to the comprehensive script (see Appendix D) which can be applied on a future release of Gaia catalogue.

Appendix A

Trials

A.1 Changes in v_y

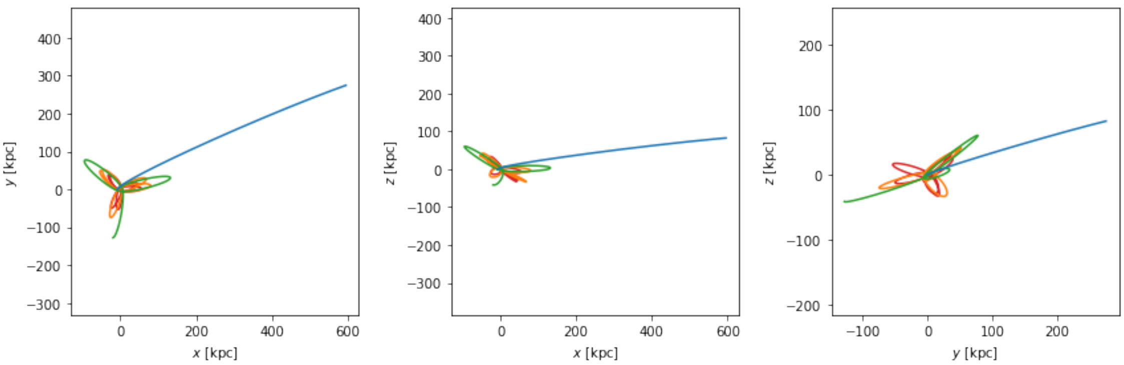

Figure A.1: Orbits with set $x = -8$ kpc, $v_x = 100$ km.s^{-1}, $v_z = 200$ km.s^{-1} and v_y is changing : red = 200 km.s^{-1}, orange = 250 km.s^{-1}, green = 300 km.s^{-1} and blue = 400 km.s^{-1}.

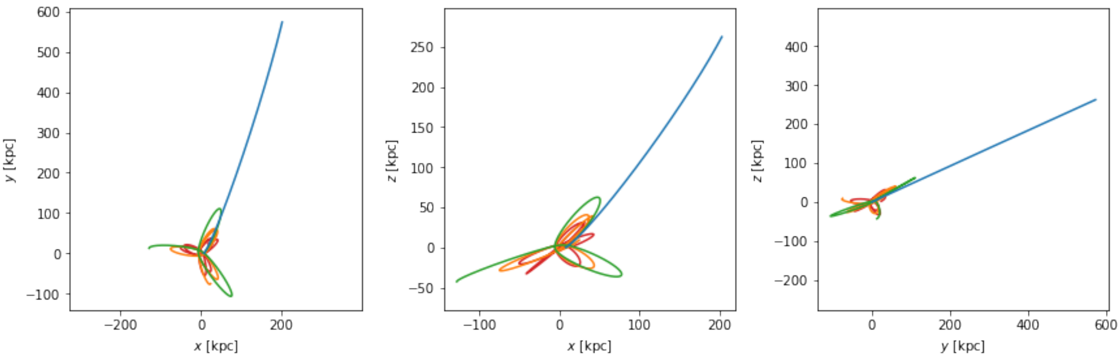

Figure A.2: Orbits with set $x = -8$ kpc, $v_x = 300$ km.s^{-1}, $v_z = 200$ km.s^{-1} and v_y is changing : red = 220 km.s^{-1}, orange = 270 km.s^{-1}, green = 320 km.s^{-1} and blue = 400 km.s^{-1}.

A.2 Changes in v_x

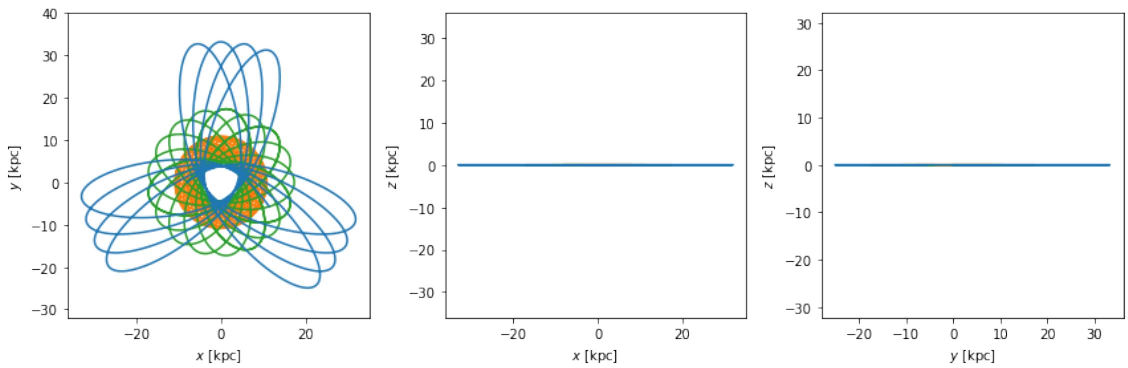

Figure A.3: Orbits with set $x = -8$ kpc, $v_y = 220\,\mathrm{km.s^{-1}}$, $v_z = 0\,\mathrm{km.s^{-1}}$ and v_x is changing : red = 0 km.s^{-1}, orange = 100 km.s^{-1}, green = 200 km.s^{-1} and blue = 300 km.s^{-1}.

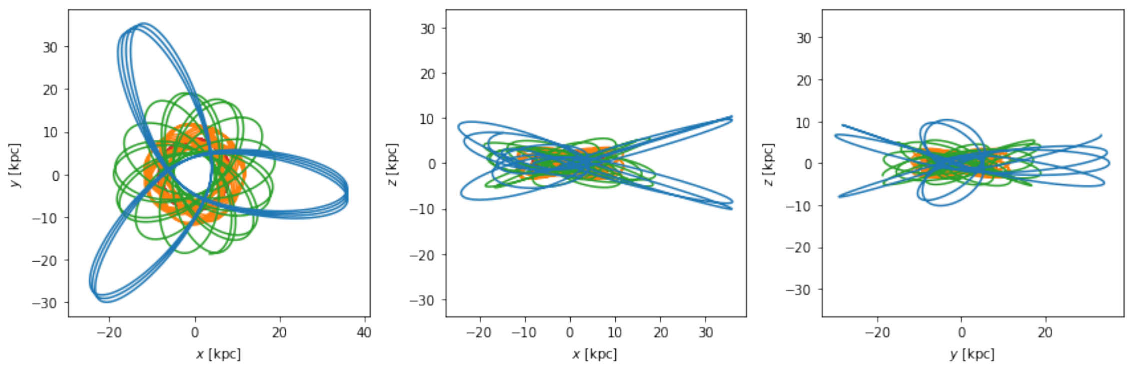

Figure A.4: Orbits with set $x = -8$ kpc, $v_y = 220km/s$, $v_z = 100km/s$ and v_x is changing : red = 0 km.s^{-1}, orange = 100 km.s^{-1}, green = 200 km.s^{-1} and blue = 300 km.s^{-1}.

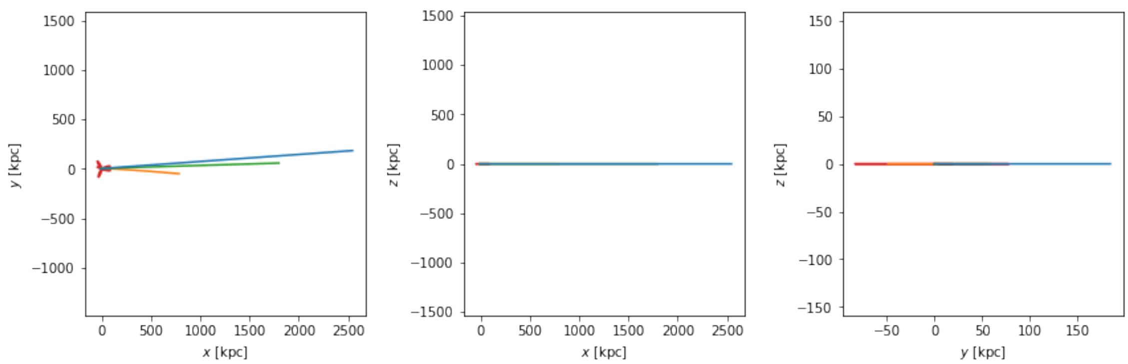

Figure A.5: Orbits with set $x = -8$ kpc, $v_y = 220\,\mathrm{km.s^{-1}}$, $v_z = 0\,\mathrm{km.s^{-1}}$ and v_x is changing : red = 400 km.s^{-1}, orange = 500 km.s^{-1}, green = 600 km.s^{-1} and blue = 700 km.s^{-1}.

A.3 Changes in v_z

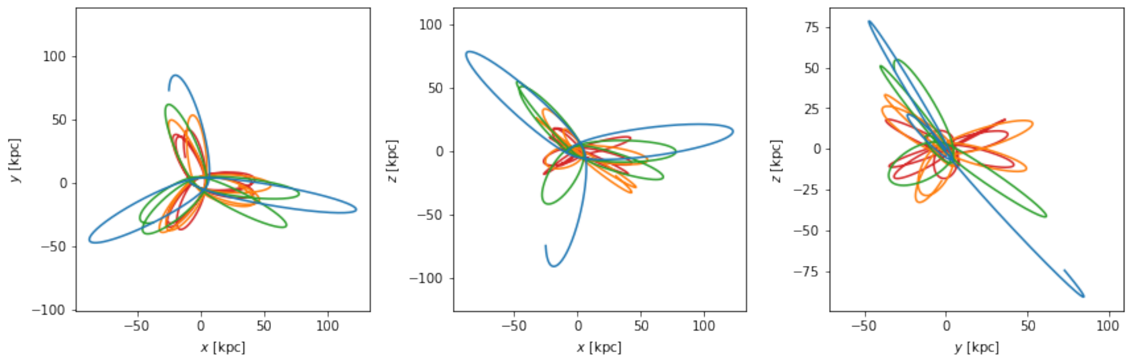

Figure A.6: Orbits with set $x = -8$ kpc, $v_x = 300$ km.s^{-1}, $v_y = -220$ km.s^{-1} and v_z is changing : red = 150 km.s^{-1}, orange = 200 km.s^{-1}, green = 250 km.s^{-1} and blue = 300 km.s^{-1}.

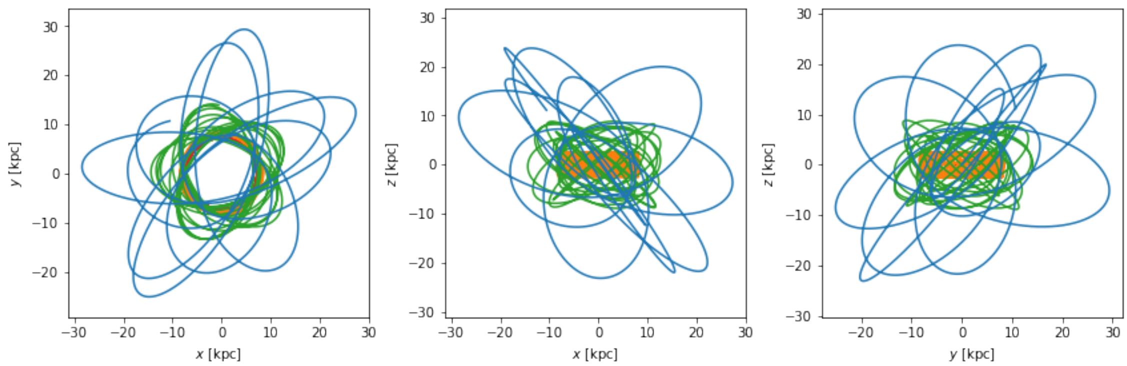

Figure A.7: Orbits with set $x = -8$ kpc, $v_x = 0$ km.s^{-1}, $v_y = 220$ km.s^{-1} and v_z is changing : red = 0 km.s^{-1}, orange = 100 km.s^{-1}, green = 200 km.s^{-1} and blue = 300 km.s^{-1}.

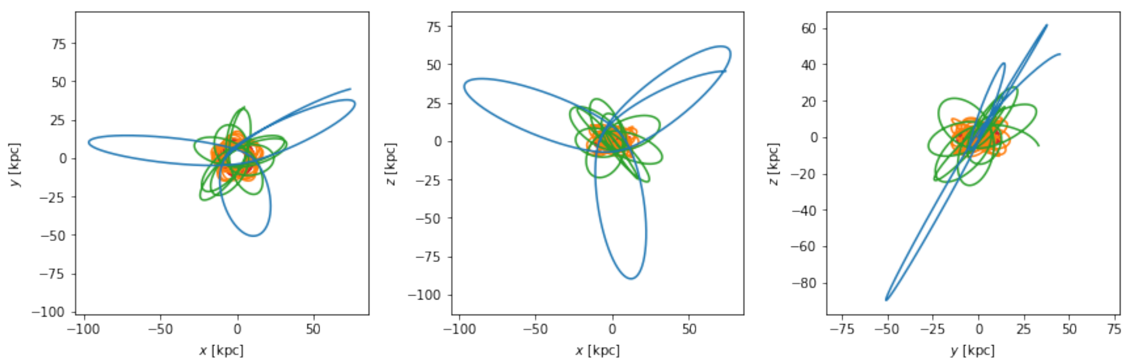

Figure A.8: Orbits with set $x = -8$ kpc, $v_x = 100$ km.s^{-1}, $v_y = 220$ km.s^{-1} and v_z is changing : red = 100 km.s^{-1}, orange = 200 km.s^{-1}, green = 300 km.s^{-1} and blue = 400 km.s^{-1}.

Appendix B

Tables

Table B.1: Neg unbound

Gaia DR2	Other name	Identified as	Spectral type	Parent	Found?
2629296824480015744	UCAC4 438-122419	High proper-motion Star	non	non	YES
1598160152636141568	TYC 3872-472-1	Star	non	[CCB99] 1 – Cluster of Stars	YES
2356640863029393792	TYC 5850-2203-1	High proper-motion Star	non	non	YES
5951114420631264640	non	non	non	non	NO
3793467471202249472	PM J11295-0233B	High proper-motion Star	non	PM J11295-0233 – Double or multiple star	YES
4065480978657619968	non	non	non	non	YES
4103096400926398592	non	Star	non	C 1829-160 – Open (galactic) Cluster	YES
5795144396911674368	RAVE J151403.9-723451	Star	non	non	YES
5878409248569969792	[DCD2015] 1085	Star	non	Cl Trumpler 22 – Open (galactic) Cluster	YES
5716044263405220096	non	non	non	non	NO
2948057206859070336	non	non	non	non	NO
5253575237405660160	non	non	non	non	NO
6385725872108796800	non	Star	non	non	YES
2798329939631122432	non	non	non	non	NO
1677490397616254592	non	non	non	non	NO
1679237212355219328	TYC 4168-762-1	Star	K	non	YES
5412495010218365568	non	non	non	non	NO
4863753908114937728	non	Star	non	non	YES
5931224697615320064	non	non	non	non	NO
1359836093873456768	non	Star	non	non	YES
5672759960942885376	non	non	non	non	NO
5305975869928712320	non	non	non	non	NO
5953456066818230528	non	non	non	non	NO
73753560659651584	V* V Ari	Peculiar Star	C-H3.5	non	YES
4269007246718955008	non	non	non	non	NO
5932173855446728064	non	Star	non	non	YES
330414789019026944	TYC 2319-713-1	High proper-motion Star	non	NGC 752 – Open (galactic) Cluster	YES
4594877960270902912	non	non	non	non	NO
5956359499060605824	TYC 7898-721-1	High proper-motion Star	non	non	YES
1765600930139450752	TYC 1126-382-1	High proper-motion Star	non	non	YES
1396335030896548992	TYC 3060-523-1	Star	non	non	YES
1398409401317253504	non	non	non	non	NO
1651722380546929152	non	non	non	non	NO
2853089398265954432	TYC 1732-2222-1	High proper-motion Star	non	non	YES
3006234119426679936	non	non	non	non	NO
2233912206910720000	non	Star	non	non	YES
5916830097537967744	non	non	non	non	NO
6397497209236655872	non	Star	non	non	YES
6505889848642319872	TYC 8826-415-1	Star	non	non	YES
6053231975369894400	non	non	non	non	NO
5231593594752514304	HD 95123B	Star	non	non	YES
1337186910255681792	non	non	non	non	NO
1426059301257128704	non	non	non	non	NO
1995066395528322560	non	Star	non	non	YES
6257774467036174848	BD-18 4046	Star	non	non	YES
1552278116525348096	non	High-velocity Star	non	non	YES
5966712023814100736	non	non	non	non	NO
2041630300642968320	non	Star	non	non	YES
1341967655532896896	TYC 3077-1097-1	Star	non	non	YES
4589100675205457792	non	non	non	non	NO

Table B.2: Pos unbound

Gaia DR2	Other name	Identified as	Spectral type	Parent	Found?
413902566644674432	non	non	non	non	NO
3705761936916676864	non	Star	non	non	YES
5800686352131080704	non	Star	non	non	YES
2251311188142608000	non	Star	non	non	YES
489354627948864128	non	Star	non	non	YES
4038969206316480512	non	non	non	non	NO
6061453917139569280	TYC 8652-540-1	High proper-motion Star	non	non	YES
5869501039771336192	TYC 8991-3270-1	Star	non	NAME HIP 67014 Cluster – Open (galactic) Cluster	YES
5195254636665583232	non	Possible Star of RR Lyr type	non	non	YES
1752925794453337600	non	Star	non	non	YES
939821616976287104	HD 53229B	Star	non	non	YES
4296894160078561280	non	non	non	non	NO
4902647036002699136	CRTS J005231.1-611030	Variable Star of RR Lyr type	non	non	YES
4747063907290066176	non	Star	non	non	YES
4649982970496758528	non	non	non	non	NO
5212110596595560192	TYC 9383-3064-1	Star	non	non	YES
1772711540555984256	non	non	non	non	NO
5637997011047611264	non	Star	non	non	YES
5212817273334550016	UCAC2 630088	Star	non	non	YES
1825842828672942208	non	non	non	non	NO
5190987741276442752	TYC 9511-1175-1	Star	non	non	YES
5191438266165988352	non	Star	non	non	YES
1774513537034328704	non	Star	non	non	YES
1732532430739244544	HD 202276B	Star	non	non	YES
4150939038071816320	UCAC4 389-084888	Star	non	non	YES
4076739732812337536	non	non	non	non	NO
1949388868571283200	non	Star	non	non	YES
3252546886080448384	non	Star	non	non	YES
6101408687905214208	non	non	non	non	NO
4937516982126408192	TYC 8047-350-1	Star	non	non	YES
1400950785006036224	non	Star	non	non	YES
5373040581643937664	non	Star	non	non	YES
2260163008363761664	non	Star	non	non	YES
5482348392671802624	non	Star	non	non	YES
2099408640243333632	HD 180683B	High proper-motion Star	non	non	YES
1334468195956624768	non	non	non	non	NO
5300505902646873088	non	Star	non	non	YES
1042515801147259008	non	Star	non	non	YES
430092737933320448	TYC 4018-2839-1	Star	B5III	non	YES

Table B.3: Neg almost unbound

Gaia DR2	Other name	Identified as	Spectral type	Parent	Found?
1200541391862812416	non	non	non	non	NO
5702040883306193792	non	non	non	non	NO
1364579829416779008	non	non	non	non	NO
6373269470519250944	non	non	non	non	NO
4846918289148074112	HD 21921B	High proper-motion Star	non	non	YES
1119572256080801664	non	non	non	non	NO
2251344379650046592	non	non	non	non	NO
2275940209948721024	non	non	non	non	NO
781931511002696448	G 146-76	Peculiar Star	non	NAME AF06 Stream – Moving Group	YES
342645451424632192	non	non	non	non	NO
564961308084113152	TYC 4500-416-1	Star	non	non	YES
2653208801494625792	non	non	non	non	NO
1752892151975412864	non	non	non	non	NO
4183218195494618496	non	non	non	non	NO
5563305674344057856	RAVE J065045.0-415052	Star	non	non	YES
4707028318100144768	non	non	non	non	NO
5828888825409356672	non	non	non	non	NO
6633823489736710784	non	non	non	non	NO
1955636637237196416	non	non	non	non	NO
881107975226164096	TYC 2471-121-1	Star	non	non	YES
29649366130846592	non	non	non	non	NO
6519251698057832448	non	non	non	non	NO
3541413604586581120	non	non	non	non	NO
1106005210308880384	BD+67 428	High proper-motion Star	F8	non	YES
1940380874743387776	WISEA J234310.57+484601.8	High proper-motion Star	non	non	YES
5728832958015766016	non	non	non	non	NO
6293344217947325184	BD-17 3902B	High proper-motion Star	non	non	YES
4486176358099463424	non	non	non	non	NO
1609904551728783232	TYC 3855-382-1	Star	non	[CCB99] 1 – Cluster of Stars	YES
125750427611380480	G 37-37	High proper-motion Star	F5	NAME Alessi Teutsch 9 – Open (galactic) Cluster	YES
1945845069576623872	G 188-20	High proper-motion Star	non	non	YES
1320868130475121024	non	non	non	non	NO
5645506675466437888	non	non	non	non	NO

Table B.3: Neg almost unbound

Gaia DR2	Other name	Identified as	Spectral type	Parent	Found?
114797397716085120	TYC 1776-1105-1	High proper-motion Star	non	non	YES
1417302275257773440	non	non	non	non	NO
5510547051995715968	non	non	non	non	NO
4584126591977439360	non	non	non	non	NO
6056115135337482496	non	Star	non	non	YES
1579434541901976576	TYC 4162-874-1	Star	non	non	YES
1353777750444932736	non	non	non	non	NO
2933107731372185472	HD 49981B	Star	non	non	YES
2044665811751803264	non	non	non	non	NO
5845269761962968704	non	non	non	non	NO
4570149462726186880	non	non	non	non	NO
5315800624771913856	non	non	non	non	NO
1642467103981470208	TYC 4195-1681-1	Star	non	non	YES

Table B.4: Pos almost unbound

Gaia DR2	Other name	Identified as	Spectral type	Parent	Found?
3787795258218885504	non	non	non	non	NO
6373201816194315008	L 80-129	High proper-motion Star	non	non	YES
2070737152266402432	TYC 3573-250-1	Star	non	non	YES
3479908092359677568	TYC 7218-391-1	Star	non	non	YES
1597988246569491968	TYC 3869-36-1	High proper-motion Star	non	non	YES
4956675937880693632	TYC 7556-168-1	Star	non	non	YES
3266449244243890176	TYC 4707-283-1	High proper-motion Star	non	non	YES
1923489734738800384	non	non	non	non	NO
2874415010402716672	non	non	non	non	NO
5414925927344979328	non	non	non	non	NO
6062623763163117952	non	non	non	non	NO
5342232472016842368	non	non	non	non	NO
5590900667426327296	TYC 7111-718-1	Peculiar Star	CEMP	Cl Collinder 135 – Open (galactic) Cluster	YES
1255095276181144320	Ross 50	High proper-motion Star	non	** LDS 4481 – Double or multiple star	YES
6393302366217688576	non	non	non	non	NO
3746122603590442240	TYC 1458-499-1	High proper-motion Star	non	non	YES
4882046242548316928	non	non	non	non	NO
5213104619530689536	TYC 9381-194-1	Star	non	non	YES
3752558526183725440	2MASS J10223698-1403456	High proper-motion Star	non	non	YES
4315136329343371648	non	non	non	non	NO
5717948445741886720	BD-16 2232	Star	non	non	YES
5274368209136879232	non	non	non	non	NO
1160564523465002240	non	non	non	non	NO
4667751460653912192	non	non	non	non	NO
5845797287008869760	non	non	non	non	NO
4036750258757682560	L 487-64	High proper-motion Star	G0	non	YES
4984034291144272000	TYC 7544-438-1	Star	non	non	YES
5276145153069304192	non	non	non	non	NO
6191511986469199616	LP 855-50	High proper-motion Star	K0	non	YES
6870578373607170432	non	non	non	non	NO
1475587111768060416	LSPM J1333+3801	High proper-motion Star	non	non	YES
4619887932790526080	non	non	non	non	NO
4936942349861633664	2MASS J02133603-5050247	Star	non	non	YES
2503491051919554304	LSPM J0239+0306	High proper-motion Star	non	non	YES
4757201919907218688	TYC 8883-469-1	Star	non	non	YES
2098721617280444928	non	non	non	non	NO
5613018443338345984	TYC 6545-3036-1	High proper-motion Star	non	non	YES
3456480072256611200	LSPM J0548+3803	High proper-motion Star	non	non	YES
5606065883412646016	non	non	non	non	NO
5352190302148489088	non	non	non	non	NO
16196841364837632	non	non	non	non	NO
5390421455289729920	TYC 7729-974-1	High proper-motion Star	non	non	YES
4958781983684033920	CD-44 457	High proper-motion Star	non	non	YES
4048994828196689536	non	non	non	non	NO
1300296199200698112	BD+25 3130	High proper-motion Star	G5	non	YES
5577394644543448576	CD-36 3161	Star	non	non	YES

Table B.5: Neg disk

Gaia DR2	Other name	Identified as	Spectral type	Parent	Found?
2133314619611880448	KIC 12253381	Peculiar Star	Flat	non	YES
1920314448236775680	TYC 3235-1494-1	Star	non	non	YES
3192796881606263424	BD-08 813	High proper-motion Star	non	non	YES
5308680118768823424	non	non	non	non	NO
1625310187102498048	WISEA J162935.84+605759.5	High proper-motion Star	non	non	YES
1625710134457648768	non	non	non	non	NO
2195270489228213632	non	non	non	non	NO

Table B.5: Neg disk

Gaia DR2	Other name	Identified as	Spectral type	Parent	Found?
2000849551816850304	HD 235766	High proper-motion Star	G5	NGC 7243 – Open (galactic) Cluster	YES
3122530185851683712	G 99-52	Spectroscopic binary	G	non	YES
5896455773444937856	non	non	non	non	NO
294072906063827072	V* RU Psc	Variable Star of RR Lyr type	A2	non	YES
920140878529848448	LP 207-42	High proper-motion Star	non	non	YES
6000574886009287040	non	non	non	non	NO
5776753866644350464	TYC 9448-1871-1	High proper-motion Star	non	non	YES
5860101417932919680	non	non	non	non	NO
4513860789615413760	non	non	non	non	NO
480595265487672832	TYC 4106-733-1	Star	non	non	YES
6308763386763044736	TYC 5592-687-1	High proper-motion Star	non	non	YES
1688719984748642304	G 255-32	Spectroscopic binary	G0	non	YES
4495396652151998976	non	non	non	non	NO
2090864232309634816	non	non	non	non	NO
5191563228620951424	V* DR Oct	Variable Star of RS CVn type	G3V	non	YES
6781994978064672640	non	non	non	non	NO
5849568818100798080	non	non	non	non	NO
4441393313920391936	TYC 976-1534-1	High proper-motion Star	non	non	YES
2034860263988296576	non	non	non	non	NO
1392290786611040896	non	non	non	non	NO
4595657857609180032	TYC 2088-248-1	High proper-motion Star	non	non	YES
3139352198360754432	non	non	non	non	NO
5963832505983654016	non	non	non	non	NO
2077355426293880192	TYC 3143-1430-1	Star	Flat	non	YES
2914965720791328896	TYC 6494-1066-1	Star	non	non	YES
2009730410301470976	non	non	non	non	NO
2915376182225431808	TYC 6489-1462-1	High proper-motion Star	non	non	YES
1932767242055230464	non	non	non	non	NO
5928269111633141888	non	non	non	non	NO
1475828798168058624	Ross 1012	High proper-motion Star	non	non	YES
5353743534120235392	non	non	non	non	NO
2919416028462413824	non	non	non	non	NO
4538465351549887872	TYC 2120-1484-1	Star	non	non	YES
1637426255485074176	TYC 4421-2499-1	Star	non	non	YES
5333193588752777344	non	non	non	non	NO
4539042114116981376	non	non	non	non	NO
6850000528157100288	WISEA J200254.66-265144.9	High proper-motion Star	non	non	YES
2049034819964604544	non	non	non	non	NO
1992856136631521536	HD 236166	High proper-motion Star	F8	Cl Stock 12 – Open (galactic) Cluster	YES

Table B.6: Pos disk

Gaia DR2	Other name	Identified as	Spectral type	Parent	Found?
4662889729473501440	HD 29907	Spectroscopic binary	F8V	non	YES
5852318353092534912	non	non	non	non	NO
6296338871010615040	non	non	non	non	NO
5791622699835843584	non	non	non	non	NO
5417661890229376000	UCAC2 14806330	Star	non	non	YES
3757326794580265728	non	non	non	non	NO
3154504568102808960	non	non	non	non	NO
2181314147624198144	non	non	non	non	NO
5457918549973306368	CD-25 8298	Star	non	non	YES
3197517394261798528	non	non	non	non	NO
4800713718174677760	HD 273309	Star	G5	non	YES
5412243359495900928	V* CD Vel	Variable Star of RR Lyr type	F	NAME HIP 45189 Cluster – Moving Group	YES
5852502555639970432	non	non	non	non	NO
2031847980092771072	non	non	non	non	NO
1585172927447080576	HD 105791	High proper-motion Star	F6wl	non	YES
5623162022214495232	non	non	non	non	NO
4469560259203065472	non	non	non	non	NO
3727858341063107072	TYC 896-386-1	High proper-motion Star	non	non	YES
2568471982962665984	LSPM J0145+0655	High proper-motion Star	non	non	YES
2059201183675241472	HD 227836	Be Star	B5Iae	non	YES
4750673363445602816	LTT 1465	High proper-motion Star	non	non	YES
3531611252266342400	L 611-42	High proper-motion Star	non	non	YES
502193041112416128	non	non	non	non	NO
3782121816873925632	Ross 891	High proper-motion Star	G5	non	YES
4106441738062136576	non	non	non	non	NO
4503751978450487040	non	non	non	non	NO
2067295891327946112	[D75b] Em* 20-104	Emission-line Star	non	non	YES
5304876049053402752	non	non	non	non	NO
3952411360285636992	HD 107550	High proper-motion Star	G0	non	YES
5046136739402105088	L 442-25	High proper-motion Star	K4	non	YES
5620283432058111488	non	non	non	non	NO
5298707857534947456	non	non	non	non	NO
1965743485564884224	non	non	non	non	NO
5715254298659729408	TYC 5993-199-1	Star	non	non	YES
664160724609806464	LP 367-226	High proper-motion Star	non	non	YES

Table B.6: Pos disk

Gaia DR2	Other name	Identified as	Spectral type	Parent	Found?
302808702040930048	TYC 2294-1561-1	High proper-motion Star	non	non	YES
3069023032306067968	non	non	non	non	NO
2015794663606952704	BD+61 2481	Emission-line Star	B3	non	YES
2905773322545989760	CD-29 2277	High proper-motion Star	F6	non	YES
6526120553355791104	HD 220127	Peculiar Star	G3/5	non	YES
4247666481872680960	non	non	non	non	NO
5972823006364164096	non	non	non	non	NO
5514031743641855232	non	non	non	non	NO
5118271574130792064	L 584-7	High proper-motion Star	K2	non	YES
1433378406566126848	non	non	non	non	NO
3813349321492771072	non	non	non	non	NO
5359450854141307776	non	non	non	non	NO
5531451173227717760	non	non	non	non	NO
951746576492018560	non	non	non	non	NO
5344098927348277376	non	non	non	non	NO
5360415095782938624	TYC 8614-934-1	Star	non	non	YES
5225454471572336384	non	non	non	non	NO
4535916271280601728	TYC 2111-228-1	Star	non	non	YES
6613986062287306752	L 572-28	High proper-motion Star	K2	non	YES
5420008488562024064	V* BN Ant	Variable Star of RR Lyr type	non	non	YES
5576566845428758528	non	non	non	non	NO
5351472080535357568	non	non	non	non	NO
4587107436723034752	non	non	non	non	NO
5493664562047619072	non	non	non	non	NO
4603153125299443328	non	non	non	non	NO
5354554767533822336	TYC 8601-1101-1	High proper-motion Star	non	non	YES

Table B.7: Neg chaotic

Gaia DR2	Other name	Identified as	Spectral type	Parent
552553937839959040	TYC 4515-1197-1	High proper-motion Star	non	non
2334178733827591424	CD-27 16505	Star	non	Cl Blanco 1 – Open (galactic) Cluster
2128652694610890368	KIC 10737052	Star	Flat	non
3140943088608549504	TYC 176-1434-1	Star	non	non
5759671677898613632	G 114-42	High proper-motion Star	non	non
6627657909558558464	HD 214362	Horizontal Branch Star	Gwl	non
1970645963090365568	TYC 3194-514-1	Star	non	non
2337925457137730304	TYC 6982-671-1	High proper-motion Star	non	non
6320525725934951040	2MASS J15082179-0850103	Star	non	non
4420705899564396288	BD+01 3070	Spectroscopic binary	G0	non
2171801001226378240	LSPM J2134+5156	High proper-motion Star	non	non
2941810984378083456	TYC 5941-2406-1	Star	non	non
3664415691211443712	TYC 316-252-1	High proper-motion Star	non	non
5035174402313161472	TYC 6428-1841-1	High-velocity Star	non	non
1072693474023066880	TYC 4385-694-1	Star	non	non
4694041711386658176	TYC 9143-1182-1	Star	non	non
4243579356635038336	TYC 499-37-1	High proper-motion Star	non	non
6356252535213950592	TYC 9465-50-1	High proper-motion Star	non	non
6183013242623029504	TYC 6712-1166-1	High proper-motion Star	non	non
4184479678933255552	HD 182018	Star	G6/8IV	NGC 6774 – Open (galactic) Cluster
2302356324700179328	BD+84 460	Star	G0	non
1673933988600769920	TYC 4403-643-1	Star	non	non
6378030424586123904	HD 220746C	High proper-motion Star	non	non
5480067077841998336	non	High proper-motion Star	non	TYC 8895-665-1 – Double or multiple star
5195968563309851136	CD-80 328	High proper-motion Star	sdG	non
1140145286868945024	TYC 4530-1147-1	Star	non	non
891085356054040960	LSPM J0659+3321	High proper-motion Star	non	non
3199894504040883584	UCAC2 29396153	High proper-motion Star	non	non
2770355924279857664	TYC 1177-1558-1	High proper-motion Star	non	non
2081319509311902336	LSPM J2015+4411	High proper-motion Star	non	non
5744816966569350528	RAVE J092322.5-075135	Star	non	non
1811095354044523392	2MASS J20420916+1621507	Star	non	NGC 6950 – Open (galactic) Cluster
6551158700861223424	HD 221342	High proper-motion Star	G3V	non
1737165669660120320	BD+07 4625	High proper-motion Star	G0	non
5055571610024137984	RAVE J033633.4-304509	Star	non	non
1817451458968642688	TYC 1646-459-1	Star	non	non
940752284849363072	TYC 2449-1891-1	Star	non	non
792568908045816192	TYC 3833-254-1	Star	non	non
4572382295963226368	TYC 2059-269-1	Star	non	non
504867225197304448	TYC 3692-2062-1	Star	non	Cl Stock 2 – Open (galactic) Cluster
893048667206860800	TYC 2456-2178-1	High proper-motion Star	non	non
793616845706502784	G 116-53	High proper-motion Star	non	non
439191261064356352	Ross 338	High proper-motion Star	G1	non
6275751035471571200	HD 122581	High proper-motion Star	K0(III)	non
1361428148055015552	TYC 3085-46-1	Star	non	non
6507096906250238848	L 285-90	High proper-motion Star	non	non
3835834433064146560	LSPM J1012+0254	High proper-motion Star	non	non
3846427888295815552	Ross 889	Peculiar Star	sdA4	non

Table B.7: Neg chaotic

Gaia DR2	Other name	Identified as	Spectral type	Parent
1226104831048552448	LP 500-6	High proper-motion Star	non	non
6316390492767441024	Ross 805	High proper-motion Star	F8	non
2191903372311859456	TYC 4248-1360-1	High proper-motion Star	non	non
4718885485854328064	2MASS J01481644-5717024	High proper-motion Star	non	non
6641546493765032960	TYC 8775-2328-1	Star	non	non
2702535057780289536	HD 212457	High proper-motion Star	G8	non
5732564082004083456	LP 727-7 B	High proper-motion Star	non	LP 727-7 – Double or multiple star
2118226399500645504	TYC 3526-321-1	Star	non	non
2649847525728693888	TYC 5235-1079-1	High proper-motion Star	non	non
2028277384814680832	TYC 2151-5733-1	Star	non	non
4910466865777710976	non	High proper-motion Star	non	TYC 8477-435-1 – Double or multiple star
2181083044026715264	TYC 3585-2705-1	High proper-motion Star	non	NAME Alessi Teutsch 11 – Open (galactic) Cluster
851071757096083712	Ross 106	High proper-motion Star	G8	non
5103298283049065472	HD 20793	Peculiar Star	C-H	non
4566984690305380736	TYC 1548-189-1	Star	non	non
2107579008072631680	KIC 10256752	Peculiar Star	G8III	non
3673986531909636736	G 65-33	High proper-motion Star	non	non
2080510887227649152	KIC 10083815	Star	non	non
2265206777438235776	LP 45-210	High proper-motion Star	non	non
5154102081099625344	RAVE J025745.6-160215	Star	non	non
2436947439975372672	TYC 5825-482-1	High proper-motion Star	non	non
2237777196440231808	TYC 4232-1133-1	Star	non	non
6558932694746826240	TYC 8443-1432-1	Star	non	non
4821671436294995456	CD-37 2255	High proper-motion Star	non	non
6103374133661596416	TYC 7814-133-1	Peculiar Star	non	non
6545771884159036928	HD 214161	High proper-motion Star	G5/8wF(0)	NAME RHLS Stream – Stellar Stream
623635680945526528	BD+19 2303	High proper-motion Star	K0	non
2903405485599544576	UCAC2 19571912	Star	non	non
4455192670185376384	TYC 943-452-1	Star	non	non
1290953133502546176	V* UU Boo	Variable Star of RR Lyr type	kA9.5hF6	non
3071335756231224704	TYC 4847-1119-1	High proper-motion Star	non	non
4531308286776328832	TYC 1596-2403-1	Star	non	non
4457069811409865344	TYC 954-704-1	High proper-motion Star	non	non
1950656158802910720	TYC 2725-2222-1	Star	non	non
2268551839703582208	TYC 4583-2519-1	High proper-motion Star	non	non
2239017857871461632	TYC 4231-1589-1	Star	non	non
2615363057216037760	TYC 5804-1393-1	High proper-motion Star	non	non
6392159934981124096	TYC 9124-1533-1	Star	non	non
1313575928841343872	BD+32 2828	Star	K0	non
5076297953963412608	TYC 6438-1019-1	High proper-motion Star	non	non
2269713095781309184	V* BD Dra	Variable Star of RR Lyr type	non	non
2870310155539081088	TYC 2752-605-1	Star	non	non
2363830054168002688	RAVE J003416.7-191736	High proper-motion Star	non	non
3959238258047032704	LSPM J1240+2337	High proper-motion Star	non	non
2626144254057562112	BD-05 5751	Star	non	non
6266830628920120704	UCAC4 380-071856	Star	non	non
4826773621221700608	TYC 7050-188-1	Star	non	non
2147214821704469888	TYC 3905-1063-1	Star	non	non
4461010048771329280	TYC 974-427-1	High proper-motion Star	non	non
2043452431931201920	LSPM J1912+3330	High proper-motion Star	non	non
1607208755375882368	G 201-5	High proper-motion Star	sdF6	[CCB99] 1 – Cluster of Stars
2127331734467335424	KIC 9335536	Peculiar Star	G5III	non
1478088363286014464	TYC 2549-500-1	Star	non	non
6680420204104678272	V* V1645 Sgr	Variable Star of RR Lyr type	non	non
6564274294034705664	V* RT Gru	Variable Star of RR Lyr type	non	non
522534933950730240	HD 6755	Spectroscopic binary	G5	non
1377443466922030592	TYC 3053-744-1	Star	non	non
1336408284224866432	LSPM J1731+3627	High proper-motion Star	non	non
2708409091279404672	Wolf 1033	High proper-motion Star	non	non
1433708328773917312	TYC 3894-668-1	Star	non	non
3815294941677802240	BD+05 2464	High proper-motion Star	K0	non
1404135760954238336	TYC 3496-1423-1	High proper-motion Star	non	non
1550695060299764096	BD+45 2101	Star	K2	non
4587905579084735616	LP 335-14	High proper-motion Star	non	non
2066609315039202176	LSPM J2048+4210	High proper-motion Star	non	non
4398079054075869312	TYC 5031-553-1	Star	non	non
4538449614789801216	Ross 712	High proper-motion Star	non	non
4605090494850292096	TYC 2630-1370-1	High proper-motion Star	non	non
1493960427808328960	TYC 3473-1260-1	Star	non	non
1925108559452411008	TYC 3242-298-1	Star	non	non
1298632603747777280	TYC 2043-799-1	Star	non	non
2526579799671207424	TYC 4678-123-1	High proper-motion Star	non	non
1506860143038459520	TYC 3472-559-1	Star	non	[CCB99] 1 – Cluster of Stars
5100858608481937664	TYC 5877-1160-1	High proper-motion Star	non	non
1639640431384973696	TYC 4181-495-1	Star	non	non
1582847494714290304	TYC 4154-98-1	Star	non	non
1348030500087634048	TYC 3094-168-1	Star	non	non
4580011085590958208	HD 335619	High proper-motion Star	G0	non
4591420374159969280	TYC 2623-2203-1	Star	non	non
1509813568711438592	TYC 3468-78-1	Star	non	[CCB99] 1 – Cluster of Stars
1301137566113736832	TYC 2049-839-1	Star	non	non

Table B.8: Pos chaotic

Gaia DR2	Other name	Identified as	Spectral type	Parent
3599211082567628544	LP 674-41	High proper-motion Star	non	non
3064774107059078784	TYC 4861-1053-1	Star	non	non
2950350478876130304	BD-15 1418	Star	non	non
2447968154259005952	LP 644-28	High proper-motion Star	non	non
6428374141448297856	V* BP Pav	Variable Star of RR Lyr type	non	non
5998904105069858688	L 335-67	High proper-motion Star	non	non
4762924396880464384	TYC 8517-1859-1	Star	non	non
6296953704168228480	V* V348 Vir	Variable Star of RR Lyr type	non	non
5769449054987032448	L 19-83	High proper-motion Star	non	non
5054369367074945920	TYC 7023-181-1	Star	non	Cl Alessi 13 – Open (galactic) Cluster
5193278023996815616	TYC 9510-619-1	High proper-motion Star	non	non
5146340967820821632	UCAC3 152-5958	Star	non	non
5267888748456751232	UCAC2 1809133	Star	non	non
4730405859452760576	CRTS J032144.6-564541	Variable Star of RR Lyr type	non	non
6353115284942387456	TYC 9481-812-1	High proper-motion Star	non	non
5282079908816150912	CD-65 485	Star	non	non
5282242086781047168	TYC 8921-1298-1	Star	non	non
6683166376130924032	L 495-50	High proper-motion Star	non	non
3797589054963808512	UCAC4 455-051704	High proper-motion Star	non	non
4307232966684928384	PM J19057+0756	High proper-motion Star	non	non
2777565593820729856	G 33-31	High proper-motion Star	non	non
5208155137874230912	2MASS J06550661-8006563	Star	non	non
588856788129452160	BD+09 2190	High proper-motion Star	sdA5	non
4734666153476613504	TYC 8492-1481-1	High proper-motion Star	non	non
4734755664890851200	UCAC2 8179555	Star	non	non
4626864192334085888	UCAC2 531138	Star	non	non
4964933510723543168	RAVE J021744.1-363555	Star	non	non
1244437400735546112	TYC 1460-1049-1	Star	non	non
5200827129096636544	UCAC2 415404	Star	non	non
6324687789762798464	HD 127355	High proper-motion Star	G5	non
6512401225221384704	HD 217272	Star	G6wF8	non
6385400760264688512	TYC 9337-1695-1	Star	non	non
3806699299073433344	TYC 4912-1-1	Star	non	non
1247991091035963520	TYC 1462-208-1	Peculiar Star	non	non
6386477555809737856	TYC 9342-1391-1	Star	non	non
4862207784311126016	TYC 7032-251-1	Star	non	Cl Alessi 13 – Open (galactic) Cluster
3844838887835297280	HD 81795	High proper-motion Star	G5V	non
4711891007057179648	TYC 8850-853-1	High proper-motion Star	non	non
6520812798415222656	CD-44 14966	Star	non	non
4900813149391611264	TYC 8844-423-1	Star	non	non
1132102462389590400	BD+79 320	Star	K	non
6346277349116427264	UCAC2 102171	Star	non	non
6307365499463905536	HD 134440	High proper-motion Star	K2V	NAME Kapteyn Moving Group
6307374845312759552	HD 134439	High proper-motion Star	sd:K1Fe-1	NAME Kapteyn Moving Group
5057497580734781952	CD-28 1174	Star	non	Cl Alessi 13 – Open (galactic) Cluster
4715160649697053824	TYC 8489-732-1	High proper-motion Star	non	non
3577444188310927744	LP 734-90	High proper-motion Star	non	non
5413574829416159104	2MASS J10172697-4625524	Red Giant Branch star	non	NGC 3201
5413573798619609216	Cl* NGC 3201 CWFD 3-294	Star	non	non
5413576586067377536	2MASS J10173259-4621502	Red Giant Branch star	non	NGC 3201 – Globular Cluster
3730191126780515456	TYC 304-107-1	Star	non	non
3971657344961894272	TYC 1437-1372-1	High proper-motion Star	non	non
231238462236707584	LSPM J0351+4204	High proper-motion Star	non	non
2424060064186725248	TYC 5265-755-1	High proper-motion Star	non	non
4751529401967463552	CD-50 823	Star	non	non
4653997738423471360	L 56-29	High proper-motion Star	non	non
4980593648680183936	UCAC2 13266111	Star	non	non
5823006506924947328	TYC 9031-2866-1	High proper-motion Star	non	non
4906911251332870144	TYC 8472-779-1	Star	non	non
1071252804552690816	TYC 4386-1860-1	High proper-motion Star	G/K	non
5842054137097439488	TYC 9236-463-1	Star	non	non
4883113181143602176	TYC 7033-640-1	Star	non	Cl Alessi 13 – Open (galactic) Cluster
3908734807060595072	TYC 879-273-1	High proper-motion Star	non	non
3434201256555048960	TYC 1892-841-1	Star	non	non
3879209827478196352	TYC 831-56-1	Star	non	non
6482660432121632128	L 351-88	High proper-motion Star	non	non
6371799320393190656	L 81-49	High proper-motion Star	non	non
3190054012411722624	TYC 5308-309-1	Star	non	non
504003696244270848	TYC 4524-1431-1	Star	non	non
6372407831359927424	TYC 9326-66-1	Star	non	non
3383882824167531520	TYC 1883-1391-1	Star	non	non
2889506421672509568	UCAC2 17416555	Star	non	non
3461875483189072128	TYC 7244-764-1	Star	non	non
1038229698662764160	TYC 3812-944-1	Star	non	non
4928460029970821120	CD-51 243	High proper-motion Star	non	non
298698310964114944	TYC 1759-1060-1	High proper-motion Star	non	non
5806792348219626624	CD-71 1234	High proper-motion Star	non	non
1277437691759222912	TYC 2564-1522-1	Star	non	non
6877318036287069312	LP 814-12	High proper-motion Star	non	non
6364276324397946752	TYC 9462-1508-1	Star	non	non
2267527438464178048	TYC 4441-1180-1	Star	non	non

Table B.8: Pos chaotic

Gaia DR2	Other name	Identified as	Spectral type	Parent
383301130813177216	TYC 2786-593-1	Star	non	non
5421568180165014912	RAVE J095741.1-384517	Star	non	non
4813751280379747200	HD 272315	Star	K5	non
4931105420587401728	2MASS J01352654-4632029	Star	non	non
6191486899564622336	TYC 6718-648-1	High proper-motion Star	non	non
1279615519352234368	TYC 2019-456-1	High proper-motion Star	non	non
301364008186460288	TYC 2309-1257-1	Star	non	non
3857833427353671808	TYC 256-1067-1	High proper-motion Star	non	non
2268999748957513984	TYC 4570-1633-1	High proper-motion Star	non	non
1064335437601392128	TYC 4138-1339-1	High proper-motion Star	non	non
3888444625639625984	LP 430-8	High proper-motion Star	non	non
4618646000047515392	TYC 9491-1476-1	Star	non	non
764719481103766528	LP 214-44 A	High proper-motion Star	non	LP 214-44 – Double or multiple star
2973921362472716416	TYC 5898-381-1	Star	non	non
5362308592238769536	CD-47 6493	High proper-motion Star	F8	non
5046991472253724800	TYC 7026-864-1	Star	non	Cl Alessi 13 – Open (galactic) Cluster
5807140176154682368	TYC 9277-2713-1	Star	non	non
6436505888927135488	TYC 9080-1695-1	Star	non	non
2313475887653200512	TYC 6992-1023-1	High proper-motion Star	non	non
3513599946132439168	2MASS J12290348-2207371	Star	non	non
4937893152542087296	RAVE J021154.1-491556	Star	non	non
4500186227885057024	G 183-9	Spectroscopic binary	non	non
4547041920197256832	LP 447-59	High proper-motion Star	non	non
5004328703108221952	G 267-157	High proper-motion Star	K3	non
4953206394579079680	TYC 7552-328-1	Star	non	non
1100785485013392768	TYC 4118-1080-1	Star	non	non
52624073910834176	HD 284248	High proper-motion Star	sdG0	non
3813460543965876096	TYC 267-308-1	Variable Star	non	non
137859658405173120	G 95-11	High proper-motion Star	non	non
6390596914778480256	UCAC3 53-404390	Star	non	non
5481840968055553920	CD-60 1432	High proper-motion Star	non	non
5535092927533941248	TYC 7657-1253-1	High proper-motion Star	non	non
3499183390187177984	UCAC2 22704670	High proper-motion Star	non	non
951685592253095168	TYC 2949-170-1	High proper-motion Star	non	NGC 2281 – Open (galactic) Cluster
6396342618948599808	2MASS J21361418-6949088	Star	non	non
5332879510732322176	TYC 8981-4210-1	Star	non	C 1155-642 – Open (galactic) Cluster
876358870971624320	Wolf 1059 B	High proper-motion Star	non	Wolf 1059 – Double or multiple star
1434752516926946432	TYC 3900-634-1	Star	non	non
5495524836939301504	RAVE J060203.9-583732	Star	non	non
2922567228793800576	CPD-23 1590	Star	non	non
1551726917602582016	GPM 203.368419+46.694288	Star	non	non
5112760993651401728	TYC 5873-24-1	High proper-motion Star	non	non
1503763918296355200	BD+46 1897	Star	K2	non
5331557897713152640	CPD-43 3058	High proper-motion Star	non	NAME HIP 45189 Cluster – Moving Group
4287154411213419520	LP 571-2	High proper-motion Star	non	non
5576178064990910592	UCAC2 14983555	Star	non	non
5483771126358762240	IRAS 06505-5817	Star	non	non
4655099208591539072	HD 268957	Peculiar Star	F5	NGC 1901 – Open (galactic) Cluster
2910106394792543616	WISEA J060656.42-272309.3	High proper-motion Star	non	non
2910503176753011840	L 595-22	High proper-motion Star	sdG0	non
5463139855815272704	CD-30 8081	Star	non	non
4664603524502409600	HD 270890	Star	K7	non
5116285645676878848	HIP 10807	Starr	Fp	non
3160714468040914816	TYC 756-964-1	High proper-motion Star	non	non
5319910393077917952	TYC 8570-1842-1	Peculiar Star	CEMP	non

Appendix C

Script for rotation of positions of intersections and comparing them with positions of stellar-mass black holes

```
import astropy.coordinates as coord
from astropy.table import QTable
import astropy.units as u
import matplotlib as mpl
import matplotlib.pyplot as plt
import numpy
%matplotlib inline
import pandas as pd
from pandas import DataFrame
import gala.coordinates as gc
import gala.dynamics as gd
import gala.potential as gp
from gala.units import galactic

data = []
allmincross =  QTable.read('allmincross.csv')
milky_way = gp.MilkyWayPotential(units=galactic)
H = gp.Hamiltonian(milky_way)
for i in range(len(allmincross)):
        x = allmincross[i]['X-cross [kpc]']
        y = allmincross[i]['Y-cross [kpc]']
        V_circ = milky_way.circular_velocity([x,y,0.])
        v_x = -V_circ * (y/abs(x+y))
        v_y = -V_circ * (x/abs(x+y))
        v_z = V_circ *0
        w= gd.PhaseSpacePosition(pos =  [x, y,0.] * u.kpc,
        vel = [v_x.value[0],v_y.value[0], 0] * u.km/u.s)
        t = allmincross[i]['Time [0.00001 Myr]'] * 0.00001
        dt = t/10000
        orbit = H.integrate_orbit(w, dt=-dt*u.Myr,t1=0*u.Myr, t2=-t*u.Myr)
        data.append(orbit[9999])
```

```
x = []
y = []
for i in range(len(data)):
        x.append(data[i].x.value)
        y.append(data[i].y.value)

BHdata1 =  QTable.read('BHdata.csv')
c = coord.SkyCoord(ra=BHdata1['Ra'],dec=BHdata1['Dec'],
                distance=BHdata1['R'], unit=(u.hourangle, u.deg, u.kpc))
galcen = c.transform_to(coord.Galactocentric(z_sun=0*u.pc,galcen_distance=8.1*u.kpc))

fig,ax = plt.subplots(1, 1, figsize=(10,10))
ax.scatter(x,y, marker = 'o', color = 'cyan',label= 'Stars crosses of disk')
ax.scatter(galcen.x.value,galcen.y.value , marker = 'o', color = 'blue',label= 'Positions of BHs')
ax.set_aspect('equal')
ax.grid(True, which='both')
#ax.set_xlim(-25,25)
#ax.set_ylim(-25,25)
ax.set_xlabel('x (kpc)')
ax.set_ylabel('y (kpc)')
ax.axhline(y=0, color='k')
ax.axvline(x=0, color='k')
ax.legend()
```

Appendix D

Python Script for the future

```
import astropy.coordinates as coord
from astropy.table import QTable
import astropy.units as u
import matplotlib as mpl
import matplotlib.pyplot as plt
import numpy
%matplotlib inline
import pandas as pd
from pandas import DataFrame
import math
import gala.coordinates as gc
import gala.dynamics as gd
import gala.potential as gp
from gala.units import galactic
import os
import gc

##############################
#doplnit
#gaia_data_neg = QTable.read('data_neg.fits')
#gaia_data_pos = QTable.read('data_pos.fits')
##############################

def createFolder(directory):
        try:
                if not os.path.exists(directory):
                        os.makedirs(directory)
        except OSError:
                print ('Error: Creating directory. ' +  directory)

negunbound=[]
for i in range(0,len(gaia_data_neg),80):
        print(i)
        a = gaia_data_neg[i:i+80]
        c = coord.SkyCoord(ra=a['ra'],
                        dec=a['dec'],
                        distance=coord.Distance(parallax=u.Quantity(a['parallax'])),
                        pm_ra_cosdec=a['pmra'],
                        pm_dec=a['pmdec'],
```

```
                radial_velocity=a['radial_velocity'])
        galcen = c.transform_to(coord.Galactocentric(z_sun=0*u.pc,galcen_distance=8.1*u.kpc))
        milky_way = gp.MilkyWayPotential()
        H = gp.Hamiltonian(milky_way)
        w= gd.PhaseSpacePosition(galcen.cartesian)
        orbitfor = H.integrate_orbit(w, dt=0.1*u.Myr,t1=0*u.Myr, t2=10000*u.Myr)
        eccentricity = orbitfor.eccentricity()
        for j in range(0,len(c)):
                a = math.isnan(eccentricity[j])
                if a == True:
                        negunbound.append(i+j)
                        mypath = os.path.join('.', 'data', 'najdene', 'neg', str(i+j))
                        createFolder(mypath)
                        print(i+j)
                        break
print(len(negunbound))
print(negunbound)

posunbound=[]
for i in range(0,len(gaia_data_pos),80):
        print(i)
        a = gaia_data_pos[i:i+80]
        c = coord.SkyCoord(ra=a['ra'],
                dec=a['dec'],
                distance=coord.Distance(parallax=u.Quantity(a['parallax'])),
                pm_ra_cosdec=a['pmra'],
                pm_dec=a['pmdec'],
                radial_velocity=a['radial_velocity'])
        galcen =c.transform_to(coord.Galactocentric(z_sun=0*u.pc,galcen_distance=8.1*u.kpc))
        milky_way = gp.MilkyWayPotential()
        H = gp.Hamiltonian(milky_way)
        w= gd.PhaseSpacePosition(galcen.cartesian)
        orbitfor = H.integrate_orbit(w, dt=0.1*u.Myr,t1=0*u.Myr, t2=10000*u.Myr)
        eccentricity = orbitfor.eccentricity()
        for j in range(0,len(c)):
                a = math.isnan(eccentricity[j])
                if a == True:
                        posunbound.append(i+j)
                        mypath = os.path.join('.', 'data', 'najdene', 'pos', str(i+j))
                        createFolder(mypath)
                        print(i+j)
                        break
print(len(posunbound))
print(posunbound)

# crossing

for j in range(len(negunbound)):
        a = negunbound[j]
        icrs = coord.SkyCoord(ra=gaia_data_neg[a]['ra'],
                dec=gaia_data_neg[a]['dec'],
                distance=coord.Distance(parallax=
                        u.Quantity(gaia_data_neg[a]['parallax'])),
                pm_ra_cosdec=gaia_data_neg[a]['pmra'],
                pm_dec=gaia_data_neg[a]['pmdec'],
```

```
                        radial_velocity=gaia_data_neg[a]['radial_velocity'])

        galcen = icrs.transform_to(coord.Galactocentric(z_sun=0*u.pc,
                galcen_distance=8.1*u.kpc))
        milky_way = gp.MilkyWayPotential()
        H = gp.Hamiltonian(milky_way)
        w= gd.PhaseSpacePosition(galcen.cartesian)

        orbitfor = H.integrate_orbit(w, dt=0.00001*u.Myr,t1=0*u.Myr, t2=200*u.Myr)

        MAM1 = orbitfor.w()
        ZZZ1 = MAM1[2]
        MyPos1 =[]
        for i in range(len(ZZZ1)):
                if abs(ZZZ1[i])<0.000005:
                        MyPos1.append(i)

        data1 = []
        for j in range(len(MyPos1)):
                c1 = orbitfor[MyPos1[j]]
                row1 = [MyPos1[j],c1.x.value,c1.y.value,c1.z.value,c1.v_x.value,
                        c1.v_y.value,c1.v_z.value]
                data1.append(row1)

        mypath1 = os.path.join('.', 'data', 'najdene', 'neg', str(a),'future_cross.csv')
        df = pd.DataFrame(data = data1, columns = ['Time[0.00001 Myr]', 'X[kpc]', 'Y[kpc]',
                'Z[kpc]', 'V_x [kpc/Myr]',        'V_y [kpc/Myr]','V_z [kpc/Myr]'])
        df.to_csv(mypath1)

        orbitback = H.integrate_orbit(w, dt=-0.00001*u.Myr,t1=0*u.Myr, t2=-200*u.Myr)

        MAM2 = orbitback.w()
        ZZZ2 = MAM2[2]
        MyPos2 =[]
        for i in range(len(ZZZ2)):
                if abs(ZZZ2[i])<0.000005:
                MyPos2.append(i)

        data2 =[]
        for j in range(len(MyPos2)):
                c2 = orbitback[MyPos2[j]]
                row2 = [-MyPos2[j],c2.x.value,c2.y.value,c2.z.value,c2.v_x.value,
                        c2.v_y.value,c2.v_z.value]
                data2.append(row2)

        mypath2 = os.path.join('.', 'data', 'najdene', 'neg', str(a),'past_cross.csv')
        df = pd.DataFrame(data = data2, columns = ['Time[0.00001 Myr]', 'X[kpc]', 'Y[kpc]',
                        'Z[kpc]', 'V_x [kpc/Myr]','V_y [kpc/Myr]','V_z [kpc/Myr]'])
        df.to_csv(mypath2)

for j in range(len(posunbound)):
        a = posunbound[j]
        icrs = coord.SkyCoord(ra=gaia_data_neg[a]['ra'],
                        dec=gaia_data_neg[a]['dec'],
                        distance=coord.Distance(parallax=
```

```
                        u.Quantity(gaia_data_neg[a]['parallax'])),
                pm_ra_cosdec=gaia_data_neg[a]['pmra'],
                pm_dec=gaia_data_neg[a]['pmdec'],
                radial_velocity=gaia_data_neg[a]['radial_velocity'])

galcen = icrs.transform_to(coord.Galactocentric(z_sun=0*u.pc,
        galcen_distance=8.1*u.kpc))
milky_way = gp.MilkyWayPotential()
H = gp.Hamiltonian(milky_way)
w= gd.PhaseSpacePosition(galcen.cartesian)

orbitfor = H.integrate_orbit(w, dt=0.00001*u.Myr,t1=0*u.Myr, t2=200*u.Myr)

MAM1 = orbitfor.w()
ZZZ1 = MAM1[2]
MyPos1 =[]
for i in range(len(ZZZ1)):
        if abs(ZZZ1[i])<0.000005:
                MyPos1.append(i)

data1= []
for j in range(len(MyPos1)):
        c1 = orbitfor[MyPos1[j]]
        row1 = [MyPos1[j],c1.x.value,c1.y.value,c1.z.value,c1.v_x.value,
                c1.v_y.value,c1.v_z.value]
        data1.append(row1)

mypath1 = os.path.join('.', 'data', 'najdene', 'pos', str(a),'future_cross.csv')
df = pd.DataFrame(data = data1, columns = ['Time[0.00001 Myr]', 'X[kpc]', 'Y[kpc]',
         'Z[kpc]', 'V_x [kpc/Myr]','V_y [kpc/Myr]','V_z [kpc/Myr]'])
df.to_csv(mypath1)

orbitback = H.integrate_orbit(w, dt=-0.00001*u.Myr,t1=0*u.Myr, t2=-200*u.Myr)

MAM2 = orbitback.w()
ZZZ2 = MAM2[2]
MyPos2 =[]
for i in range(len(ZZZ2)):
if abs(ZZZ2[i])<0.000005:
        MyPos2.append(i)

data2 =[]
for j in range(len(MyPos2)):
        c2 = orbitback[MyPos2[j]]
        row2 = [-MyPos2[j],c2.x.value,c2.y.value,c2.z.value,c2.v_x.value,
                c2.v_y.value, c2.v_z.value]
        data2.append(row2)

mypath2 = os.path.join('.', 'data', 'najdene', 'pos', str(a),'past_cross.csv')
df = pd.DataFrame(data = data2, columns = ['Time[0.00001 Myr]', 'X[kpc]', 'Y[kpc]',
        'Z[kpc]', 'V_x [kpc/Myr]','V_y [kpc/Myr]','V_z [kpc/Myr]'])
df.to_csv(mypath2)
```

Bibliography

Abadi, M. G., Navarro, J. F., & Steinmetz, M. (2009). An Alternative Origin for Hypervelocity Stars. *Astrophysical Journal, Letters*, *691*(2), L63–L66.

Adams, W. S., & Joy, A. H. (1919). The Motions in Space of Some Stars of High Radial Velocity. *Proceedings of the National Academy of Science*, *5*(7), 239–241.

Allen, C., & Poveda, A. (1972). *On the Reproducibility of Run-Away Stars Formed in Collapsing Clusters*, vol. 31 of *Astrophysics and Space Science Library*, (p. 114).

Allen, L. B. (1925). Two Red Variable Stars with High Velocities. *Publications of the Astronomical Society of the Pacific*, *37*, 94–94.

Aslanov, A. A., & Barannikov, A. A. (1989). Optical Variability of the Runaway Ofp-Star HD108. *Soviet Astronomy Letters*, *15*, 316.

Aslanov, A. A., Kornilova, L. N., & Cherepashchuk, A. M. (1984). A Search for Relativistic Companions of Runaway Ob-Stars. *Soviet Astronomy Letters*, *10*, 278–281.

Bidelman, W. P. (1948). Two High-Velocity Stars of Early Type. *Publications of the Astronomical Society of the Pacific*, *60*(355), 264.

Blaauw, A. (1956). On the Luminosities, Motions, and Space Distribution of the Nearer Northern O-B5 Stars. *Astrophysical Journal*, *123*, 408.

Blaauw, A. (1959). Empirical data and position in the Hertzsprung-Russell diagram for O and B-type stars. In J. L. Greenstein (Ed.) *The Hertzsprung-Russell Diagram*, vol. 10 of *IAU Symposium*, (p. 105).

Blaauw, A. (1961). On the origin of the O- and B-type stars with high velocities (the "run-away" stars), and some related problems. *Bulletin Astronomical Institute of the Netherlands*, *15*, 265.

Bovy, J. (2015). galpy: A python Library for Galactic Dynamics. *Astrophysical Journal, Supplement*, *216*(2), 29.

Bromley, B. C., Kenyon, S. J., Geller, M. J., Barcikowski, E., Brown, W. R., & Kurtz, M. J. (2006). Hypervelocity Stars: Predicting the Spectrum of Ejection Velocities. *Astrophysical Journal*, *653*(2), 1194–1202.

Brown, W. R. (2015). Hypervelocity Stars. *Annual Review of Astronomy and Astrophysics*, *53*(1), 15–49.
URL https://doi.org/10.1146/annurev-astro-082214-122230

Brown, W. R., Geller, M. J., Kenyon, S. J., & Kurtz, M. J. (2005). Discovery of an Unbound Hypervelocity Star in the Milky Way Halo. *Astrophysical Journal, Letters*, *622*(1), L33–L36.

Brown, W. R., Geller, M. J., Kenyon, S. J., & Kurtz, M. J. (2006a). A Successful Targeted Search for Hypervelocity Stars. *Astrophysical Journal, Letters*, *640*(1), L35–L38.

Brown, W. R., Geller, M. J., Kenyon, S. J., & Kurtz, M. J. (2006b). Hypervelocity Stars. I. The Spectroscopic Survey. *Astrophysical Journey*, *647*(1), 303–311.

Brown, W. R., Geller, M. J., Kenyon, S. J., Kurtz, M. J., & Bromley, B. C. (2007a). Hypervelocity Stars. II. The Bound Population. *Astrophysical Journal*, *660*(1), 311–318.

Brown, W. R., Geller, M. J., Kenyon, S. J., Kurtz, M. J., & Bromley, B. C. (2007b). Hypervelocity Stars. III. The Space Density and Ejection History of Main-Sequence Stars from the Galactic Center. *Astrophysical Journal*, *671*(2), 1708–1716.

Cherepashchuk, A. M., & Aslanov, A. A. (1984). Search for relativistic companions in 'non-X-ray' binary systems. *Astrophysics and Space Science*, *102*(1), 97–122.

Cherepashchuk, A. M., & Kukarkin, B. V. (1976). The Possibility of the Search for Relativistic Objects Using the Ellipsoidal Variability of the Run-Away Stars. *Information Bulletin on Variable Stars*, *1137*, 1.

Corral-Santana, J. M., Casares, J., Muñoz-Darias, T., Bauer, F. E., Martínez-Pais, I. G., & Russell, D. M. (2016). BlackCAT: A catalogue of stellar-mass black holes in X-ray transients. *Astronomy and Astrophysics*, *587*, A61.

Cropper, M., Katz, D., Sartoretti, P., Prusti, T., de Bruijne, J. H. J., Chassat, F., Charvet, P., Boyadjian, J., Perryman, M., Sarri, G., Gare, P., Erdmann, M., Munari, U., Zwitter, T., Wilkinson, M., Arenou, F., Vallenari, A., Gómez, A., Panuzzo, P., Seabroke, G., Allende Prieto, C., Benson, K., Marchal, O., Huckle, H., Smith, M., Dolding, C., Janßen, K., Viala, Y., Blomme, R., Baker, S., Boudreault, S., Crifo, F., Soubiran, C., Frémat, Y., Jasniewicz, G., Guerrier, A., Guy, L. P., Turon, C., Jean-Antoine-Piccolo, A., Thévenin, F., David, M., Gosset, E., & Damerdji, Y. (2018). Gaia Data Release 2. Gaia Radial Velocity Spectrometer. *Astronomy and Astrophysics*, *616*, A5.

Edelmann, H., Napiwotzki, R., Heber, U., Christlieb, N., & Reimers, D. (2005). HE 0437-5439: An Unbound Hypervelocity Main-Sequence B-Type Star. *Astrophysical Journal*, *634*(2), L181–L184.

ESA (2014-2020). GAIA DATA RELEASE SCENARIO. (Date of access 26.01.2020).
URL https://www.cosmos.esa.int/web/gaia/release

ESA (2017). Gaia Spacecraft.
URL https://sci.esa.int/web/gaia/-/40924-gaia-spacecraft

ESA (2018). Gaia archive.
URL https://gea.esac.esa.int/archive/http://arxiv.org/abs/1603.07347

Fragione, G., & Gualandris, A. (2019). Hypervelocity stars from star clusters hosting intermediate-mass black holes. *Monthly Notices of the Royal Astronomical Society*, *489*(4), 4543–4556.

Gaia Collaboration, Brown, A. G. A., Vallenari, A., Prusti, T., de Bruijne, J. H. J., Babusiaux, C., Bailer-Jones, C. A. L., Biermann, M., Evans, D. W., Eyer, L., Jansen, F., Jordi, C., Klioner, S. A., Lammers, U., Lindegren, L., Luri, X., Mignard, F., Panem, C., Pourbaix, D., Randich, S., Sartoretti, P., Siddiqui, H. I., Soubiran, C., van Leeuwen, F., Walton, N. A., Arenou, F., Bastian, U., Cropper, M., Drimmel, R., Katz, D., Lattanzi, M. G., Bakker, J., Cacciari, C., Castañeda, J., Chaoul, L., Cheek, N., De Angeli, F., Fabricius, C., Guerra, R., Holl, B., Masana, E., Messineo, R., Mowlavi, N., Nienartowicz, K., Panuzzo, P., Portell, J., Riello, M., Seabroke, G. M., Tanga, P., Thévenin, F., Gracia-Abril, G., Comoretto, G., Garcia-Reinaldos, M., Teyssier, D., Altmann, M., Andrae, R., Audard, M., Bellas-Velidis, I., Benson, K., Berthier, J., Blomme, R., Burgess, P., Busso, G., Carry, B., Cellino, A., Clementini, G., Clotet, M., Creevey, O., Davidson, M., De Ridder, J., Delchambre, L., Dell'Oro, A., Ducourant, C., Fernández-Hernández, J., Fouesneau, M., Frémat, Y., Galluccio, L., García-Torres, M., González-Núñez, J., González-Vidal, J. J., Gosset, E., Guy, L. P., Halbwachs, J. L., Hambly, N. C., Harrison, D. L., Hernández, J., Hestroffer, D., Hodgkin, S. T., Hutton, A., Jasniewicz, G., Jean-Antoine-Piccolo, A., Jordan, S., Korn, A. J., Krone-Martins, A., Lanzafame, A. C., Lebzelter, T., Löffler, W., Manteiga, M., Marrese, P. M., Martín-Fleitas, J. M., Moitinho, A., Mora, A., Muinonen, K., Osinde, J., Pancino, E., Pauwels, T., Petit, J. M., Recio-Blanco, A., Richards, P. J., Rimoldini, L., Robin, A. C., Sarro, L. M., Siopis, C., Smith, M., Sozzetti, A., Süveges, M., Torra, J., van Reeven, W., Abbas, U., Abreu Aramburu, A., Accart, S., Aerts, C., Altavilla, G., Álvarez, M. A., Alvarez, R., Alves, J., Anderson, R. I., Andrei, A. H., Anglada Varela, E., Antiche, E., Antoja, T., Arcay, B., Astraatmadja, T. L., Bach, N., Baker, S. G., Balaguer-Núñez, L., Balm, P., Barache, C., Barata, C., Barbato, D., Barblan, F., Barklem, P. S., Barrado, D., Barros, M., Barstow, M. A., Bartholomé Muñoz, S., Bassilana, J. L., Becciani, U., Bellazzini, M., Berihuete, A., Bertone, S., Bianchi, L., Bienaymé, O., Blanco-Cuaresma, S., Boch, T., Boeche, C., Bombrun, A., Borrachero, R., Bossini, D., Bouquillon, S., Bourda, G., Bragaglia, A., Bramante, L., Breddels, M. A., Bressan, A., Brouillet, N., Brüsemeister, T., Brugaletta, E., Bucciarelli, B., Burlacu, A., Busonero, D., Butkevich, A. G., Buzzi, R., Caffau, E., Cancelliere, R., Cannizzaro, G., Cantat-Gaudin, T., Carballo, R., Carlucci, T., Carrasco, J. M., Casamiquela, L., Castellani, M., Castro-Ginard, A., Charlot, P., Chemin, L., Chiavassa, A., Cocozza, G., Costigan, G., Cowell, S., Crifo, F., Crosta, M., Crowley, C., Cuypers, J., Dafonte, C., Damerdji, Y., Dapergolas, A., David, P., David, M., de Laverny, P., De Luise, F., De March, R., de Martino, D., de Souza, R., de Torres, A., Debosscher, J., del Pozo, E., Delbo, M., Delgado, A., Delgado, H. E., Di Matteo, P., Diakite, S., Diener, C., Distefano, E., Dolding, C., Drazinos, P., Durán, J., Edvardsson, B., Enke, H., Eriksson, K., Esquej, P., Eynard Bontemps, G., Fabre, C., Fabrizio, M., Faigler, S., Falcão, A. J., Farràs Casas, M., Federici, L., Fedorets, G., Fernique, P., Figueras, F., Filippi, F., Findeisen, K., Fonti, A., Fraile, E., Fraser, M., Frézouls, B., Gai, M., Galleti, S., Garabato, D., García-Sedano, F., Garofalo, A., Garralda, N., Gavel, A., Gavras, P., Gerssen, J., Geyer, R., Giacobbe, P., Gilmore, G., Girona, S., Giuffrida, G., Glass, F., Gomes, M., Granvik, M., Gueguen, A., Guerrier, A., Guiraud, J., Gutiérrez-Sánchez, R., Haigron, R., Hatzidimitriou, D., Hauser, M., Haywood, M., Heiter, U., Helmi, A., Heu, J., Hilger, T., Hobbs, D., Hofmann, W., Holland, G., Huckle, H. E., Hypki, A., Icardi, V., Janßen, K., Jevardat de Fombelle, G., Jonker, P. G., Juhász, Á. L., Julbe, F., Karampelas, A., Kewley, A., Klar, J., Kochoska, A., Kohley, R., Kolenberg, K., Kontizas, M., Kontizas, E., Koposov, S. E., Kordopatis, G., Kostrzewa-Rutkowska, Z., Koubsky, P., Lambert, S., Lanza, A. F., Lasne, Y., Lavigne, J. B., Le Fustec, Y., Le Poncin-Lafitte, C., Lebreton, Y., Leccia, S., Leclerc, N., Lecoeur-Taibi, I., Lenhardt (2018). Gaia Data Release 2. Summary of the contents and survey properties. *Astronomy and Astrophysics*, *616*, A1.

Gaia Collaboration, Prusti, T., de Bruijne, J. H. J., Brown, A. G. A., Vallenari, A., Babusiaux, C., Bailer-Jones, C. A. L., Bastian, U., Biermann, M., Evans, D. W., Eyer, L., Jansen, F., Jordi, C., Klioner, S. A., Lammers, U., Lindegren, L., Luri, X., Mignard, F., Milligan, D. J., Panem, C., Poinsignon, V., Pourbaix, D., Randich, S., Sarri, G., Sartoretti, P., Siddiqui, H. I., Soubiran, C., Valette, V., van Leeuwen, F., Walton, N. A., Aerts, C., Arenou, F., Cropper, M., Drimmel, R., Høg, E., Katz, D., Lattanzi, M. G., O'Mullane, W., Grebel, E. K., Holland, A. D., Huc, C., Passot, X., Bramante, L., Cacciari, C., Castañeda, J., Chaoul, L., Cheek, N., De Angeli, F., Fabricius, C., Guerra, R., Hernández, J., Jean-Antoine-Piccolo, A., Masana, E., Messineo, R., Mowlavi, N., Nienartowicz, K., Ordóñez-Blanco, D., Panuzzo, P., Portell, J., Richards, P. J., Riello, M., Seabroke, G. M., Tanga, P., Thévenin, F., Torra, J., Els, S. G., Gracia-Abril, G., Comoretto, G., Garcia-Reinaldos, M., Lock, T., Mercier, E., Altmann, M., Andrae, R., Astraatmadja, T. L., Bellas-Velidis, I., Benson, K., Berthier, J., Blomme, R., Busso, G., Carry, B., Cellino, A., Clementini, G., Cowell, S., Creevey, O., Cuypers, J., Davidson, M., De Ridder, J., de Torres, A., Delchambre, L., Dell'Oro, A., Ducourant, C., Frémat, Y., García-Torres, M., Gosset, E., Halbwachs, J. L., Hambly, N. C., Harrison, D. L., Hauser, M., Hestroffer, D., Hodgkin, S. T., Huckle, H. E., Hutton, A., Jasniewicz, G., Jordan, S., Kontizas, M., Korn, A. J., Lanzafame, A. C., Manteiga, M., Moitinho, A., Muinonen, K., Osinde, J., Pancino, E., Pauwels, T., Petit, J. M., Recio-Blanco, A., Robin, A. C., Sarro, L. M., Siopis, C., Smith, M., Smith, K. W., Sozzetti, A., Thuillot, W., van Reeven, W., Viala, Y., Abbas, U., Abreu Aramburu, A., Accart, S., Aguado, J. J., Allan, P. M., Allasia, W., Altavilla, G., Álvarez, M. A., Alves, J., Anderson, R. I., Andrei, A. H., Anglada Varela, E., Antiche, E., Antoja, T., Antón, S., Arcay, B., Atzei, A., Ayache, L., Bach, N., Baker, S. G., Balaguer-Núñez, L., Barache, C., Barata, C., Barbier, A., Barblan, F., Baroni, M., Barrado y Navascués, D., Barros, M., Barstow, M. A., Becciani, U., Bellazzini, M., Bellei, G., Bello García, A., Belokurov, V., Bendjoya, P., Berihuete, A., Bianchi, L., Bienaymé, O., Billebaud, F., Blagorodnova, N., Blanco-Cuaresma, S., Boch, T., Bombrun, A., Borrachero, R., Bouquillon, S., Bourda, G., Bouy, H., Bragaglia, A., Breddels, M. A., Brouillet, N., Brüsemeister, T., Bucciarelli, B., Budnik, F., Burgess, P., Burgon, R., Burlacu, A., Busonero, D., Buzzi, R., Caffau, E., Cambras, J., Campbell, H., Cancelliere, R., Cantat-Gaudin, T., Carlucci, T., Carrasco, J. M., Castellani, M., Charlot, P., Charnas, J., Charvet, P., Chassat, F., Chiavassa, A., Clotet, M., Cocozza, G., Collins, R. S., Collins, P., Costigan, G., Crifo, F., Cross, N. J. G., Crosta, M., Crowley, C., Dafonte, C., Damerdji, Y., Dapergolas, A., David, P., David, M., De Cat, P., de Felice, F., de Laverny, P., De Luise, F., De March, R., de Martino, D., de Souza, R., Debosscher, J., del Pozo, E., Delbo, M., Delgado, A., Delgado, H. E., di Marco, F., Di Matteo, P., Diakite, S., Distefano, E., Dolding, C., Dos Anjos, S., Drazinos, P., Durán, J., Dzigan, Y., Ecale, E., Edvardsson, B., Enke, H., Erdmann, M., Escolar, D., Espina, M., Evans, N. W., Eynard Bontemps, G., Fabre, C., Fabrizio, M., Faigler, S., Falcão, A. J., Farràs Casas, M., Faye, F., Federici, L., Fedorets, G., Fernández-Hernández, J., Fernique, P., Fienga, A., Figueras, F., Filippi, F., Findeisen, K., Fonti, A., Fouesneau, M., Fraile, E., Fraser, M., Fuchs, J., Furnell, R., Gai, M., Galleti, S., Galluccio, L., Garabato, D., García-Sedano, F., Garé, P., Garofalo, A., Garralda, N., Gavras, P., Gerssen, J., Geyer, R., Gilmore, G., Girona, S., Giuffrida, G., Gomes, M., González-Marcos, A., González-Núñez, J., González-Vidal, J. J., Granvik, M., Guerrier, A., Guillout, P., Guiraud, J., Gúrpide, A., Gutiérrez-Sánchez, R., Guy, L. P., Haigron, R., Hatzidimitriou, D., Haywood, M., Heiter, U., Helmi, A., Hobbs, D., Hofmann, W., Holl, B., Holland , G., Hunt, J. A. S., Hypki, A., Icardi, V., Irwin, M., Jevardat de Fombelle, G., Jofré, P., Jonker, P. G., Jorissen, A., Julbe, F., Karampelas, (2016). The Gaia mission. *Astronomy and Astrophysics*, *595*, A1.

Greenstein, J. L. (1957). Some high-velocity Population I stars. *Astronomical Journal*, *62*, 16.

Greenstein, J. L., Macrae, D. A., & Fleischer, R. (1956). Two B-Type Stars of High Velocity. *Publications of the Astronomical Society of the Pacific*, *68*(402), 242.

Hattori, K., Valluri, M., Castro, N., Roederer, I. U., Mahler, G., & Khullar, G. (2019). Origin of a Massive Hyper-runaway Subgiant Star LAMOST-HVS1: Implication from Gaia and Follow-up Spectroscopy. *Astrophysical Journal*, *873*(2), 116.

Hernquist, L. (1990). An Analytical Model for Spherical Galaxies and Bulges. *Astrophysical journal*, *356*, 359.

Hills, J. G. (1988). Hyper-velocity and tidal stars from binaries disrupted by a massive Galactic black hole. *Nature*, *331*(6158), 687–689.

Hirsch, H. A., Heber, U., O'Toole, S. J., & Bresolin, F. (2005). ¡ASTROBJ¿US 708¡/ASTROBJ¿ - an unbound hyper-velocity subluminous O star. *Astronomy and Astrophysics*, *444*(3), L61–L64.

Hodge, P. W. (2020). Milky way galaxy.
URL https://www.britannica.com/place/Milky-Way-Galaxy

Humason, M. L., & Zwicky, F. (1947). A Search for Faint Blue Stars. *Astrophysical Journal*, *105*, 85.

Katz, D., Sartoretti, P., Cropper, M., Panuzzo, P., Seabroke, G. M., Viala, Y., Benson, K., Blomme, R., Jasniewicz, G., Jean-Antoine, A., Huckle, H., Smith, M., Baker, S., Crifo, F., Damerdji, Y., David, M., Dolding, C., Frémat, Y., Gosset, E., Guerrier, A., Guy, L. P., Haigron, R., Janßen, K., Marchal, O., Plum, G., Soubiran, C., Thévenin, F., Ajaj, M., Allende Prieto, C., Babusiaux, C., Boudreault, S., Chemin, L., Delle Luche, C., Fabre, C., Gueguen, A., Hambly, N. C., Lasne, Y., Meynadier, F., Pailler, F., Panem, C., Royer, F., Tauran, G., Zurbach, C., Zwitter, T., Arenou, F., Bossini, D., Gerssen, J., Gómez, A., Lemaitre, V., Leclerc, N., Morel, T., Munari, U., Turon, C., Vallenari, A., & Žerjal, M. (2019). Gaia Data Release 2. Properties and validation of the radial velocities. *Astronomy and Astrophysics*, *622*, A205.

Koposov, S. E., Boubert, D., Li, T. S., Erkal, D., Da Costa, G. S., Zucker, D. B., Ji, A. P., Kuehn, K., Lewis, G. F., Mackey, D., Simpson, J. D., Shipp, N., Wan, Z., Belokurov, V., Bland-Hawthorn, J., Martell, S. L., Nordlander, T., Pace, A. B., De Silva, G. M., Wang, M.-Y., & S5 collaboration (2020). Discovery of a nearby 1700 km s^{-1} star ejected from the Milky Way by Sgr A*. *Monthly Notices of the RAS*, *491*(2), 2465–2480.

Kramer, H. J. (2002). Gaia (global astrometric interferometer for astrophysics).
URL https://directory.eoportal.org/web/eoportal/satellite-missions/content/-/article/gaia-satellite-mission

Lindegren, L., Hernández, J., Bombrun, A., Klioner, S., Bastian, U., Ramos-Lerate, M., de Torres, A., Steidelmüller, H., Stephenson, C., Hobbs, D., Lammers, U., Biermann, M., Geyer, R., Hilger, T., Michalik, D., Stampa, U., McMillan, P. J., Castañeda, J., Clotet, M., Comoretto, G., Davidson, M., Fabricius, C., Gracia, G., Hambly, N. C., Hutton, A., Mora, A., Portell, J., van Leeuwen, F., Abbas, U., Abreu, A., Altmann, M., Andrei, A., Anglada, E., Balaguer-Núñez, L., Barache, C., Becciani, U., Bertone, S., Bianchi, L., Bouquillon, S., Bourda, G., Brüsemeister, T., Bucciarelli, B., Busonero, D., Buzzi, R., Cancelliere, R., Carlucci, T., Charlot, P., Cheek, N., Crosta, M., Crowley, C., de Bruijne, J., de Felice, F., Drimmel, R., Esquej, P., Fienga, A., Fraile, E., Gai, M., Garralda, N., González-Vidal, J. J., Guerra, R., Hauser, M., Hofmann, W., Holl, B., Jordan, S., Lattanzi, M. G., Lenhardt, H., Liao, S., Licata, E., Lister, T., Löffler, W., Marchant, J., Martin-Fleitas, J. M., Messineo, R., Mignard, F., Morbidelli, R., Poggio, E., Riva, A., Rowell, N., Salguero, E., Sarasso, M., Sciacca, E., Siddiqui, H., Smart, R. L., Spagna, A., Steele, I., Taris, F., Torra, J., van Elteren, A., van Reeven, W., & Vecchiato, A. (2018). Gaia Data Release 2. The astrometric solution. *Astronomy and Astrophysics*, *616*, A2.

Luri, X., Brown, A. G. A., Sarro, L. M., Arenou, F., Bailer-Jones, C. A. L., Castro-Ginard, A., de Bruijne, J., Prusti, T., Babusiaux, C., & Delgado, H. E. (2018). Gaia Data Release 2. Using Gaia parallaxes. *Astronomy and Astrophysics*, *616*, A9.

McMillan, S. (2019). Leapfrog Integrator.
URL http://www.physics.drexel.edu/~steve/Courses/Comp_Phys/Integrators/leapfrog/

Mikulášek, Z., & Krtička, J. (2005). Základy fyziky hvězd.
URL https://astro.physics.muni.cz/download/documents/skripta/F3080.pdf

Miyamoto, M., & Nagai, R. (1975). Three-dimensional models for the distribution of mass in galaxies. *Publications of the Astronomical Society of Japan*, *27*, 533–543.

Oort, J. H. (1922). Some peculiarities in the motion of stars of high velocity. *Bulletin of the Astronomical Institutes of the Netherlands*, *1*, 133.

Oort, J. H. (1926). *The Stars of High Velocity*. Ph.D. thesis, -.

Oort, J. H. (1930). The estimated number of high velocities among stars selected according to proper motion. *Bulletin of the Astronomical Institutes of the Netherlands*, *5*, 189.

Pearson Education (2004a). Anatomy of the Milky way.
URL https://www.physast.uga.edu/~rls/1020/ch19/19-01b.jpg

Pearson Education (2004b). Orbits of stars in different regions of our Galaxy.
URL https://www.physast.uga.edu/~rls/1020/ch19/19-18.jpg

Pline (2013). Gaia orbit.
URL https://commons.wikimedia.org/wiki/File:Gaia_orbit-fr.png

Ponman, T. (2013). Dynamics in a Gravitational Field. In *Formation & Evolution of Galaxies*, chap. 2. (Unpublished).
URL http://www.sr.bham.ac.uk/~tjp/FEG/hand2.pdf

Poveda, A., Ruiz, J., & Allen, C. (1967). Run-away Stars as the Result of the Gravitational Collapse of Proto-stellar Clusters. *Boletin de los Observatorios Tonantzintla y Tacubaya*, *4*, 86–90.

Price-Whelan, A., Sipőcz, B., Lenz, D., Greco, J., Major, S., Koposov, S., Oh, S., & Lim, P. L. (2020). adrn/gala: v1.1.

Price-Whelan, A. M. (2017). Gala: A Python package for galactic dynamics. *The Journal of Open Source Software*, *2*, 388.

Price-Whelan, A. M. (2020a). Defining a Milky Way potential model.
URL https://gala-astro.readthedocs.io/en/latest/potential/define-milky-way-model.html

Price-Whelan, A. M. (2020b). Hamiltonian.
URL https://gala-astro.readthedocs.io/en/latest/api/gala.potential.hamiltonian.Hamiltonian.html#gala.potential.hamiltonian.Hamiltonian

Price-Whelan, A. M. (2020c). LeapfrogIntegrator.
URL https://gala-astro.readthedocs.io/en/latest/api/gala.integrate.LeapfrogIntegrator.html#gala.integrate.LeapfrogIntegrator

Price-Whelan, A. M. (2020d). Phase Space Position.
URL https://gala-astro.readthedocs.io/en/latest/api/gala.dynamics.PhaseSpacePosition.html#gala.dynamics.PhaseSpacePosition

Przybilla, N., Fernanda Nieva, M., Heber, U., & Butler, K. (2008). HD 271791: An Extreme Supernova Runaway B Star Escaping from the Galaxy. *Astrophysical Journal*, *684*(2), L103.

Schwarzschild, M. (1952). Perigalactic and apogalactic distances of high-velocity stars. *Astronomical Journal*, *57*, 57.

Silk, J., Antonuccio-Delogu, V., Dubois, Y., Gaibler, V., Haas, M. R., Khochfar, S., & Krause, M. (2012). Jet interactions with a giant molecular cloud in the Galactic centre and ejection of hypervelocity stars. *Astronomy and Astrophysics*, *545*, L11.

Soubiran, C., Jasniewicz, G., Chemin, L., Zurbach, C., Brouillet, N., Panuzzo, P., Sartoretti, P., Katz, D., Le Campion, J. F., Marchal, O., Hestroffer, D., Thévenin, F., Crifo, F., Udry, S., Cropper, M., Seabroke, G., Viala, Y., Benson, K., Blomme, R., Jean-Antoine, A., Huckle, H., Smith, M., Baker, S. G., Damerdji, Y., Dolding, C., Frémat, Y., Gosset, E., Guerrier, A., Guy, L. P., Haigron, R., Janßen, K., Plum, G., Fabre, C., Lasne, Y., Pailler, F., Panem, C., Riclet, F., Royer, F., Tauran, G., Zwitter, T., Gueguen, A., & Turon, C. (2018). Gaia Data Release 2. The catalogue of radial velocity standard stars. *Astronomy and Astrophysics*, *616*, A7.

Sterken, C. (1988). Photometric and spectrographic study of the runaway star 53 Arietis. *Astronomy and Astrophysics*, *189*, 81–88.

Trumpler, R. (1924). The High Velocity Star C. D. -26°16876. *Publications of the Astronomical Society of the Pacific*, *36*(214), 343.

University of Michigan (2019). Hyper-runaway star ejected from the Milky Way Disk.
URL https://tinyurl.com/y2ongtg3

Wikipedia (2020a). Leapfrog integration - Wikipedia.
URL https://en.wikipedia.org/wiki/Leapfrog_integration

Wikipedia (2020b). Milky way.
URL https://en.wikipedia.org/wiki/Milky_Way

Wikipedia (2020c). Navarro–frenk–white profile.
URL https://en.wikipedia.org/wiki/Navarro\IL2\textendashFrenk\IL2\textendashWhite_profile

Yu, Q., & Tremaine, S. (2003). Ejection of Hypervelocity Stars by the (Binary) Black Hole in the Galactic Center. *Astrophysical Journal*, *599*(2), 1129–1138.